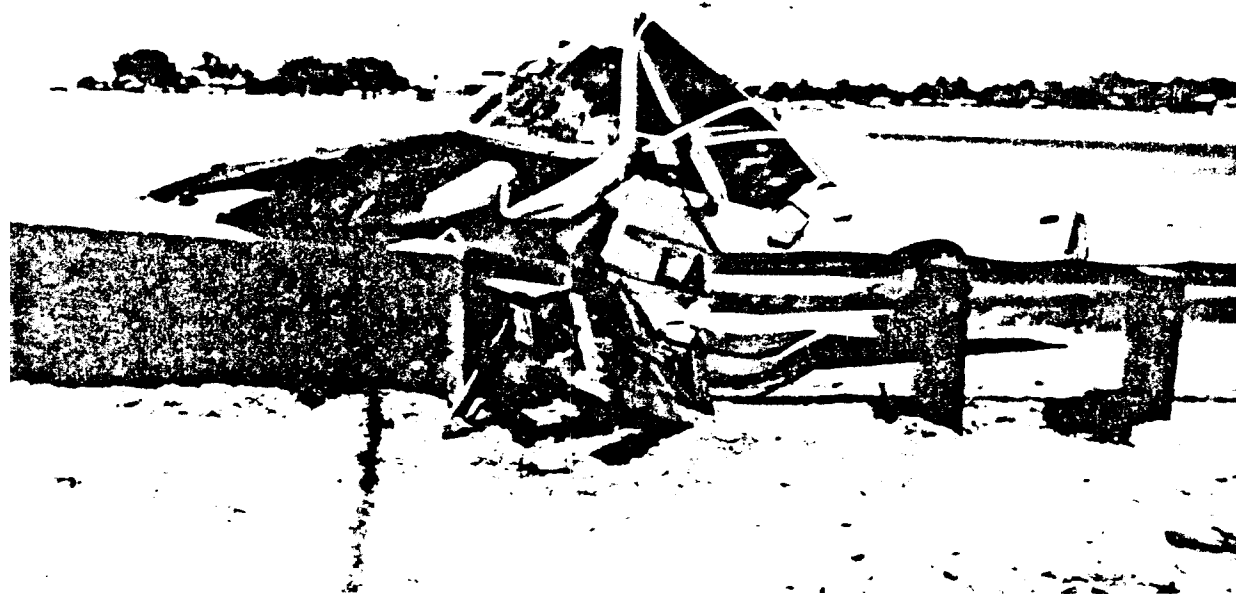


Guardrail-Bridge Rail Transition Designs, Volume I: Research Report

Publication No. FHWA/RD-86/178

April 1988



REPRODUCED BY
U.S. DEPARTMENT OF COMMERCE
NATIONAL TECHNICAL INFORMATION SERVICE
SPRINGFIELD, VA. 22161




U.S. Department of Transportation
Federal Highway Administration

Research, Development, and Technology
Turner-Fairbank Highway Research Center
6300 Georgetown Pike
McLean, Virginia 22101-2296

FOREWORD

This report, "Guardrail-Bridge Rail Transition Designs," Volume I, presents the results of research conducted on transitions by the Southwest Research Institute for the Federal Highway Administration (FHWA), Office of Safety and Traffic Operations Research and Development under contract Number DTFH61-83-C-00028. This work was conducted as part of Program A5, "Safety Design," and is intended for engineers concerned with roadside safety hardware. A series of transitions from W-beam or three beam approach guardrails to straight or flared end blocks were crash tested with 4,500 lb cars and evaluated using the criteria in NCHRP Report No. 230. A curved guardrail/transition was also tested and developed. The computer program that was developed as an aid for designing independent end blocks should be used with caution because it has only been validated against the results of one full-scale test.

Copies of this report are being given widespread distribution by FHWA Transmittal Memorandum. Sufficient copies of Volume I are being distributed to provide a minimum of one copy to each regional office, division office and State highway agency. Direct distribution is being made to the division offices. Additional copies may be obtained from the National Technical Information Service, 5285 Port Royal Road, Springfield, Virginia 22161.


for Stanley R. Byington, Director
Office of Safety and Traffic
Operations Research and Development
Federal Highway Administration

NOTICE

This document is disseminated under the sponsorship of the Department of Transportation in the interest of information exchange. The United States Government assumes no liability for the contents or use thereof.

The contents of this report reflect the views of the contractor, who is responsible for the accuracy of the data presented herein. The contents do not necessarily reflect the official policy of the Department of Transportation.

This report does not constitute a standard, specification, or regulation.

The United States Government does not endorse products or manufacturers. Trade or manufacturer's names appear herein only because they are considered essential to the objective of this document.

1. Report No. FHWA/RD-86/178		2. Government Accession No. PB89 124531AS		3. Recipient's Catalog No.																	
4. Title and Subtitle GUARDRAIL-BRIDGE RAIL TRANSITION DESIGNS VOLUME 1, RESEARCH REPORT				5. Report Date April 1988																	
				6. Performing Organization Code																	
7. Author(s) M. E. Bronstad, L. R. Calcote, M. H. Ray, J. B. Mayer				8. Performing Organization Report No. 06-7642-1																	
9. Performing Organization Name and Address Southwest Research Institute 6220 Culebra Road San Antonio, TX 78284				10. Work Unit No. 31T2322																	
				11. Contract or Grant No. DTFH61-83-C-00028																	
12. Sponsoring Agency Name and Address Safety Design Division Federal Highway Administration 6300 Georgetown Pike McLean, VA 22101-2296				13. Type of Report and Period Covered Final Report July 1983 - February 1987																	
				14. Sponsoring Agency Code																	
15. Supplementary Notes FHWA Contract Manager (COTR): C. F. McDevitt (HSR-20)																					
16. Abstract This project was concerned with the transition designs used between W-beam and thrie guardrail, and rigid bridge rail parapets or wingwalls. State designs submitted to the Federal Highway Administration (FHWA) were rated and designs selected for crash test evaluation. New designs were also formulated and subjected to crash test evaluation. Most of the crash tests were conducted with 4500-lb (2000-kg) cars at 60 mph (95 km/h) and a 25-degree angle. Design drawings are presented along with recommendations for use of these transition designs. Guidelines for transition features are given and design procedures for independent end blocks are given. This volume is the first in a series. The others in the series are:																					
<table border="0" style="width: 100%; border-collapse: collapse;"> <thead> <tr> <th style="text-align: center;"><u>Vol. No.</u></th> <th style="text-align: center;"><u>FHWA No.</u></th> <th style="text-align: center;"><u>Short Title</u></th> <th style="text-align: center;"><u>NTIS (PB) No.</u></th> </tr> </thead> <tbody> <tr> <td style="text-align: center;">1</td> <td style="text-align: center;">RD-86/178</td> <td style="text-align: center;">Research Report</td> <td></td> </tr> <tr> <td style="text-align: center;">2</td> <td style="text-align: center;">RD-86/179</td> <td style="text-align: center;">Appendix B</td> <td></td> </tr> <tr> <td style="text-align: center;">3</td> <td style="text-align: center;">RD-86/180</td> <td style="text-align: center;">Appendixes C and D</td> <td></td> </tr> </tbody> </table>						<u>Vol. No.</u>	<u>FHWA No.</u>	<u>Short Title</u>	<u>NTIS (PB) No.</u>	1	RD-86/178	Research Report		2	RD-86/179	Appendix B		3	RD-86/180	Appendixes C and D	
<u>Vol. No.</u>	<u>FHWA No.</u>	<u>Short Title</u>	<u>NTIS (PB) No.</u>																		
1	RD-86/178	Research Report																			
2	RD-86/179	Appendix B																			
3	RD-86/180	Appendixes C and D																			
17. Key Words Guardrail, Bridge rail, Transition, Crash test, Highway safety			18. Distribution Statement No restrictions. This document is available to the public through the National Technical Information Service, Springfield, VA 22161.																		
19. Security Classif. (of this report) Unclassified		20. Security Classif. (of this page) Unclassified		21. No. of Pages 188	22. Price																

METRIC (SI*) CONVERSION FACTORS

APPROXIMATE CONVERSIONS TO SI UNITS

Symbol When You Know Multiply By To Find Symbol

LENGTH

in	inches	2.54	millimetres	mm
ft	feet	0.3048	metres	m
yd	yards	0.914	metres	m
mi	miles	1.61	kilometres	km

AREA

in ²	square inches	645.2	millimetres squared	mm ²
ft ²	square feet	0.0929	metres squared	m ²
yd ²	square yards	0.836	metres squared	m ²
mi ²	square miles	2.59	kilometres squared	km ²
ac	acres	0.395	hectares	ha

MASS (weight)

oz	ounces	28.35	grams	g
lb	pounds	0.454	kilograms	kg
T	short tons (2000 lb)	0.907	megagrams	Mg

VOLUME

fl oz	fluid ounces	29.57	millilitres	mL
gal	gallons	3.785	litres	L
ft ³	cubic feet	0.0328	metres cubed	m ³
yd ³	cubic yards	0.0765	metres cubed	m ³

NOTE: Volumes greater than 1000 L shall be shown in m³.

TEMPERATURE (exact)

°F	Fahrenheit temperature	5/9 (after subtracting 32)	Celsius temperature	°C
----	------------------------	----------------------------	---------------------	----

APPROXIMATE CONVERSIONS TO SI UNITS

Symbol When You Know Multiply By To Find Symbol

LENGTH

mm	millimetres	0.039	inches	in
m	metres	3.28	feet	ft
m	metres	1.09	yards	yd
km	kilometres	0.621	miles	mi

AREA

mm ²	millimetres squared	0.0016	square inches	in ²
m ²	metres squared	10.764	square feet	ft ²
km ²	kilometres squared	0.39	square miles	mi ²
ha	hectares (10 000 m ²)	2.53	acres	ac

MASS (weight)

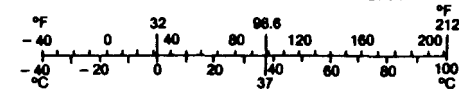
g	grams	0.0353	ounces	oz
kg	kilograms	2.205	pounds	lb
Mg	megagrams (1 000 kg)	1.103	short tons	T

VOLUME

mL	millilitres	0.034	fluid ounces	fl oz
L	litres	0.264	gallons	gal
m ³	metres cubed	35.315	cubic feet	ft ³
m ³	metres cubed	1.308	cubic yards	yd ³

TEMPERATURE (exact)

°C	Celsius temperature	9/5 (then add 32)	Fahrenheit temperature	°F
----	---------------------	-------------------	------------------------	----



These factors conform to the requirement of FHWA Order 5190.1A.



* SI is the symbol for the International System of Measurements

Table of Contents

Volume 1: Guardrail-Bridge Rail Transition Designs

<u>Section</u>	<u>Page</u>
1. Introduction and Research Approach.....	1
a. Statement of the Problem.....	1
b. Objectives and Scope.....	5
c. Research Approach and Report Organization.....	7
2. Current Designs.....	11
a. Review of State Current Designs.....	11
b. Selection of Candidate Transition Systems.....	16
c. Component Testing.....	19
d. Analysis of Candidate Configurations.....	29
3. Summary of Full-Scale Crash Tests.....	55
a. Test Procedures.....	55
b. W-Beam/Wingwall Transitions.....	60
c. Three-Beam/Wingwall Transitions.....	77
d. W-Beam Approach at Intersecting Roadways.....	82
e. W-Beam/Independent Block.....	99
f. W-Beam/Tapered Curb.....	104
4. Design of Independent Anchor Blocks.....	109
a. Introduction.....	109
b. Ultimate Strength of Soils.....	112
c. Analysis of the Independent Block.....	117
d. Independent Block Analysis Program.....	122
e. Design of Independent Anchor Blocks.....	122
f. Summary.....	132
5. Conclusions and Recommendations.....	133
a. Conclusions.....	133
b. Recommendations.....	137
Appendix A. Transition Configurations.....	162
References	168

Table of Contents (continued)

Volume 2: Guardrail - Bridge Rail Transition Designs

<u>Section</u>		<u>Page</u>
Appendix B.	Full-Scale Crash Test Reports.....	1
	Test LA-1.....	9
	Test LA-1M.....	16
	Test T-5.....	24
	Test NC-1.....	48
	Test NC-1M.....	67
	Test NC-2M.....	90
	Test T-6.....	114
	Test T-1.....	136
	Test T-7.....	159
	Test T-2.....	182
	Test T-3.....	205
	Test WA-1.....	227
	Test WA-1M.....	237
	Test WA-2M.....	244
	Test WA-3M.....	265
	Test WA-4M.....	272
	Test WA-5M.....	304
	Test NV-1.....	326
	Test IB-1.....	350
	Test TC-1.....	373

Volume 3: Guardrail - Bridge Rail Transition Designs

Appendix C.	Ratings of State Transition Designs.....	1
Appendix D.	BARRIER VII Plots for Selected Transitions.....	26

List of Figures

Volume 1: Guardrail - Bridge Rail Transition Designs

<u>Figure</u>		<u>Page</u>
1.	Definition of roadside barrier elements.....	2
2.	Bridge end drainage.....	3
3.	Bridge end adapter block for guardrail attachment.....	4
4.	End block that is integral part of abutment.....	6
5.	Post property tests.....	20
6.	Previous pendulum test.....	25
7.	Pendulum test result for W6X15.5 with soil paddle.....	26
8.	Post elastic-plastic response.....	27
9.	BARRIER VII post simulation.....	28
10.	BARRIER VII plot for a rigid transition.....	32
11.	Rub rail retrofit.....	39
12.	Simulation for impact at 450 in.....	40
13.	Simulation for impact at 487.5 in.....	46
14.	Washington test simulation.....	52
15.	Test LA-1 photographs.....	61
16.	Sequential photographs, Test LA-1.....	62
17.	Test LA-1M photographs.....	63
18.	Sequential photographs, Test LA-1M.....	65
19.	Before and after photographs, Test T-5.....	66
20.	Sequential photographs, Test T-5.....	67
21.	Test NC-1 photographs.....	68
22.	Sequential photographs, Test NC-1.....	69

List of Figures (continued)

<u>Figure</u>		<u>Page</u>
23.	Test NC-1M photographs.....	71
24.	Sequential photographs, Test NC-1M.....	72
25.	Test NC-2M photographs.....	73
26.	Sequential photographs, Test NC-2M.....	74
27.	Before and after photographs, Test T-6.....	75
28.	Sequential photographs, Test T-6.....	76
29.	Test T-1 photographs.....	78
30.	Sequential photographs, Test T-1.....	79
31.	Before and after photographs, Test T-7.....	80
32.	Sequential photographs, Test T-7.....	81
33.	Test T-2 photographs.....	83
34.	Sequential photographs, Test T-2.....	84
35.	Test T-3 photographs.....	85
36.	Sequential photographs, Test T-3.....	86
37.	Test WA-1 photographs.....	87
38.	Sequential photographs, Test WA-1.....	89
39.	Test WA-1M photographs.....	90
40.	Sequential photographs, Test WA-1M.....	91
41.	Test WA-2M photographs.....	92
42.	Sequential photographs, Test WA-2M.....	93
43.	Test WA-3M photographs.....	95
44.	Sequential photographs, Test WA-3M.....	96
45.	Sequential photographs, Test WA-4M.....	97

List of Figures (continued)

<u>Figure</u>		<u>Page</u>
46.	Test WA-4M photographs.....	98
47.	Test WA-5M photographs.....	100
48.	Sequential photographs, Test WA-5M.....	101
49.	Test NV-1 photographs.....	102
50.	Sequential photographs, Test NV-1.....	103
51.	Before and after photographs, Test IB-1.....	105
52.	Sequential photographs, Test IB-1.....	106
53.	Before and after photographs, Test TC-1.....	107
54.	Sequential photographs, Test TC-1.....	108
55.	Critical load case for an independent anchor block.....	110
56.	Idealized wall-force/time history.....	111
57.	Force-displacement behavior of a dynamically loaded guardrail post.....	113
58.	Seiler's lateral post soil pressure distribution.....	116
59.	Forces resisting yaw rotation.....	121
60.	Independent block analysis program.....	123
61.	Independent block analysis program sample input screen.....	127
62.	Independent block analysis program sample output.....	128
63.	Design curves for load cases nos. 1 and 2.....	129
64.	Design curves for the critical load case.....	130
65.	Safety shape parapet end consideration.....	135
66.	G4(2W) W-beam transition - tapered wingwall.....	138
67.	W-beam transition on tapered wingwall.....	139
68.	Tapered wingwall geometry - W-beam and thrie beam transitions	140

List of Figures (continued)

<u>Figure</u>		<u>Page</u>
69.	Tapered wingwall geometry for G4(1S) and G4(2W) systems.....	141
70.	Wingwall reinforcement drawings for both tapered and straight wingwalls.....	142
71.	W-beam transition/curved wingwall North Carolina State standards.....	143
72.	Modified North Carolina standard.....	146
73.	G4(2W) W-beam transition - straight wingwall.....	147
74.	G4(1S) W-beam transition - straight wingwall.....	148
75.	W-beam wingwall attachment details - straight wingwall.....	149
76.	G9 (wood post) thrie beam transition - tapered wingwall.....	150
77.	G9 (steel post) thrie beam transition - tapered wingwall.....	151
78.	Tapered wingwall details for G9 thrie beam transition.....	152
79.	G9 (steel post) transition - flat wingwall.....	153
80.	G9 (wood post) transition - flat wingwall.....	154
81.	Modified thrie beam transition - flat wingwall.....	155
82.	Intersecting roadway transition design.....	156
83.	Independent end block drawing.....	158
84.	Barrier construction details, tapered curb.....	160
85.	LA-1 test installation drawing.....	163
86.	WA-1 test installation drawing.....	164
87.	NV-1 test installation drawings.....	165

List of Figures (continued)

Volume 2: Guardrail - Bridge Rail Transition Designs

<u>Figure</u>		<u>Page</u>
1.	Test vehicle dimensions.....	2
2.	Dummies in test vehicle.....	4
3.	Data acquisition system.....	5
4.	Barrier and vehicle details, Test LA-1.....	11
5.	Summary of results, Test LA-1.....	12
6.	Barrier and vehicle damage, Test LA-1.....	13
7.	Barrier and vehicle details, Test LA-1M.....	18
8.	Summary of results, Test LA-1M.....	19
9.	Barrier and vehicle damage, Test LA-1M.....	20
10.	Barrier and vehicle details, Test T-5.....	26
11.	Summary of results, Test T-5.....	27
12.	Barrier and vehicle damage, Test T-5.....	40
13.	Vehicle accelerations, Test T-5.....	41
14.	Driver head accelerations, Test T-5.....	42
15.	Driver chest accelerations, Test T-5.....	43
16.	Driver femur loads, Test T-5.....	44
17.	Passenger head accelerations, Test T-5.....	45
18.	Passenger chest accelerations, Test T-5.....	46
19.	Passenger femur loads, Test T-5.....	47
20.	Barrier and vehicle details, Test NC-1.....	49
21.	Summary of results, Test NC-1.....	50
22.	Barrier and vehicle damage, Test NC-1.....	59

List of Figures (continued)

<u>Figure</u>		<u>Page</u>
23.	Vehicle accelerations, Test NC-1.....	60
24.	Driver head accelerations, Test NC-1.....	61
25.	Driver chest accelerations, Test NC-1.....	62
26.	Driver femur loads, Test NC-1.....	63
27.	Passenger head accelerations, Test NC-1.....	64
28.	Passenger chest accelerations, Test NC-1.....	65
29.	Passenger femur loads, Test NC-1.....	66
30.	Barrier and vehicle details, Test NC-1M.....	69
31.	Summary of results, Test NC-1M.....	70
32.	Barrier and vehicle damage, Test NC-1M.....	82
33.	Vehicle accelerations, Test NC-1M.....	83
34.	Driver head accelerations, Test NC-1M.....	84
35.	Driver chest accelerations, Test NC-1M.....	85
36.	Driver femur loads, Test NC-1M.....	86
37.	Passenger head accelerations, Test NC-1M.....	87
38.	Passenger chest accelerations, Test NC-1M.....	88
39.	Passenger femur loads, Test NC-1M.....	89
40.	Barrier and vehicle details, Test NC-2M.....	92
41.	Summary of results, Test NC-2M.....	93
42.	Barrier and vehicle damage, Test NC-2M.....	106
43.	Vehicle accelerations, Test NC-2M.....	107
44.	Driver head accelerations, Test NC-2M.....	108
45.	Driver chest accelerations, Test NC-2M.....	109

List of Figures (continued)

<u>Figure</u>		<u>Page</u>
46.	Driver femur loads, Test NC-2M.....	110
47.	Passenger head accelerations, Test NC-2M.....	111
48.	Passenger chest accelerations, Test NC-2M.....	112
49.	Passenger femur loads, Test NC-2M.....	113
50.	Barrier and vehicle details, Test T-6.....	116
51.	Summary of results, Test T-6.....	117
52.	Barrier and vehicle damage, Test T-6.....	129
53.	Vehicle accelerations, Test T-6.....	130
54.	Driver head accelerations, Test T-6.....	131
55.	Driver chest accelerations, Test T-6.....	132
56.	Driver femur loads, Test T-6.....	133
57.	Passenger chest accelerations, Test T-6.....	134
58.	Passenger femur loads, Test T-6.....	135
59.	Barrier and vehicle details, Test T-1.....	138
60.	Summary of results, Test T-1.....	139
61.	Barrier and vehicle damage, Test T-1.....	151
62.	Vehicle accelerations, Test T-1.....	152
63.	Driver head accelerations, Test T-1.....	153
64.	Driver chest accelerations, Test T-1.....	154
65.	Driver femur loads, Test T-1.....	155
66.	Passenger head accelerations, Test T-1.....	156
67.	Passenger chest accelerations, Test T-1.....	157
68.	Passenger femur loads, Test T-1.....	158

List of Figures (continued)

<u>Figure</u>		<u>Page</u>
69.	Barrier and vehicle details, Test T-7.....	161
70.	Summary of results, Test T-7.....	162
71.	Barrier and vehicle damage, Test T-7.....	174
72.	Vehicle accelerations, Test T-7.....	175
73.	Driver head accelerations, Test T-7.....	176
74.	Driver chest accelerations, Test T-7.....	177
75.	Driver femur loads, Test T-7.....	178
76.	Passenger head accelerations, Test T-7.....	179
77.	Passenger chest accelerations, Test T-7.....	180
78.	Passenger femur loads, Test T-7.....	181
79.	Barrier and vehicle details, Test T-2.....	184
80.	Summary of results, Test T-2.....	185
81.	Barrier and vehicle damage, Test T-2.....	197
82.	Vehicle accelerations, Test T-2.....	198
83.	Driver head accelerations, Test T-2.....	199
84.	Driver chest accelerations, Test T-2.....	200
85.	Driver femur loads, Test T-2.....	201
86.	Passenger head accelerations, Test T-2.....	202
87.	Passenger chest accelerations, Test T-2.....	203
88.	Passenger femur loads, Test T-2.....	204
89.	Barrier and vehicle details, Test T-3.....	207
90.	Summary of results, Test T-3.....	208
91.	Barrier and vehicle damage, Test T-3.....	220

List of Figures (continued)

<u>Figure</u>		<u>Page</u>
92.	Vehicle accelerations, Test T-3.....	221
93.	Driver head accelerations, Test T-3.....	222
94.	Driver chest accelerations, Test T-3.....	223
95.	Passenger head accelerations, Test T-3.....	224
96.	Passenger chest accelerations, Test T-3.....	225
97.	Passenger femur loads, Test T-3.....	226
98.	Barrier and vehicle details, Test WA-1.....	229
99.	Summary of results, Test WA-1.....	232
100.	Barrier and vehicle damage, Test WA-1.....	233
101.	Driver head accelerations, Test WA-1.....	234
102.	Driver chest accelerations, Test WA-1.....	235
103.	Driver femur loads, Test WA-1.....	236
104.	Barrier and vehicle details, Test WA-1M.....	238
105.	Summary of results, Test WA-1M.....	239
106.	Barrier and vehicle damage, Test WA-1M.....	241
107.	Barrier and vehicle details, Test WA-2M.....	246
108.	Summary of results, Test WA-2M.....	247
109.	Barrier and vehicle damage, Test WA-2M.....	248
110.	Vehicle accelerations, Test WA-2M.....	258
111.	Driver head accelerations, Test WA-2M.....	260
112.	Driver chest accelerations, Test WA-2M.....	262
113.	Driver femur loads, Test WA-2M.....	264
114.	Barrier and vehicle details, Test WA-3M.....	266

List of Figures (continued)

<u>Figure</u>		<u>Page</u>
115.	Summary of results, Test WA-3M.....	267
116.	Barrier and vehicle damage, Test WA-3M.....	269
117.	Barrier and vehicle details, Test WA-4M.....	274
118.	Summary of results, Test WA-4M.....	275
119.	Barrier and vehicle damage, Test WA-4M.....	292
120.	Vehicle accelerations, Test WA-4M.....	293
121.	Driver head accelerations, Test WA-4M.....	295
122.	Driver chest accelerations, Test WA-4M.....	297
123.	Passenger head accelerations, Test WA-4M.....	299
124.	Passenger chest accelerations, Test WA-4M.....	301
125.	Passenger femur loads, Test WA-4M.....	303
126.	Barrier and vehicle details, Test WA-5M.....	305
127.	Summary of results, Test WA-5M.....	306
128.	Barrier and vehicle damage, Test WA-5M.....	318
129.	Vehicle accelerations, Test WA-5M.....	319
130.	Driver head accelerations, Test WA-5M.....	320
131.	Driver chest accelerations, Test WA-5M.....	321
132.	Driver femur loads, Test WA-5M.....	322
133.	Passenger head accelerations, Test WA-5M.....	323
134.	Passenger chest accelerations, Test WA-5M.....	324
135.	Passenger femur loads, Test WA-5M.....	325
136.	Barrier and vehicle details, Test NV-1.....	328
137.	Summary of results, Test NV-1.....	329

List of Figures (continued)

<u>Figure</u>		<u>Page</u>
138.	Barrier and vehicle damage, Test NV-1.....	342
139.	Vehicle accelerations, Test NV-1.....	343
140.	Driver head accelerations, Test NV-1.....	344
141.	Driver chest accelerations, Test NV-1.....	345
142.	Driver femur loads, Test NV-1.....	346
143.	Passenger head accelerations, Test NV-1.....	347
144.	Passenger chest accelerations, Test NV-1.....	348
145.	Passenger femur loads, Test NV-1.....	349
146.	Barrier and vehicle details, Test IB-1.....	352
147.	Summary of results, Test IB-1.....	353
148.	Barrier and vehicle damage, Test IB-1.....	365
149.	Vehicle accelerations, Test IB-1.....	366
150.	Driver head accelerations, Test IB-1.....	367
151.	Driver chest accelerations, Test IB-1.....	368
152.	Driver femur loads, Test IB-1.....	369
153.	Passenger head accelerations, Test IB-1.....	370
154.	Passenger chest accelerations, Test IB-1.....	371
155.	Passenger femur loads, Test IB-1.....	372
156.	Barrier and vehicle details, Test TC-1.....	375
157.	Summary of results, Test TC-1.....	376
158.	Barrier and vehicle damage, Test TC-1.....	381

List of Tables

Volume 1: Guardrail - Bridge Rail Transition Designs

<u>Table</u>		<u>Page</u>
1.	Research tasks and specifications.....	8
2.	Summary of systems with lateral stiffness = G, wheel snagging = G.....	12
3.	Summary of systems with lateral stiffness = G, wheel snagging = F.....	13
4.	Summary of systems with lateral stiffness = G, wheel snagging = P.....	14
5.	Summary of systems with lateral stiffness = P, wheel snagging = P.....	15
6.	Suggested guardrail - bridge rail transitions for further analysis.....	17
7.	Summary of pendulum tests.....	21
8.	BARRIER VII/full-scale test comparisons.....	30
9.	Summary of BARRIER VII results.....	36
10.	BARRIER VII results.....	51
11.	Summary of W-beam/wingwall transition tests.....	56
12.	Summary of thrie beam/wingwall transition tests.....	57
13.	Summary of W-beam approach at intersecting roadways.....	58
14.	Summary of W-beam independent block and tapered curb tests...	59

List of Tables (continued)

Volume 2: Guardrail - Bridge Rail Transition Designs

<u>Table</u>		<u>Page</u>
1.	Data acquisition system components.....	6
2.	Data processing system components.....	7
3.	Film analysis data, Test LA-1.....	14
4.	Permanent barrier deflections, Test LA-1M.....	21
5.	Film analysis data, Test LA-1M.....	22
6.	Permanent barrier deflections, Test T-5.....	29
7.	Film analysis data, Test T-5.....	30
8.	Transducer data, Test T-5.....	34
9.	Permanent rail deflections, Test NC-1.....	52
10.	Transducer data, Test NC-1.....	53
11.	Permanent rail deflections, Test NC-1M.....	72
12.	Film analysis data, Test NC-1M.....	73
13.	Transducer data, Test NC-1M.....	76
14.	Permanent rail deflections, Test NC-2M.....	95
15.	Film analysis data, Test NC-2M.....	96
16.	Transducer data, Test NC-2M.....	100
17.	Permanent barrier deflections, Test T-6.....	119
18.	Film analysis data, Test T-6.....	120
19.	Transducer data, Test T-6.....	123
20.	Permanent barrier deflections, Test T-1.....	141
21.	Film analysis data, Test T-1.....	142
22.	Transducer data, Test T-1.....	145

List of Tables (continued)

<u>Table</u>		<u>Page</u>
23.	Permanent barrier deflections, Test T-7.....	164
24.	Film analysis data, Test T-7.....	165
25.	Transducer data, Test T-7.....	168
26.	Permanent barrier deflections, Test T-2.....	187
27.	Film analysis data, Test T-2.....	188
28.	Transducer data, Test T-2.....	191
29.	Permanent barrier deflections, Test T-3.....	210
30.	Film analysis data, Test T-3.....	211
31.	Transducer data, Test T-3.....	214
32.	Driver dummy transducer data, Test WA-1.....	230
33.	Film analysis data, Test WA-1M.....	242
34.	Film analysis data, Test WA-2M.....	249
35.	Transducer data, Test WA-2M.....	251
36.	Film analysis data, Test WA-3M.....	270
37.	Film analysis data, Test WA-4M.....	277
38.	Transducer data, Test WA-4M.....	280
39.	Film analysis data, Test WA-5M.....	308
40.	Transducer data, Test WA-5M.....	311
41.	Permanent barrier deflections, Test NV-1.....	331
42.	Film analysis data, Test NV-1.....	332
43.	Transducer data, Test NV-1.....	336
44.	Permanent barrier deflections, Test IB-1.....	355
45.	Film analysis data, Test IB-1.....	356

List of Tables (continued)

<u>Table</u>		<u>Page</u>
46.	Transducer data, Test IB-1.....	359
47.	Permanent barrier deflections, Test TC-1.....	378
48.	Film analysis data, Test TC-1.....	379

Volume 3: Guardrail - Bridge Rail Transition Designs

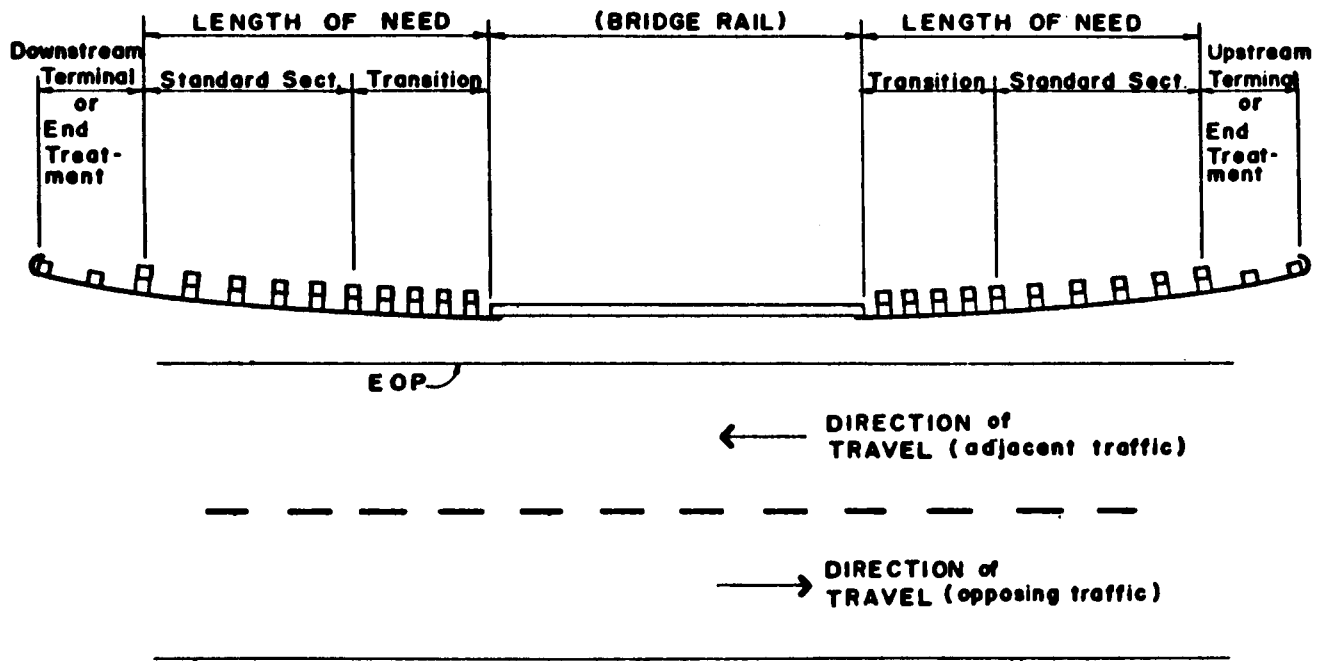
1.	State transition ratings.....	2
2.	Guardrail-bridge rail transition rating criteria.....	13
3.	Unit costs for transition elements.....	17
4.	Pertinent State comments concerning guardrail-bridge rail transitions.....	19

1. Introduction and Research Approach

a. Statement of the Problem

The 1981 Highway Safety Stewardship Report of the Secretary of Transportation to the United States Congress estimated that in 1979 about 1,390 persons were killed in 1,250 fatal accidents involving bridge ends or approach guardrail. It was further estimated that 50 percent of guardrail accidents occur at bridge approaches and that about 50 percent of bridge accidents involve bridge ends. A recent SwRI study shows that impacts involving bridge ends were by far the most severe with 29.8 percent resulting in fatal or incapacitating injuries.⁽¹⁾ Guardrail/median barrier collisions were the least severe with 9.5 percent. Thus, the severity of accidents at many of the relatively old bridges that have unprotected ends could be significantly reduced by installing approach guardrails that are properly transitioned and effectively anchored to the existing bridge rails. Other situations exist where (1) approach guardrails are installed but not properly anchored or attached to the bridge; and (2) bridge railings do not meet current standards and should be replaced with guardrails continuing across the full length of the bridge.

As shown in figure 1, the transition between the approach guardrail and the bridge end is only one part of a barrier system that protects motorists as they approach, cross, and leave a bridge. Since the bridge railing, the transition and approach guardrail, and the bridge end drainage systems are usually designed by different groups of people at different times, the designs are sometimes not well integrated. Consequently, guardrail posts may have to be offset or relocated to accommodate curbs or drainage inlets. A drainage design that does not interfere with the approach guardrail post spacing is shown in figure 2. However, the curb shown in the figure is a potential problem. Many of the older bridge railings have "brush curbs" which must be flared or treated as shown in figure 3. The flare rates of the approach guardrail and the transition zone must also be compatible. The ideal situation would be to have a good transition



2

Figure 1. Definition of roadside barrier elements.

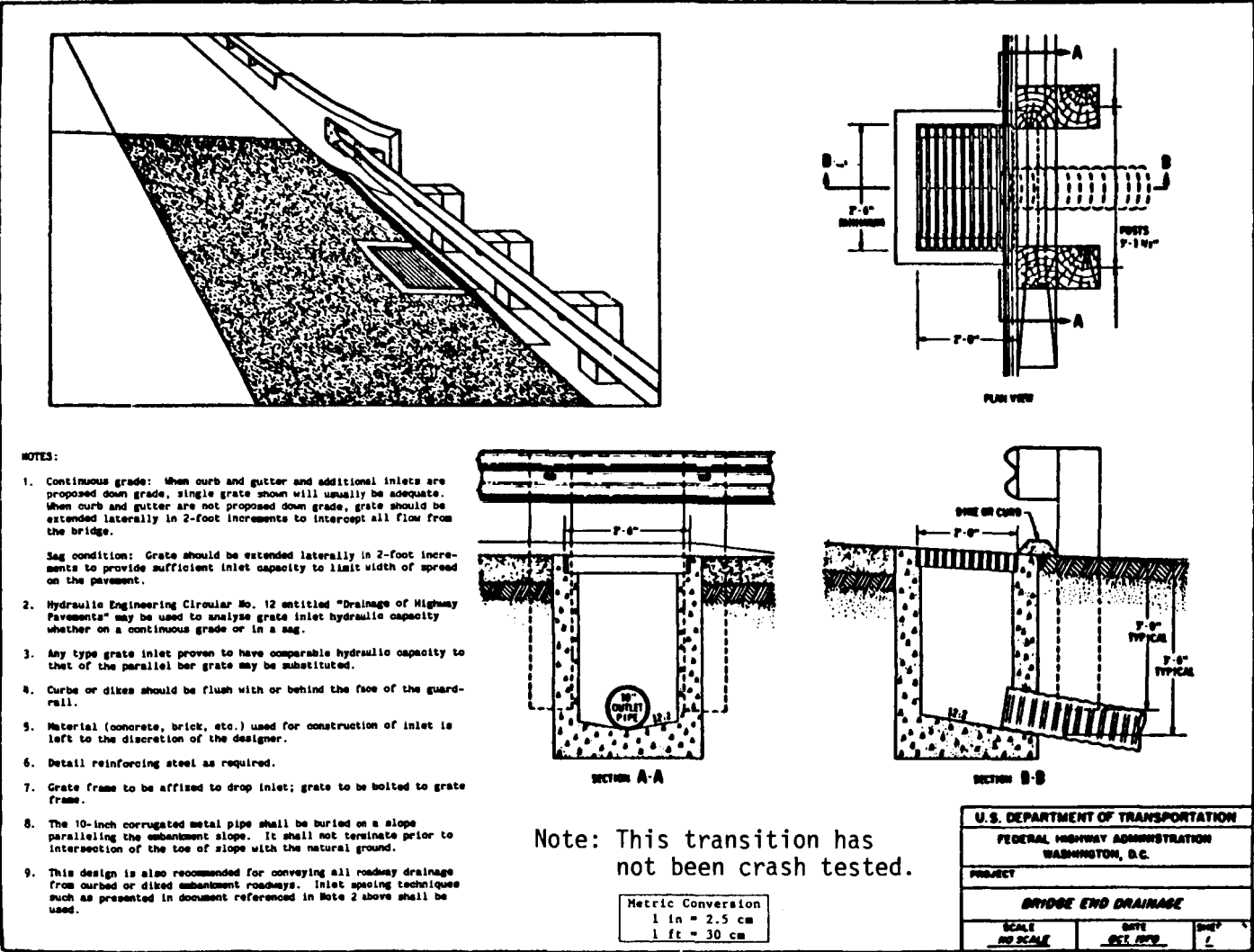


Figure 2. Bridge end drainage.

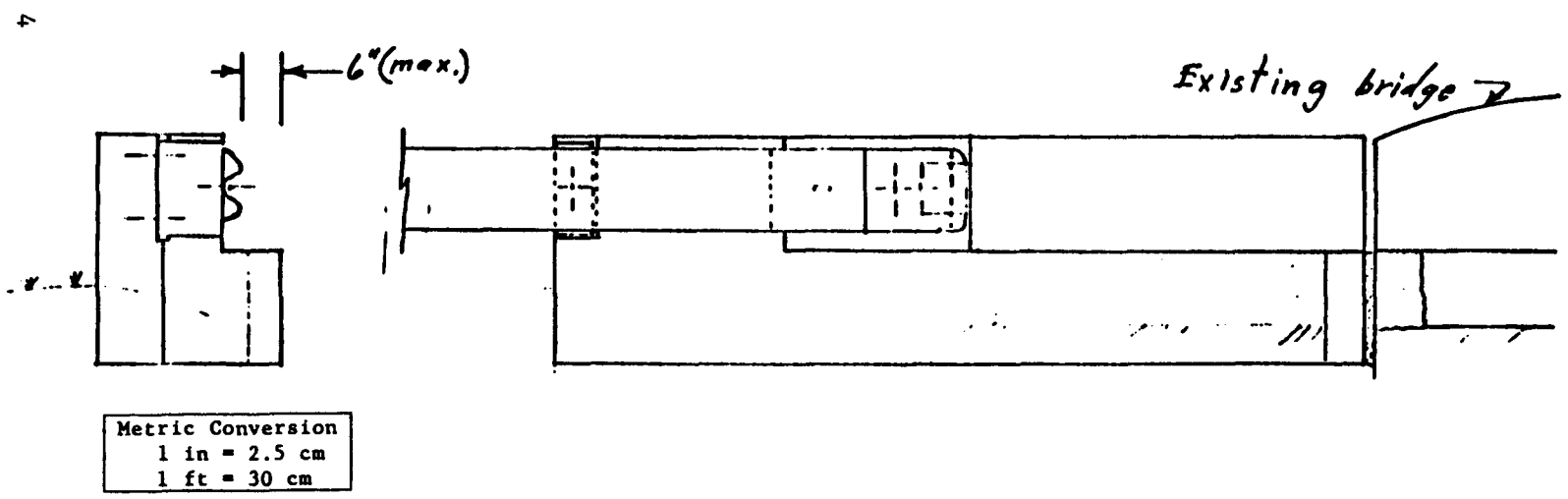
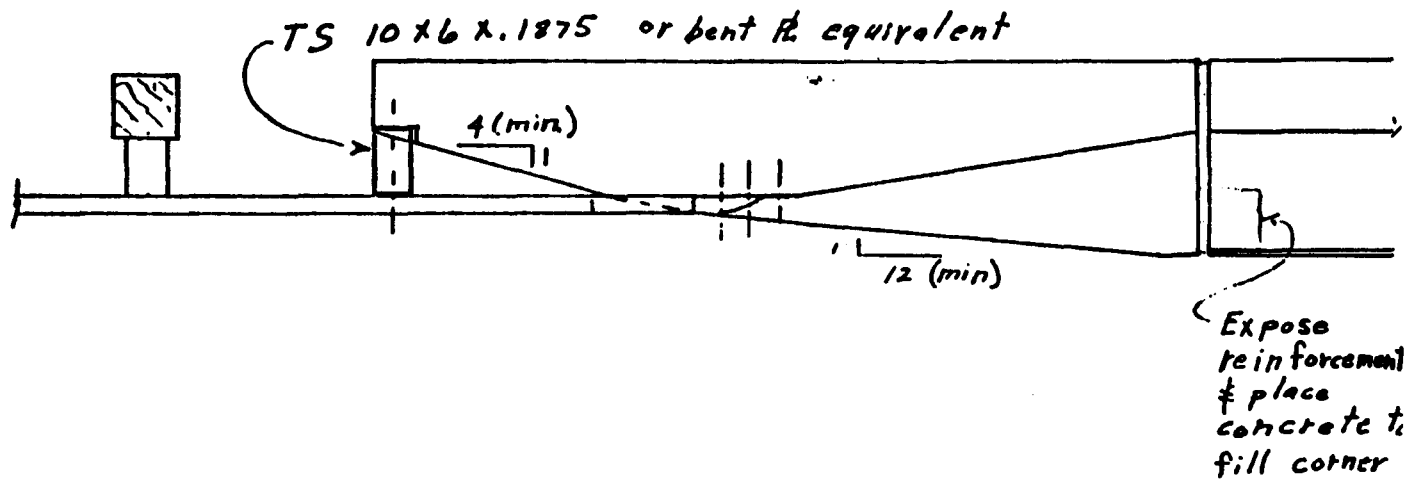


Figure 3. Bridge end adapter block for guardrail attachment.

that is reasonable in price but versatile enough so that it can be used for many different bridge ends.

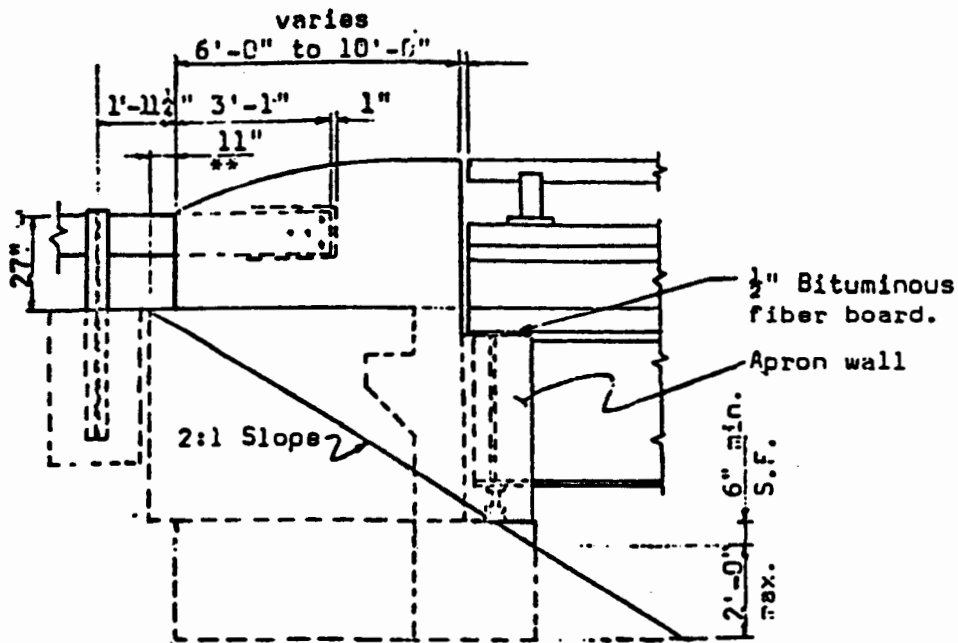
A few States have made the transition directly from a metal bridge rail to the approach guardrail. However, because there is usually an expansion joint at the end of the bridge, the approach guardrail is usually anchored to a concrete end block with an end shoe as shown in figure 3. Some problems with the end shoe bolts pulling out of the concrete have been reported. The concrete end block may either be an independent block set on the approach embankment as shown in figure 3, or it may be integral with the abutment as shown in figure 4.

At the beginning of this project, only a few crash tests had been conducted on guardrail-bridge rail transitions. Most of the tests were at 60 mph (95 km/h) and 25 degrees with standard-size sedans weighing between 3,500 (1600 kg) and 4,500 lbs (2000 kg), and some wheel snagging problems had been observed. Thus, a need existed to develop design guidelines, evaluate current designs, and develop transitions and approach guardrail systems that could be used for safety treatment at bridges.

b. Objectives and Scope

As indicated in the Statement of Work, the objectives of this study were the following:

1. To develop design guidelines for transitions and approach guardrails.
2. To test and evaluate current transition designs.
3. To design, test, and develop transitions and approach guardrail systems that can be used for safety treatment or upgrading of old bridges.



Metric Conversion	
1 in	= 2.5 cm
1 ft	= 30 cm

Figure 4. End block that is integral part of abutment.

The stated scope of work was as follows:

This requirement shall consist of reviewing the current transition and approach guardrail designs and guidelines, computer simulation and analysis of designs, making cost estimates, static and pendulum tests of barrier components, full-scale tests of transitions and approach guardrail systems, development of design guidelines and preparation of standard design drawings.

c. Research Approach and Report Organization

This project was composed of six major research tasks. These tasks, along with their corresponding specifications taken from the Statement of Work, are shown in table 1.

The review of current guardrail-bridge rail transition designs (Task A) is discussed in chapter 2. Also discussed in this chapter are the pendulum tests (Task B) required for inputs of the BARRIER VII computer program that was used for analysis purposes. Finally, details of the rating and selection process for candidate transition designs (Task C) are discussed. The final transition configurations are shown in appendix A. Ratings of the various State designs are included in appendix C.

Summaries of the 20 full-scale crash tests conducted (Task D) are given in chapter 3. Test reports are included in appendix B. Details of the independent block design (Task E) are discussed in chapter 4.

Finally, conclusions, recommendations, and design guidelines (Task F) resulting from the study are presented in chapter 5.

Table 1. Research tasks and specifications.

Task A. Review of Current Designs

1. Make a thorough review of the guardrail-bridge rail transition designs and guidelines shown in the 1977 AASHTO Barrier Guide and in the State Standard Plans that will be loaned to the contractor by FHWA. Identify potential safety shortcomings and opportunities for improving performance and reducing costs. Classify transition situations in a logical scheme (e.g., by type of bridge rail and approach guardrail). For each situation, identify the best and most cost-effective transitions and bridge end treatments.
2. Recommend: potential improvements in the selected existing designs, concepts to solve any major problems noted in this review, and designs or concepts for correction of the approaches to old bridges that should be evaluated analytically in Task C or experimentally in Tasks B and C.

NOTES:

A. Any shortcomings of the existing designs that are revealed during this state-of-the art review shall be brought to the immediate attention of the Contracting Officer's Technical Representative (COTR) by telephone.

B. Contracts with States to obtain data and information shall be arranged through the COTR.

TECHNICAL GUIDELINE

Unit cost information on guardrail-bridge rail transitions is not available from most States because the transition is not usually a separate bid item.

Task B. Laboratory Tests of Components

Make static pullout and bending tests of end shoes and pendulum tests of guardrail posts. (As a minimum, 20 static tests and 12 pendulum tests shall be conducted.)

NOTE: Should the contractor conclude that some of the funds allocated to this task would be best spent on additional full-scale testing in Task D, then the contractor shall notify the COTR. On approval of the contracting officer, this level of effort will be transferred to Task D.

Task C. Analysis and Preliminary Design

1. On approval of the COTR of the systems recommended in Task A-2, use computer simulation and other analytical tools to evaluate existing transition designs and to provide an analytical basis for designing the approach guardrail and transition sections for safety treating the ends of old bridges that will be full-scale tested in Task D.
2. After consulting with the COTR, prepare detailed designs and preliminary drawings of the approach guardrail and transition sections to be tested in Task D. Submit the drawings to the contracting officer for approval. (See Article II - Reports).

Table 1. Research tasks and specifications (continued).

NOTE: Should the contractor conclude that some of the funds allocated to this task would be best spent on additional laboratory tests of components in Task B, on full-scale testing in Task D, or on development of design guidelines in Task F, then the contractor shall notify the COTR. On approval of the contracting officer, this level of effort may be transferred to Task B, Task D, or Task F, as appropriate.

Task D. Full-Scale Tests

Conduct up to 12 full-scale tests with 4,500 lb sedans and 1,800 lb mini-compact sedans in order to evaluate selected existing transition, end block and approach guardrail designs, and to test and develop approach guardrail and transition designs for safety upgrading of the ends of old bridges. Furnish and install all of the necessary appurtenances to construct complete test layouts for testing at the contractor's test site and furnish and prepare all test vehicles, vehicle guidance systems, propulsion systems, instrumentation, personnel, film, and photographic equipment.

TECHNICAL REQUIREMENTS

1. Test procedures, test instrumentation, evaluation of the full-scale test results and the report contents shall be in accordance with the guidelines in National Cooperative Highway Research Program (NCHRP) Report No. 230. (2) These procedures may be modified by the contractor when test conditions dictate, provided the deviations are approved by the COTR. The vehicle maximum 50 msec accelerations, and the changes in vehicle velocity and momentum shall also be reported. Data shall be recorded in analog form on oscillographic records and magnetic tape. A fully-instrumented 50-th percentile male anthropometric dummy, restrained with lap and shoulder belts, shall be placed in the driver's seat and in the right front seat of each test vehicle. An onboard camera shall be used to record the motions of the dummies. Documentary real-time films shall be made to show the actual work involved in constructing the approach guardrail and transition at the test site. High-speed and real-time films, slides, and still photographs shall be made of each test.
2. The full-scale test data shall be digitized in accordance with the SAE-J211, Class 1000 specification and a magnetic data tape shall be prepared as specified in NHTSA's "Dynamic Crash Test Information Reference Guide" (3).
3. In order to measure the vehicle crush depth, a minimum of six measurements shall be made before and after each full-scale test. The depth measurement points shall be equally spaced along the length of the damaged area in order to generally describe the damage penetration profile. The maximum static crush distance (damage penetration) shall also be measured and reported, regardless of its location. End, top and lateral view photographs shall be taken of the full length of each damaged vehicle. The vehicle trajectory after impact shall also be measured and reported.

Table 1. Research tasks and specifications (continued).

NOTES:

A. Should the research findings indicate that specific sign details should be changed, or indicate a need for additional analysis and/or laboratory testing, the contractor shall promptly notify the COTR and on approval of the contracting officer, this level of effort may be transferred to Tasks B, C, or E, as appropriate.

B. For budget estimating purposes, assume that the 1,800 lb vehicle will be a 1980 or later a model Honda Civic sedan and that five vehicles will be needed. Assume that the 4,500 sedan will be a 1980 or later model and that seven vehicles will have to be purchased under the contract.

C. The test facilities must be flexible enough to accommodate the 60 mph impacts with 4,500 lb vehicles at 15 or 25 degrees, and to accommodate 60 mph impacts with 1,800 lb vehicles at 15 or 20 degrees at selected points along the test barrier.

Task E. Design of Independent Block

In order to provide guidance for designing a concrete block "dead man," determine the required mass, foundation, and other key parameters required to insure its proper functioning on an approach embankment.

Task F. Develop Design Guidelines

1. Develop design guidelines for transitions and approach guardrail that also address the problems at bridge piers and retaining wall ends. The design guidelines shall address the problems of curbs and drainage control at the bridge end, and provide answers to questions such as the following: How fast should the barrier be flared in the transition zone? How should bridge rail "brush curbs" be flared or treated? How fast should we change the barrier stiffness in the transition zone and what are the efficient ways (e.g., changing the post spacing or the rail stiffness) of doing it?
2. Prepare detailed drawings of the recommended transitions and treatments for bridge ends.

NOTES:

A. The work to be performed in developing design guidelines shall include, but not be limited to, providing design solutions to the questions and problems listed above. It is expected that the results of the laboratory and full-scale tests will raise questions that will also require design guidance.

B. The contractor shall carefully document the basis for the design decisions and discuss all assumptions so that they can be readily re-evaluated in the light of future experience or changed conditions.

C. The drawings and design guidelines shall be prepared in such a form that Texas Transportation Institute can readily incorporate the material into the "Road-side Safety Technology Text and Guide" publications that will be prepared under contract DTFH61-82-C-00088.

2. Current Designs

a. Review of State Current Designs

In order to evaluate current designs and select candidate systems, State Standard Plans for guardrail-bridge rail transitions were provided by FHWA at the start of the contract. These standards were reviewed and the various systems evaluated. A tabular form was developed by which the transitions could be concisely rated by a number of pertinent factors. In order to maintain consistency in the ratings, criteria were developed that would be adequate for most of the cases encountered. These criteria, along with the ratings of the various State transitions, are included in appendix C.

A general review of the transitions in appendix C showed that most of the States use a G4 type of approach guardrail with Michigan end shoe connections to bridge concrete parapets or safety shapes. Practically all use reduced post spacing in the transition with many also using heavier posts. However, the bridge end-to-first-post space varies considerably from less than a foot to the usual 3 ft-1 1/2 in (0.9 m). An optimum space for this first post would be desirable. Several States use regular flared W-beam end sections (rather than the Michigan shoe) that are anchored to the concrete parapet through block-outs. Strengths of connections, particularly those with block-outs, needed to be checked. Several States also use nested rails, which may or may not be a cost-effective measure. Finally, the greatest discrepancy between States concerned the trailing transitions. Requirements varied from no guardrail to those with regular post spacing to those of the same stiffened type used on the approach. Ample evidence thus existed that transition standards were indeed needed.

The various transition ratings shown in appendix C were summarized, and the results are shown in tables 2 through 5. As shown in table 2, only nine of the systems rated good in both lateral stiffness and wheel snagging. Table 3 shows the 12 systems with good lateral stiffness and

Table 2. Summary of systems with lateral stiffness = G, wheel snagging = G.

Bridge Rail End Type	Approach Railing					Other
	G4W	G4S	G4W,S	G4C,W,S	G3	
1. Parapet						
Straight	1					1 G9
Tapered/Curved			1			1 G9
2. Curb Parapet						
Straight	1					
Tapered/Curved		1				
3. Safety Shape						
Straight	1		1			
Tapered/Curved						
4. Steel Rigid						
5. Steel Semi-Rigid						1 Tubular Thrie
6. Aluminum Rigid						
7. Aluminum Semi-Rigid						

Total = 9

Table 3. Summary of systems with lateral stiffness = G, wheel snagging = F.

Bridge Rail End Type	Approach Railing					
	G4W	G4S	G4W,S	G4C,W,S	G3	Other
1. Parapet						
Straight	1			1		
Tapered/Curved	1					
2. Curb Parapet						
Straight	1			2		
Tapered/Curved						
3. Safety Shape						
Straight	1	2				
Tapered/Curved						
4. Steel Rigid			1			
5. Steel Semi-Rigid						1 G9, 1 Tubular Thrie
6. Aluminum Rigid						
7. Aluminum Semi-Rigid						

Total = 12

Table 4. Summary of systems with lateral stiffness = G, wheel snagging = P.

Bridge Rail End Type	Approach Railing					Other
	G4W	G4S	G4W,S	G4C,W,S	G3	
1. Parapet						
Straight	7	1		1		
Tapered/Curved						
2. Curb Parapet						
Straight	6	1	1	1		
Tapered/Curved						
3. Safety Shape						
Straight	2		1			
Tapered/Curved						
4. Steel Rigid						
5. Steel Semi-Rigid						
6. Aluminum Rigid	1					
7. Aluminum Semi-Rigid						

Total = 22

Table 5. Summary of systems with lateral stiffnes = P, wheel snagging = P.

Bridge Rail End Type	Approach Railing					Other
	G4W	G4S	G4W,S	G4C,W,S	G3	
1. Parapet						
Straight	2	2		1		2 GR2, 1 G4U
Tapered/Curved	1					1 GE3
2. Curb Parapet						
Straight	6	2	7	2		
Tapered/Curved						
15 3. Safety Shape						
Straight	3	5	2	1	3	1 GE3
Tapered/Curved						
4. Steel Rigid					3	
5. Steel Semi-Rigid	6	2	1			6 GR2
6. Aluminum Rigid		1				2 GE3
7. Aluminum Semi-Rigid						

Total = 63

fair wheel snagging. As indicated by the criteria of appendix C, such systems could be upgraded with a change in connection (flush to blocked) or addition of a rub rail. The 22 systems in table 4 (good lateral stiffness and poor wheel snagging) would require both the change in connection and the addition of a rub rail. Finally, the 63 systems of table 5 are those with poor ratings in both lateral stiffness and wheel snagging.

b. Selection of Candidate Transition Systems

Based on the larger number groupings of tables 2 through 5, typical configurations were selected and suggested for subsequent analysis and full-scale testing. These configurations, along with some of the expected spin-off benefits to be determined by this subsequent work, are shown in table 6. The suggested systems included the heavy post, reduced spacing configuration, standard posts with reduced spacing that are used by several of the States, and the two- or three-bridge rail transitions to box beam or W-beam guardrails that currently appear to rate poorly. The need for strengthening by reduced post spacing on trailing transitions was not apparent. Elimination of interfering curbs, block-out of connections to parapets, and the addition of rub rails appeared to be retrofits that would be suggested.

In consultation with the FHWA COTR, the final transition selections were made. Included in the final analyses were the following selected configurations and other systems that were added subsequent to this selection process:

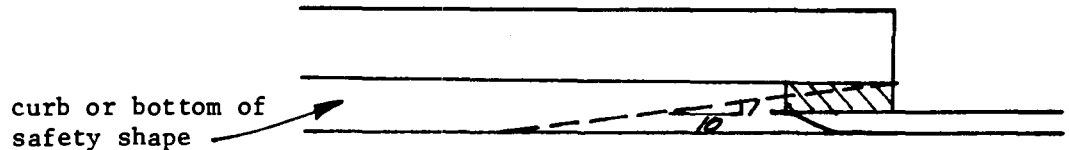
- North Carolina Type VIII System (number 1 in table 6).
- Nevada System (number 2 in table 6).
- Louisiana System (number 6 in table 6).
- Washington Bridge Approach Design (added by contract modification to check the 90-degree curved approach guardrail designed by Washington).

Table 6. Suggested guardrail - bridge rail transitions for further analysis.

1. North Carolina VIII - Rate GG - 9 standard G4S posts with tapered wingwall - not a common installation but shows extreme reduced spacing with standard G4S posts.
2. Nevada - Rate GG - 7 post G4W with straight safety shape - 3 10 in x 10 in and 4 6 in x 8 in posts - W beam laps safety shape with block-outs (37.5-ft length) - Common installation.

Questions:

- a. Are 6 in x 8 in posts satisfactory or are 8 in x 8 in posts necessary?
- b. Is 12 ft-6 in bent lap necessary or can it end at parapet end? The bend may be necessary with 2-way traffic but why not use flush connection with standard guardrail on 1-way exits?
- c. Safety shapes and curb/parapets offer same problem for wheel snagging at base. How about 10:1 taper on these?



3. Repeat System 2 with G4S system (3 W6x15.5 and 4 W6x8.5 posts).
4. Check system with GF rating and straight curb parapet (North Dakota Type IV). System has a rub rail but mounts flush with the bridge rail.
5. Check system with GP rating and straight parapet (Montana Type 2). This system can be used to check the effect of 12 in x 12 in posts on lateral strength and also the effect of a metal box blockout on connection strength.

Metric Conversion	
1 in	= 2.5 cm
1 ft	= 30 cm

Table 6. Suggested guardrail - bridge rail transitions for further analysis (continued).

6. Louisiana - Rate PP - G4W and G4S systems with 8 6 in x 8 in wood and W6x8.5 standard posts - Fairly common, but most omit the last post for 7-post system, and several use nested rails.

Questions:

- a. Is 7-post system o.k.?
 - b. Should 8 in x 8 in posts be used?
 - c. What is benefit of nested rail?
 - d. Can system be improved with addition of 1 or 2 posts at 1 ft-6 3/4 in positions (see System 1 above)?
7. Check system with PP rating and straight curb parapet (Ohio Types D and E). This system can be used to check the use of fewer posts with concrete footings.
 8. Should look at a system with sidewalks or wide curbs to eliminate the twisted configuration (see Georgia 5 or Kentucky C) and replace it with continuous W beam running across bridge. Check anchor block retrofit of Iowa Type RE-28. This will also provide a check on the use of inserts for the connection. Also check Texas Traffic Rail Type T6 (tubular W beam) for retrofit to knock out curbing and extend railing across bridge.
 9. Look at non-blocked out systems of steel semi-rigid to W beam (see Vermont and Texas). Systems rate PP and may require major upgrade. Eliminate Vermont because of 10 in granite curb. Use Texas Traffic Rail Type 301 (2-rail box beam) to W beam transition.
 10. Check wingwall design with Texas Traffic Rail Type T5. This is one of the thinner safety shape rails (top width of 7 1/2 in) with a flush Michigan shoe connection.

Metric Conversion
1 in = 2.5 cm
1 ft = 30 cm

- Thrie Beam System (added by contract modification to develop a new thrie beam transition).

On selection of these systems, it was necessary to contact the involved States to obtain information that was not available on the Standard Plans. Needed were typical construction details (geometry, steel reinforcement, and concrete strength for wingwalls, end bridge posts, etc.).

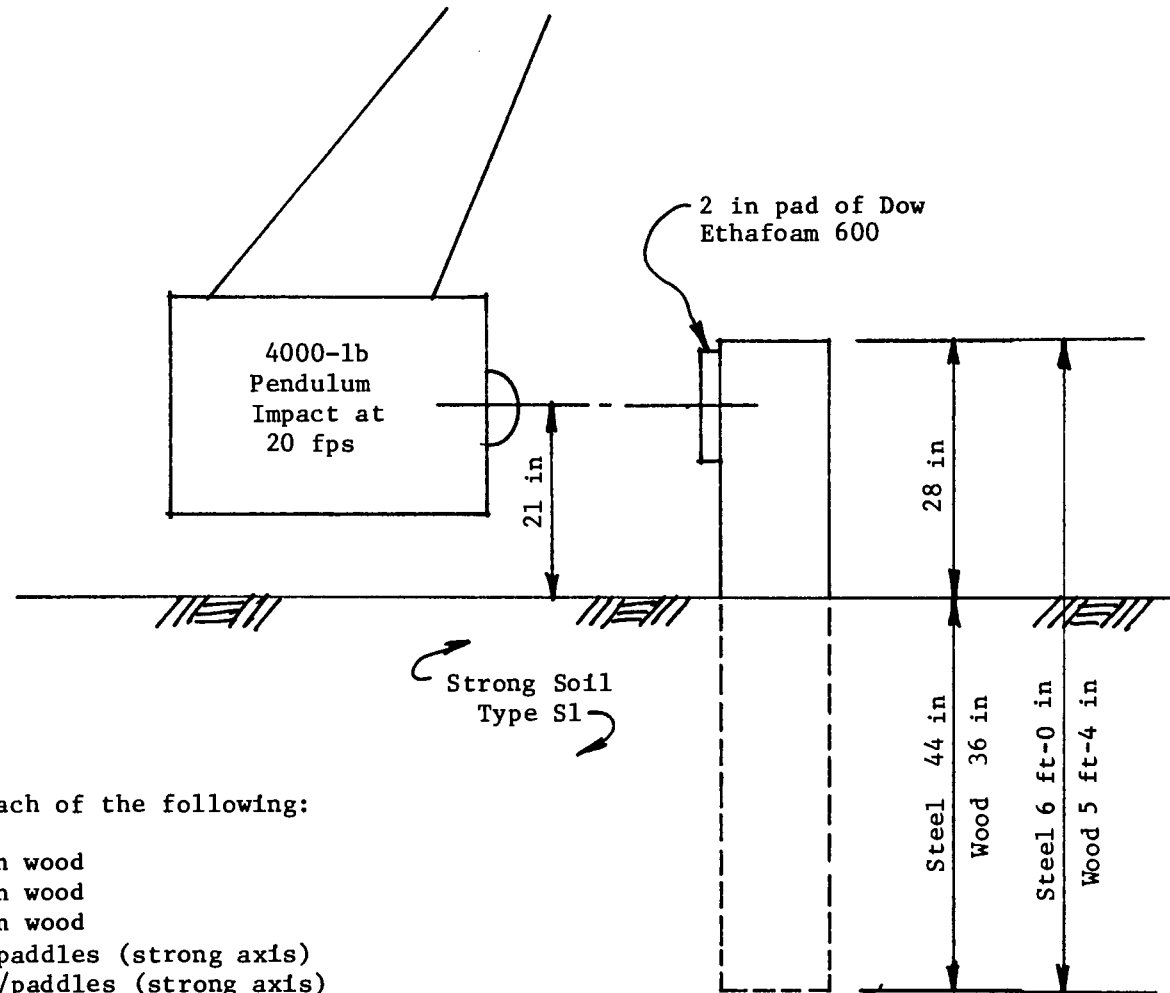
For the systems listed above, 14 full-scale crash tests were conducted on the original designs and upgrading retrofits. The final test installation configurations are shown in appendix A. Crash tests are summarized in chapter 3, and test reports are included in appendix B.

c. Component Testing

The BARRIER VII computer simulation was used for guidance in selecting test conditions for the various transition configurations. With the larger posts (12-in x 12-in (30-cm x 30-cm), 10-in x 10-in (25-cm x 25-cm), and 8-in x 8-in (20-cm x 20-cm) wood and W6x15.5 steel) used in some of the systems, it was necessary to conduct pendulum tests for determination of post properties for the BARRIER VII inputs. Test details and the test matrix are shown in figure 5.

A summary of results for the 12 pendulum tests is shown in table 7. Also shown in the table are expanded results of pendulum tests conducted in a previous SwRI study for cost-effectiveness selection of guardrails.⁽²⁾ The reason for including these will be discussed shortly.

Two important and rather surprising results can be seen from table 7. The first is that the 18-in x 24-in (46-cm x 61-cm) soil paddle used on the W6x15.5 posts apparently does little to increase either the stiffness or maximum force. The second is that the W6x15.5 posts without soil paddle are only slightly less stiff than the 10-in x 10-in (25-cm x 25-cm) wood posts (2.28 vs 2.55) but yield greater maximum force (18.3 vs



Conduct 2 tests of each of the following:

- (1) 12 in x 12 in wood
- (2) 10 in x 10 in wood
- (3) 8 in x 8 in wood
- (4) W6 x 15.5 w/paddles (strong axis)
- (5) W6 x 15.5 wo/paddles (strong axis)
- (6) W6 x 15.5 (weak axis)

<p>Metric Conversion 1 in = 2.5 cm 1 ft = 30 cm</p>

Figure 5. Post property tests.

Table 7. Summary of pendulum tests.

Test No.	Maximum Force (kips)	Time t_1 (ms)	Distance d_1 (in)	Stiffness (k/in)	Total Impulse (lb-sec)	Time t_2^* (ms)	Distance d_2 (in)	Remarks
12 in x 12 in Wood Posts								
1P12	20.7	32	7.32		2273.8	116	18.62	Soil Yield
1P12-R	23.8	25	5.76		2271.2	98	15.67	Soil Yield
Averages	22.3		6.54	3.41			17.15	
10 in x 10 in Wood Posts								
1P10	16.3	30	6.84		1544.2	100	18.12	Soil Yield
2P10	16.4	26	6.00		913.2	59	12.31	Post Fracture
Averages	16.4		6.42	2.55			18.12	
8 in x 8 in Wood Posts								
2P8	13.2	30	6.96		1287.3	103	19.75	Soil Yield
1P8-R	11.6	34	7.92		1091.0	101	20.42	Soil Yield
Averages	12.4		7.44	1.67			20.07	
W6x15.5 (Strong Axis with Soil Paddles)								
1SP-S	20.4	34	7.80		2475	128	19.42	Soil Yield
2SP-S	18.3	37	8.40		2450	142	21.10	Soil Yield
Averages	19.4		8.10	2.40			20.26	
W6x15.5 (Strong Axis without Soil Paddles)								
1SP-SA	19.2	35	8.16		2637	145	21.36	Soil Yield
2SP-SA	17.3	34	7.92		2215	135	21.84	Soil Yield
Averages	18.3		8.04	2.28			21.60	

Unused Tests:

2P12 Soil was too wet

1P8 Post fractured through opposite knots

$$* t_2 = \frac{I_{total}}{F} + \frac{t_1}{2} - 10$$

Metric Conversion
1 in = 2.5 cm
1 ft = 30 cm

Table 7. Summary of pendulum tests (continued).

Test No.	Maximum Force (kips)	Time t_1 (ms)	Distance d_1 (in)	Stiffness (k/in)	Total Impulse (lb-sec)	Time t_2^* (ms)	Distance d_2 (in)	Remarks
W6x15.5 (Weak Axis)								
1SP-WA	10.8	32	7.56		1740	167	29.28	Post Yield
2SP-WA	10.5	38	8.88		1717	173	30.36	Post Yield
Averages	10.7		8.22	1.30			29.82	
W6x8.5 (Weak Axis)†								
F-82	4.8	15	3.59		279.7	56	13.00	Post Yield
F-85	4.1	15	3.64		242.5	57	13.45	Post Yield
F-90	5.1	18	4.36		287.0	55	12.94	Post Yield
F-94	4.3	18	4.36		283.6	65	15.20	Post Yield
Averages	4.6		3.99	1.15			13.65	
W6x8.5 (Strong Axis)†								
F-81	12.7	17	4.06		571.7	44	9.95	Soil Yield
F-86	12.7	21	5.00		879.4	70	14.84	Soil Yield
F-89	10.2	15	3.65		499.6	46	10.67	Soil Yield
F-93	8.3	22	5.22		667.3	81	17.38	Soil Yield
Averages	11.0		4.48	2.46			13.21	
6 in x 8 in Wood Posts (Weak Axis) †								
F-83	11.2	22	5.19		154.1			Post Fracture
F-87	6.5	19	4.52		102.7			Post Fracture
F-91	8.0	22	5.32		606.6	77	17.09	Soil Yield
F-96	11.1	16	3.81		186.4			Post Fracture
Averages	9.2		4.71	1.95			No Plasticity	

$$* t_2 = \frac{I_{total}}{F} + \frac{t_1}{2} - 10$$

Metric Conversion
1 in = 2.5 cm
1 ft = 30 cm

† See "Development of a Cost-Effectiveness Model for Guardrail Selection," Report No. FHWA-RD-78-74, Appendix H, January 1980.

Table 7. Summary of pendulum tests (continued).

Test No.	Maximum Force (kips)	Time t_1 (ms)	Distance d_1 (in)	Stiffness (k/in)	Total Impulse (lb-sec)	Time t_2^* (ms)	Distance d_2 (in)	Remarks
6 in x 8 in Wood Posts (Strong Axis) †								
F-84	11.7	25	5.88		698.7	62	13.50	Soil Yield
F-88A	6.4	24	5.74		513.5	82	18.20	Soil Yield
F-92	7.3	19	4.63		528.5	72	16.34	Soil Yield
F-95	7.2	20	4.78		436.9	61	13.82	Soil Yield
Averages	8.2		5.26	1.56			15.47	

$$* t_2 = \frac{I_{\text{total}}}{F} + \frac{t_1}{2} - 10$$

† See "Development of a Cost Effectiveness Model for Guardrail Selection," Report No. FHWA-RD-78-84, Appendix H, January 1980.

<p>Metric Conversion 1 in = 2.5 cm 1 ft = 30 cm</p>

16.4). This contradicts the lateral stiffness rating criterion that was used in the original selection process (see table 50 in appendix C). Apparently, W6x15.5 posts are as good as the 10-in x 10-in (25-cm x 25-cm) wood posts without concrete footings or soil paddles.

As the pendulum test results became available and were inspected, it became apparent particularly with these larger posts that extrapolations of previous elastic results were not adequate. Figure 6 shows an example of a former pendulum test. The unload curve over 20 ms is the way BARRIER VII unloads when a post fails (10 time steps of 2 ms each). On comparing this figure with the W6x15.5 w/paddle test in figure 7, it can be seen that much reserve strength remains after the maximum load has been reached when these strong posts yield the soil. Thus, it was decided that the posts should be modeled with the elastic-plastic response shown by the dashed line of figure 7. The plastic response continues until the area under the curve equals the total measured impulse, as shown by the equation.

Test results of the previous SwRI study for guardrail selection were retrieved and expanded for this elastic-plastic response.⁽²⁾ Shown in table 7 are the results for W6x8.5 and 6-in x 8-in (15-cm x 20-cm) wood posts. Note that plastic action occurs for all posts except the weak axis of the 6-in x 8-in (15-cm x 20-cm) wood posts. As shown in the table, anomalous plastic response was eliminated for Test F-91 of the 6-in x 8-in (15-cm x 20-cm) wood post weak axis and for Test 2P10 of the 10-in x 10-in (25-cm x 25-cm) wood post. Test 2P10 was not repeated because of no more available posts, but the results were used in the stiffness average.

The next problem was how to model this elastic-plastic post response in BARRIER VII. It was decided to accomplish this by combination members of friction dampers and springs, as shown in figure 8. This required enlarged simulation sizes for BARRIER VII because of the added members, as shown in figure 9. However, the increased size and run times were not excessive.

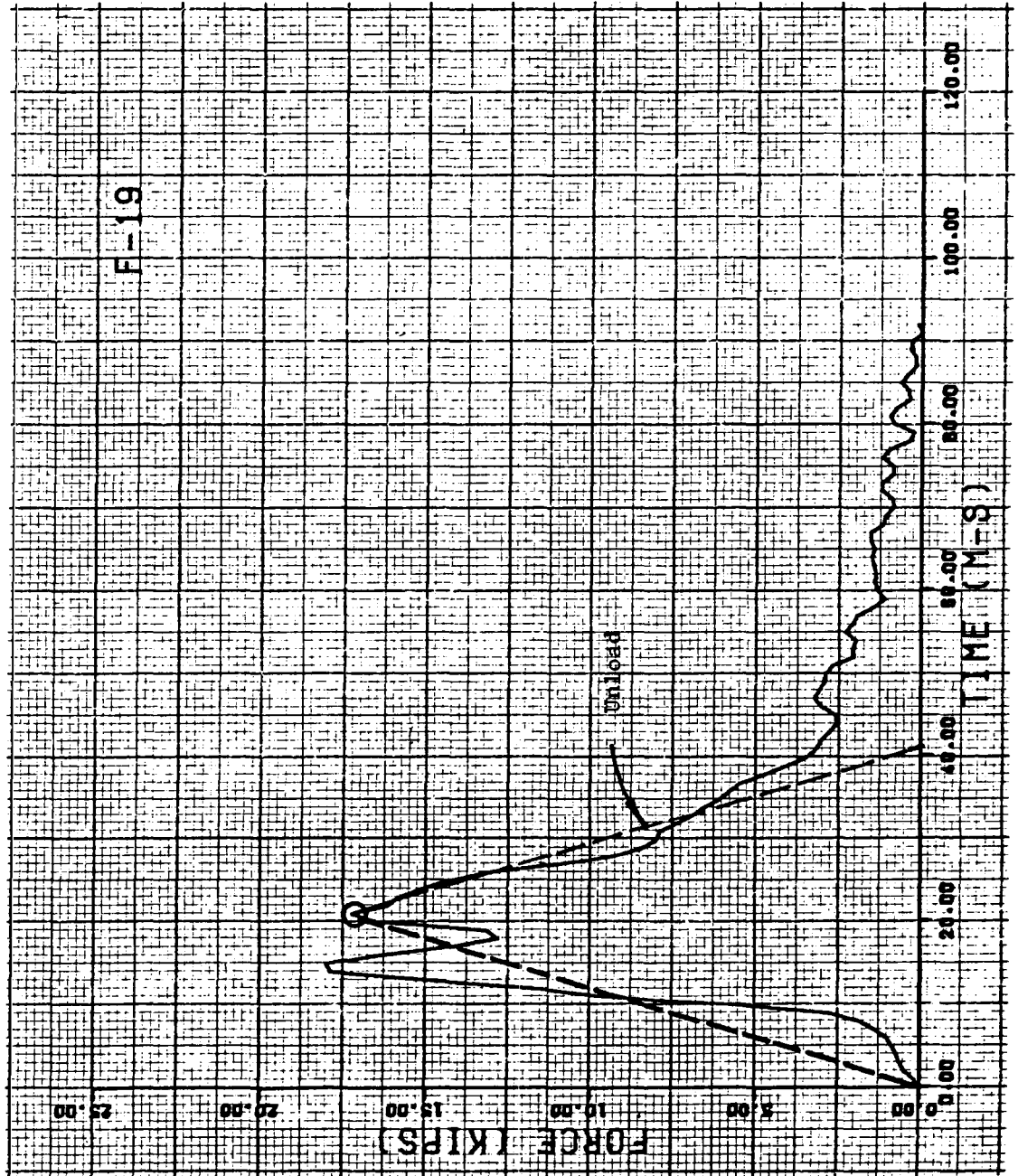
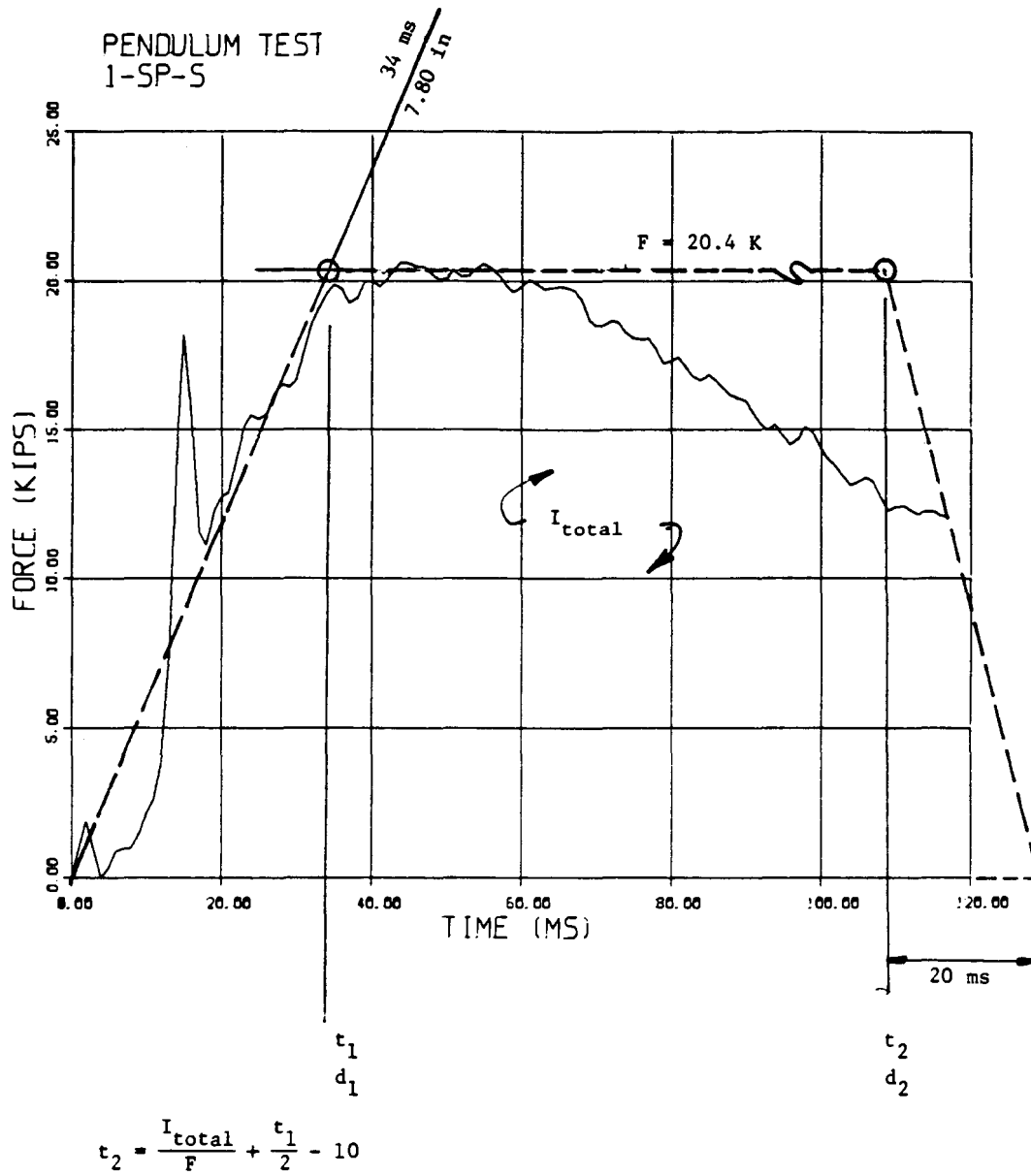


Figure 6. Previous pendulum test.



Metric Conversion
1 in = 2.5 cm
1 ft = 30 cm

Figure 7. Pendulum test result for W6x15.5 with soil paddle.

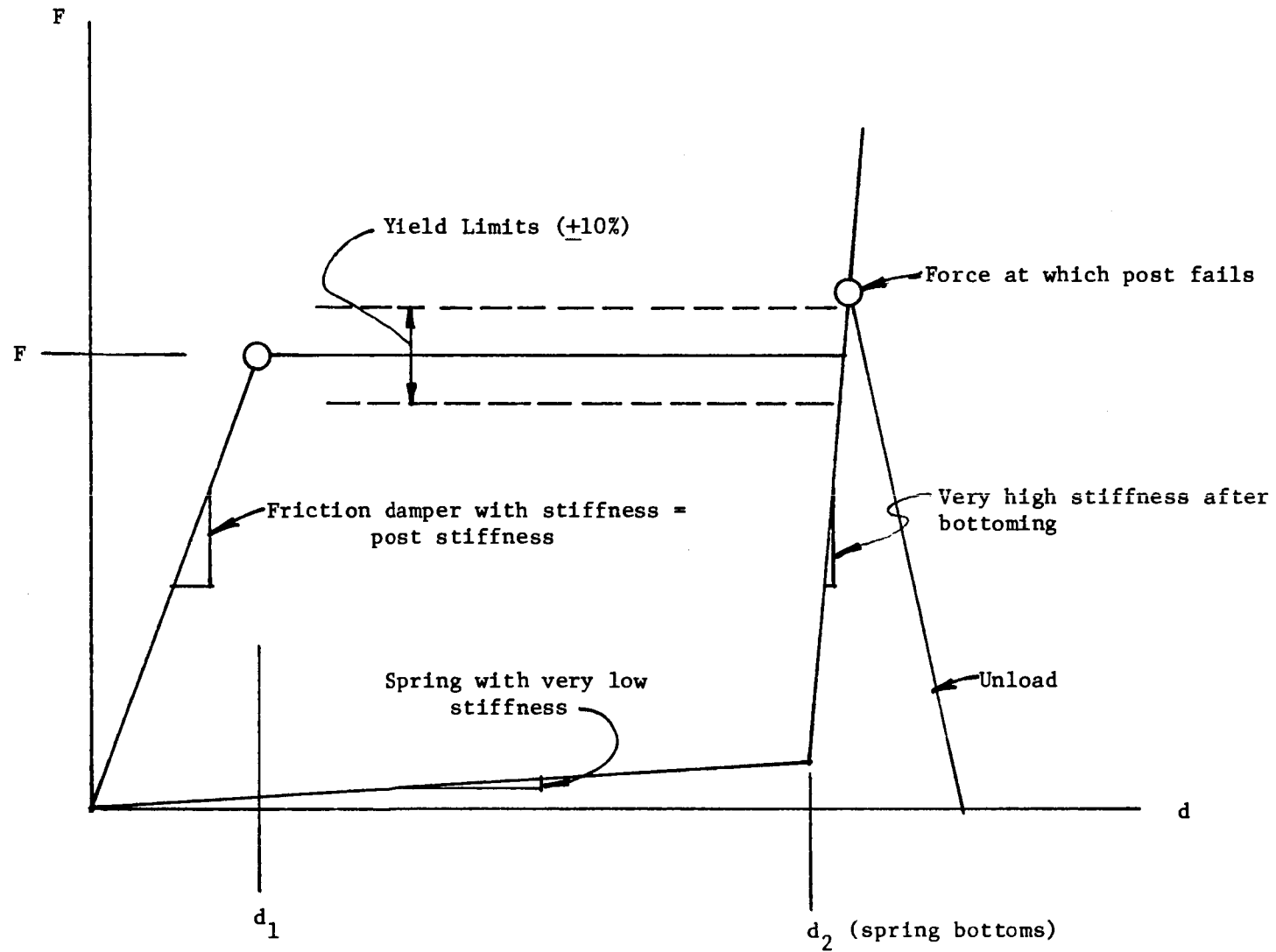


Figure 8. Post elastic-plastic response.

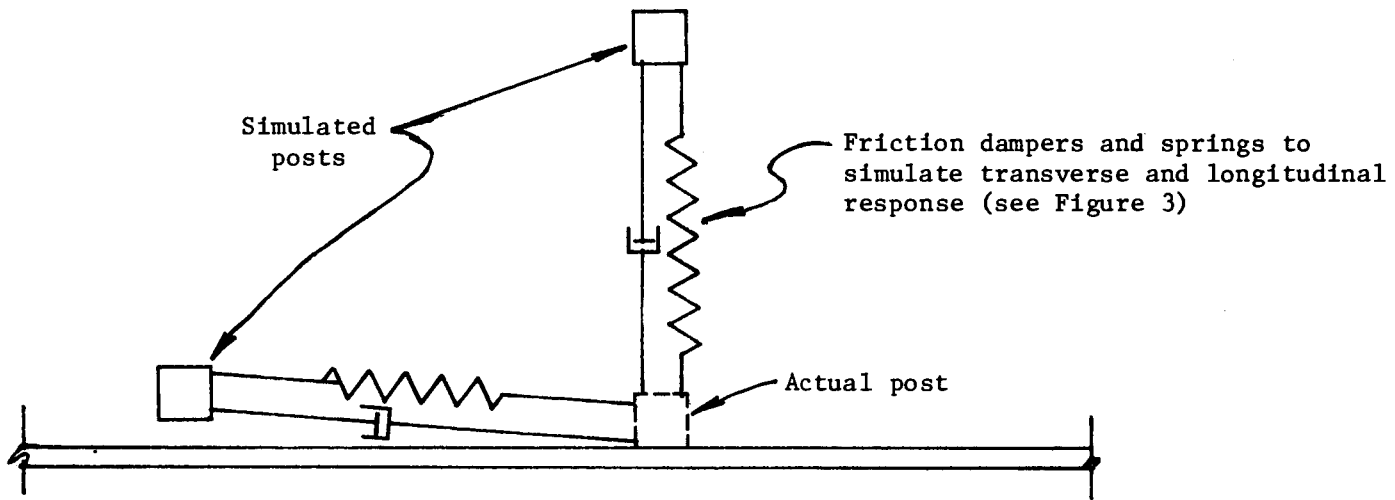


Figure 9. BARRIER VII post simulation.

Consideration was given to the question of guardrail-bridge rail connection component tests. The problem of what can be gained by static connection tests is complicated by the multiplicity of pertinent factors, such as the geometry and reinforcement of the wingwall or end post, the manner of connection (blocked, through bolts or inserts, etc.), the magnitude and direction of the anchor force, dynamic effect of increased stiffness and strength with high load rates, and so forth. Because of these problems and the unlikely probability of getting satisfactory answers from static tests, it was decided not to conduct such tests.

d. Analysis of Candidate Configurations

The BARRIER VII computer simulation was used as the analysis tool for the selected transition configurations. With the new elasto-plastic post responses for BARRIER VII inputs, the first task was to compare the program predictions with full-scale test results. Since anchor forces were measured in the test, California Test 273 was selected as the first trial. This was a rather severe test on a 75-ft (22.9-m) G4(2W) system installed in hardpan soil at the California test site. Comparisons of the test results with BARRIER VII predictions are shown in table 8. Note that only the permanent barrier deflection was reported. Test photographs show a dynamic deflection of about 0.6 of the car width, or about 0.6 (80) = 48 in (1.2 m).

The second test for comparison was SwRI Test No. 118, a transition installation similar to the T1 transition system in the AASHTO guide.⁽³⁾ Comparative results are also shown in table 8. While the table shows that much of the information was not measured, the system was selected to determine if this modeling of the rigid abutment would cause any ill-conditioning of the BARRIER VII solution. None was apparent in that no numerical instability developed and the results looked reasonable. While BARRIER VII indicated vehicle redirection, the tendency toward pocketing was apparent. Also, the test pocketing was "attributed to unsatisfactory

Table 8. BARRIER VII/full-scale test comparisons.

California Test 273⁽¹⁾
4960 lb/68 mph/24 degrees

Item	Test	BARRIER VII
Upstream Anchorage	31 k	34.67 k
Downstream Anchorage	20 k	31.74 k
Max. Lateral Deflection	28.0 in (perm)	47.44 in
Max. 50-ms Accelerations		
Lateral	6.95	8.52
Longitudinal	6.75	5.17
Exit Angle	14°	7.9°
Posts out	2 out 1 splintered	2

SwRI Test 118⁽²⁾
4297 lb/58.8 mph/28 degrees

Max. Lateral Deflection	N/R	18.37 in
Max. 50-ms Accelerations		
Lateral	N/R	10.71
Longitudinal	N/R	10.98
Exit Angle	Pocketed	16.3°
Posts out	0	0

N/R = Not Reported

- (1) E. F. Nordlin, J. R. Stoker, and R. L. Stoughton, "Dynamic Tests of Metal Beam Guardrail, Series XXVII," California Transportation Laboratory Report No. CA-DOT-TL-6392-5-74-14, April 1974.
- (2) J. D. Michie, L. R. Calcote, and M. E. Bronstad, "Guardrail Performance and Design," Final Report, NCHRP Project No. 15-1(2), January 1970.

soil compaction at the posts--inadequate consolidation (probably due to extreme dry conditions)."

Based on these comparisons, BARRIER VII/test correlation was considered adequate to proceed, and the program was exercised with a view of answering some of the questions in table 6 above. For better presentation, a first effort was made to obtain plots of the vehicle/transition interaction. Figure 10 shows a typical plot for a rigid configuration that was used as a baseline case. Plots of other transition types are included in appendix D.

A summary of the preliminary BARRIER VII results, corresponding to the plots of appendix D, is shown in table 9. Note that the first run is the rigid configuration baseline case of figure 10. With the single criterion of keeping the vehicle off of the abutment but, at the same time, allowing the vehicle to impact at any arbitrary point along the transition, these results were a bit disturbing. Impact at the third post out [9.375 ft (2.9 m) from the wingwall], as shown in the plots of appendix D, appears to be the critical point. Unfortunately, any of these flexible systems deflect and tend to pocket the vehicle in the area near the connection. As shown in table 9, this results in higher decelerations and greater lateral loads than those of the rigid configuration.

Of course, such simulations were used for guidance in selecting full-scale tests, and the situation would not likely be as bad as it appeared. Certain preliminary desirable transition features and answers could be implied as follows:

- The connection should be blocked out and the wingwall should be tapered or curved to lessen the tendency for wheel snagging.
- An 8-post transition is not significantly better than the 7-post system.

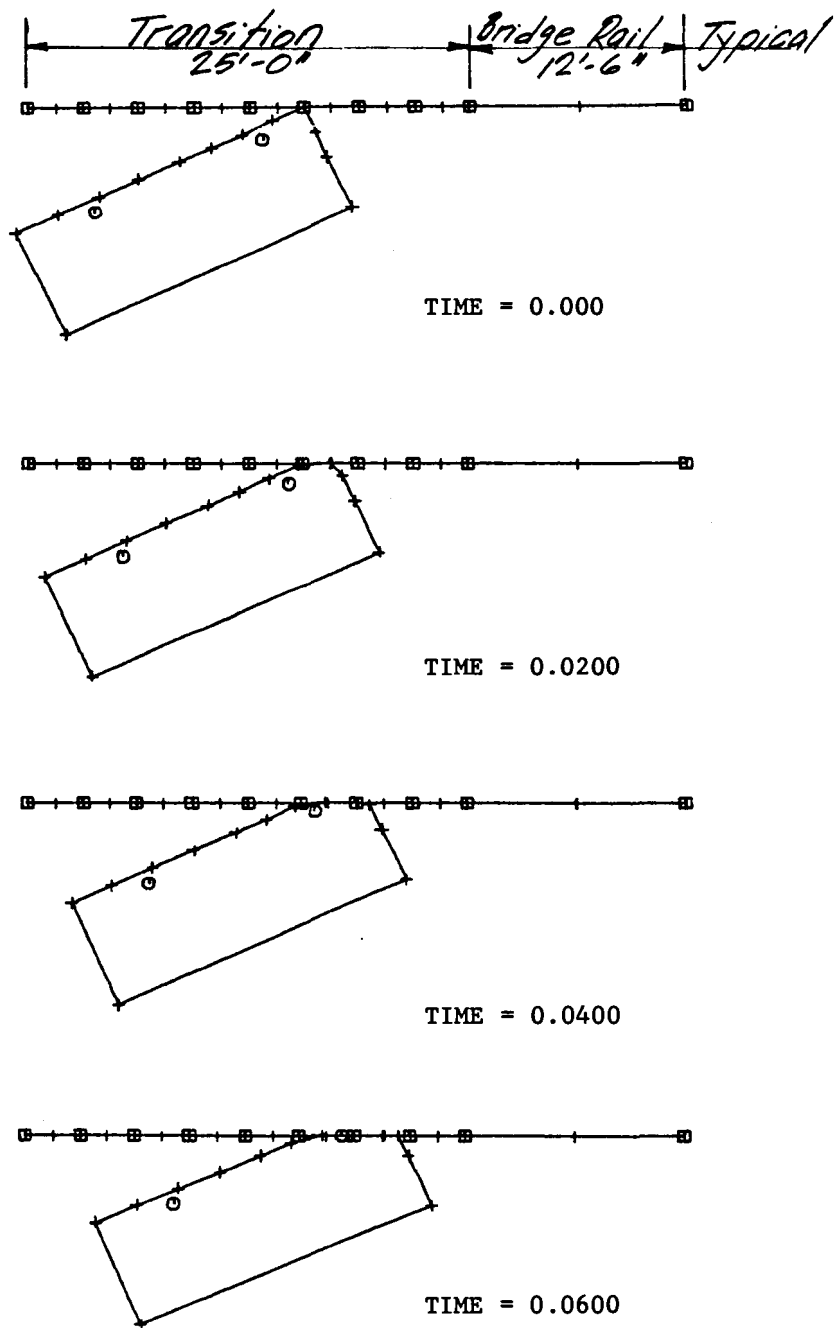


Figure 10. BARRIER VII plot for a rigid transition.

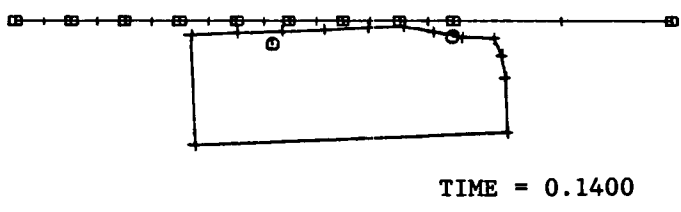
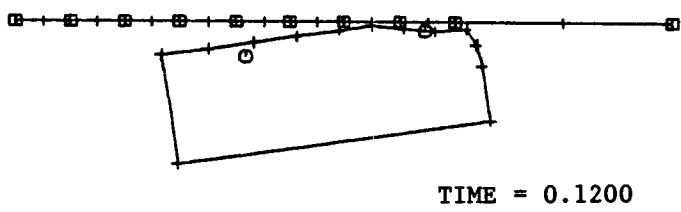
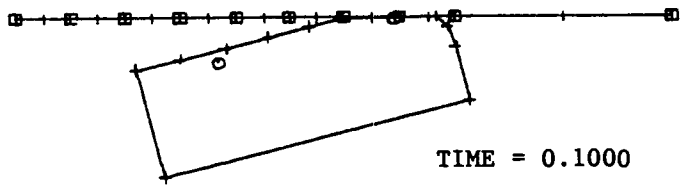
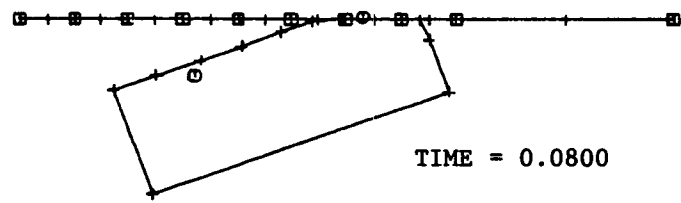
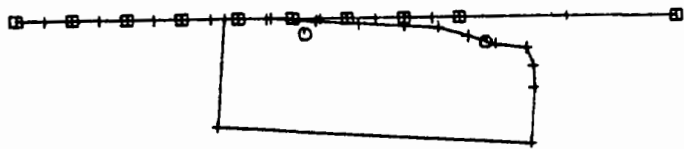
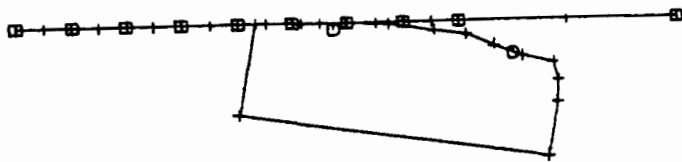


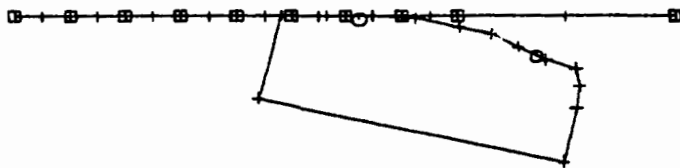
Figure 10. BARRIER VII plot for a rigid transition (continued).



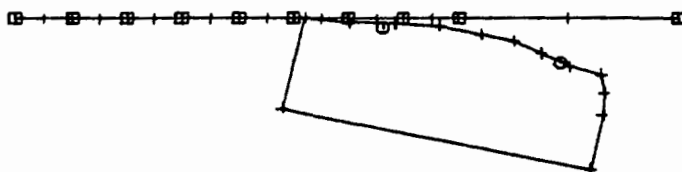
TIME = 0.1600



TIME = 0.1800



TIME = 0.2000



TIME = 0.2200

Figure 10. BARRIER VII plot for a rigid transition (continued).

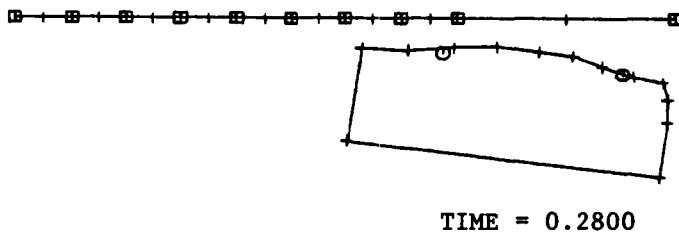
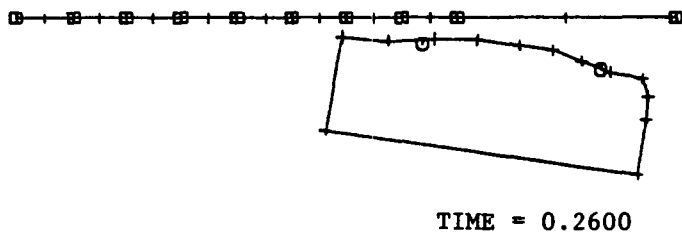
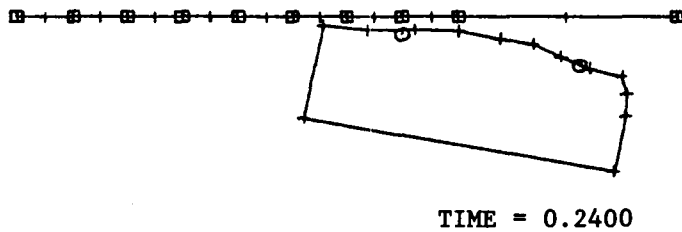


Figure 10. BARRIER VII plot for a rigid transition (continued).

Table 9. Summary of BARRIER VII results.

No.	System	Max. Deflection (in)	50-ms Averages (g's)		Max. Lateral Load (k)
			Lateral	Longitudinal	
1	Rigid	0.01	15.32	12.24	57.74
2	Configuration 1 (3 10 in x 10 in & 4 8 in x 8 in posts)	13.11	15.88	17.60	95.42
3	Configuration 2 (8 8 in x 8 in posts)	14.40	17.48	20.04	109.73
4	N.C. Type VIII Impact @ 4th Post (637.5 in)	7.43	15.64	16.62	88.65
5	N.C. Type VIII Impact @ 5th Post (600.0 in)	11.94	13.72	16.78	75.64
6	Configuration 3 (7 Std. W6x8.5 posts)	14.58	16.94	19.52	102.86
7	Configuration 3 (7 W6x8.5 posts w/nested rail)	13.54	15.22	17.38	92.41
8	Configuration 3 (7 Wooden 6 in x 8 in posts)	14.73	17.52	20.38	113.62
9	Configuration 3 (7 Wooden 8 in x 8 in posts)	14.48	17.42	20.04	109.40

<p>Metric Conversion 1 in = 2.5 cm 1 ft = 30 cm</p>
--

Table 9. Summary of BARRIER VII results (continued).

No.	System	Max. Deflection (in)	50-ms Averages (g's)		Max. Lateral Load (k)
			Lateral	Longitudinal	
10	Configuration 1 (3 W6x15.5 & 4 W6x8.5 posts)	13.85	16.48	18.42	97.64
11	Montana Type 2 (5 12 in x 12 in & 1 8 in x 8 in posts)	11.91	15.20	16.12	87.03
12	Configuration 1 (3 10 in x 10 in & 4 8 in x 8 in posts) Impact @ 525 in	18.41	9.57	8.51	16.84
13	Configuration 1 (3 10 in x 10 in & 4 8 in x 8 in posts) Impact @ 600 in	15.67	11.48	10.73	40.67

37

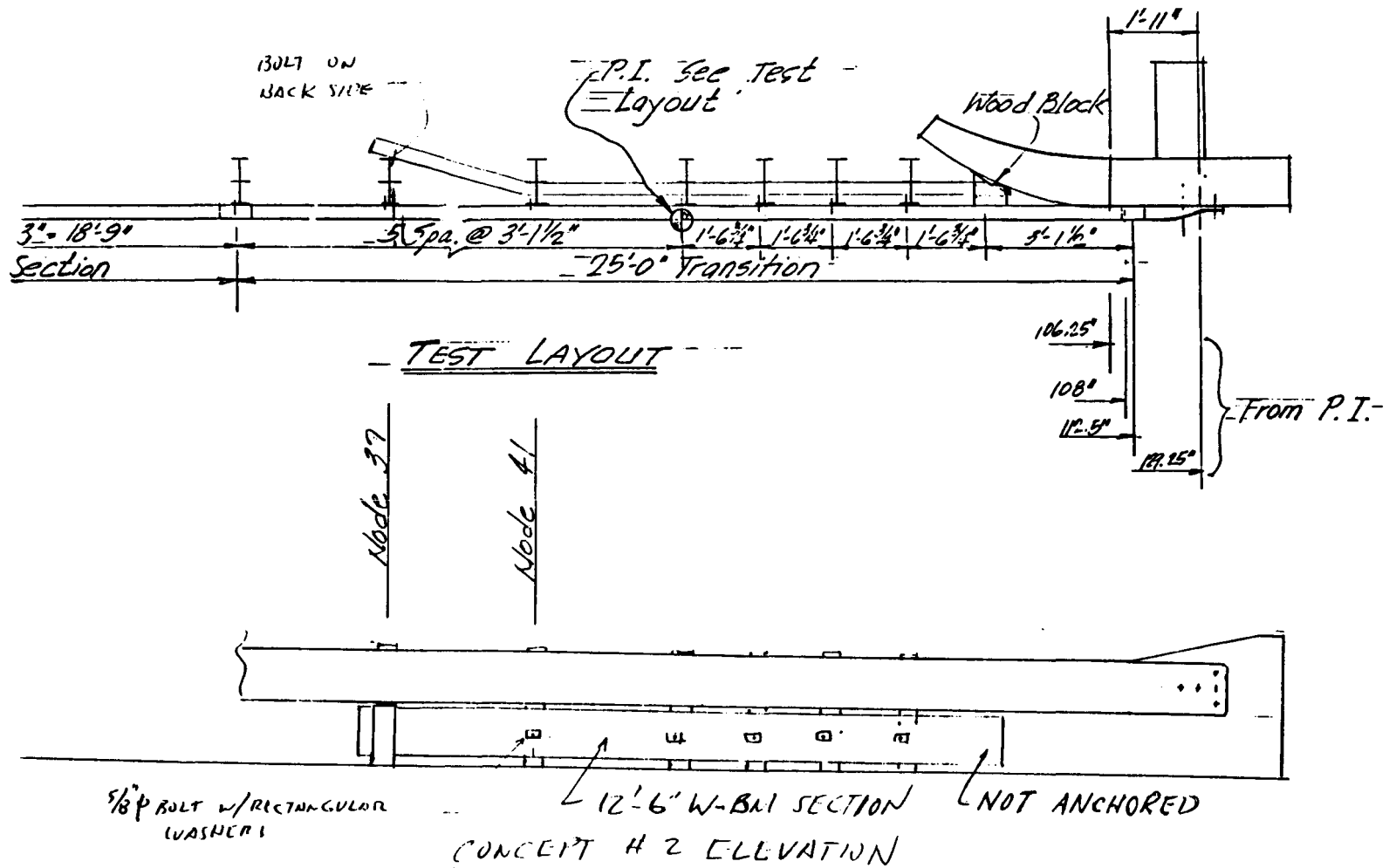
<p>Metric Conversion 1 in = 2.5 cm 1 ft = 30 cm</p>
--

- For the 7-post transition, W6x8.5 steel posts and 6-in x 8-in (15-cm x 20-cm) or 8-in x 8-in (20-cm x 20-cm) wood posts all give essentially equal responses.
- Some benefit is gained by nested rails or the larger 10-in x 10-in (25-cm x 25-cm) posts. However, neither is as good as the reduced 1 ft-6 3/4 in (0.5-m) post spacing of the North Carolina system. This simple addition of intermediate posts will likely be a cheaper retrofit than substitution of the larger posts.

Of interest in table 9 (No. 11) and the plots of appendix D is the simulation of the Montana Type 2 transition. This system is unusual with five 12-in x 12-in (30-cm x 30-cm) wood posts and one 8-in x 8-in (20-cm x 20-cm) post. Despite this strong characteristic, the pocketing tendency remains, resulting in higher longitudinal accelerations than the rigid system (No. 1). It is only slightly better than the N.C. Type VIII (No. 4) with the reduced standard post spacing.

One purpose of the BARRIER VII runs was to determine the most critical impact point on the transition. As shown in table 9, (Nos. 4 and 5 for the N.C. type and Nos. 2, 12, and 13 for Configuration 1), this point is at about the third post out [3×37.5 in = 112.5 in (2.9 m) from the connection at the wingwall]. As shown in the plots, this point causes the barrier to deflect and tends to pocket the vehicle just before it reaches the end of the wingwall. Impacts further out the transition tend to provide vehicle redirection before the wingwall is reached.

As the project progressed, BARRIER VII runs were continued to provide guidance in full-scale retrofit tests and to estimate the probable barrier response. For example, as shown in figure 11, a W-beam rub rail was used as a retrofit for the North Carolina Type VIII transition. The system appeared to work well for the test point of impact (see P.I. in figure 11). Because of this potential promise as a good retrofit for other transitions as well, it was desired to test the system for the effect of the blunt end of the rub rail. To determine the point of impact for this test, BARRIER VII simulation runs were made. Figure 12 shows the results



Metric Conversion
1 in = 2.5 cm
1 ft = 30 cm

Figure 11. Rub rail retrofit.

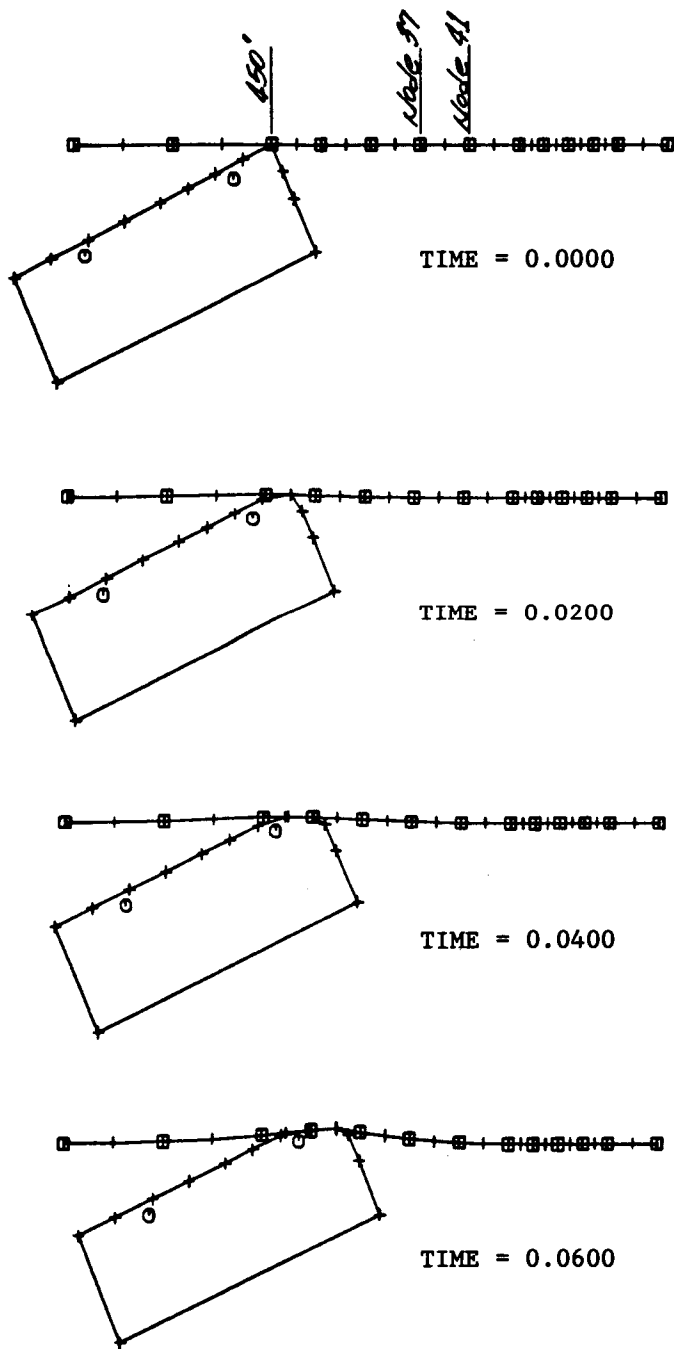


Figure 12. Simulation for impact at 450 in.

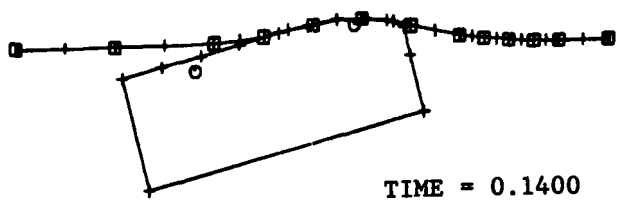
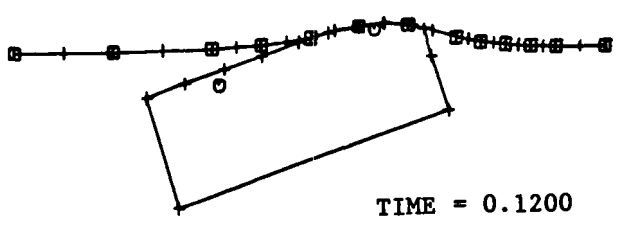
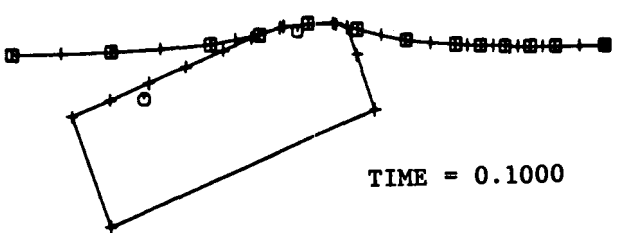
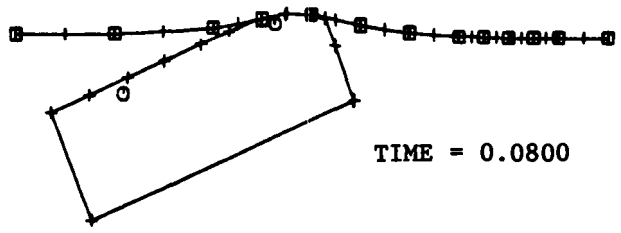


Figure 12. Simulation for impact at 450 in (continued).

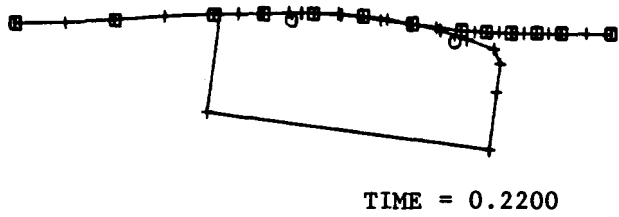
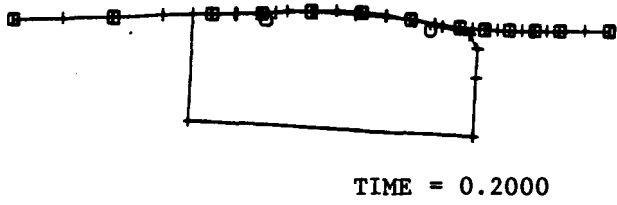
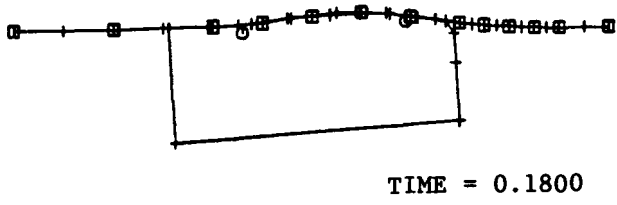
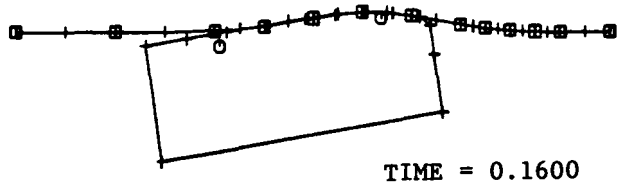
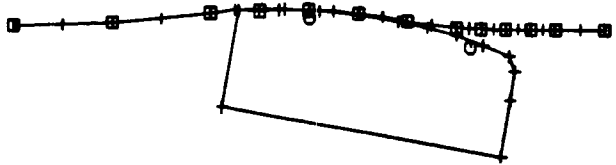
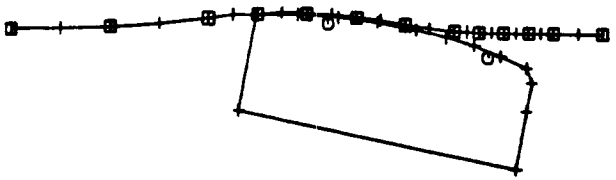


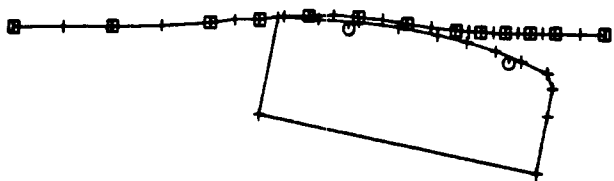
Figure 12. Simulation for impact at 450 in (continued).



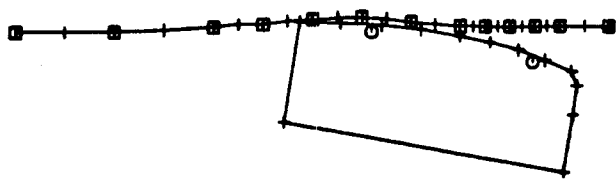
TIME = 0.2400



TIME = 0.2600

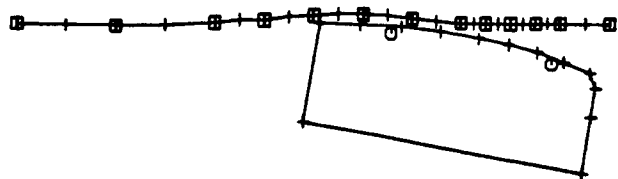


TIME = 0.2800

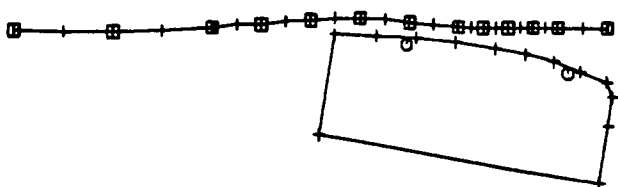


TIME = 0.3000

Figure 12. Simulation for impact at 450 in (continued).



TIME = 0.3200



TIME = 0.3400

Figure 12. Simulation for impact at 450 in (continued).

for an impact at 450 in (11.4 m), the end post of the 25-ft (7.6-m) transition. Figure 13 shows the 487.5-in (12.4-m) impact, one post inside the transition.

As shown in figure 11, the rub rail was bent at node 41 and bolted to the back of the post at node 37. These two nodes are indicated on the first sheets of figures 12 and 13. Desired was the simulation that would produce the greatest deflections at these two nodes. BARRIER VII results are shown in table 10. From these results, it is concluded that the test should be made with the impact at 450 in (11.4 m).

By contract modification, the Washington bridge approach design was added to the project. This treatment, consisting of a 90-degree curve in the approach guardrail, is applicable to sites where a local road intersects the main road near a main road bridge. The short distance available for effecting a safe transition to the bridge presents a real design problem, and this design was conceived by Washington DOT as a possible solution.

Again, BARRIER VII was used to predict the probable response of the system. Figure 14 shows the simulation plot for the test conducted on the original design. Results of the test were unsuccessful in that the vehicle was launched, landed on its front wheels, and then rolled onto its top. With its 2-dimensional character, BARRIER VII results showed continued redirection. However, it is obvious at time = 0.16 sec in figure 14 that vaulting or pocketing would occur if the contacted post did not move out of the path. This was the post that launched the vehicle in the test.

The BARRIER VII output plots of figures 12 through 14 illustrate how the program was used to provide guidance for the full-scale tests and to estimate probable barrier responses. Other plots made on the original designs and retrofitted systems are included in appendix D.

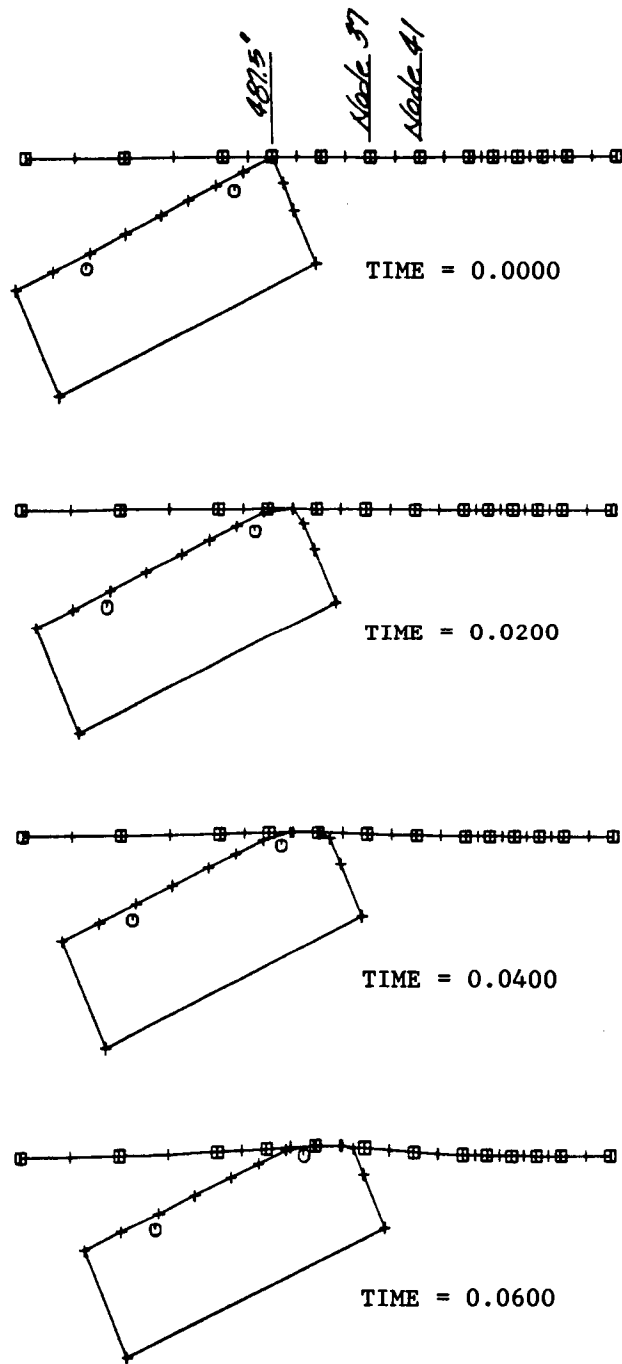


Figure 13. Simulation for impact at 487.5 in.

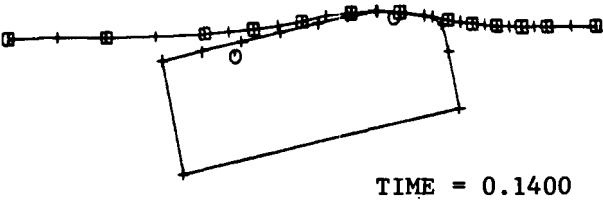
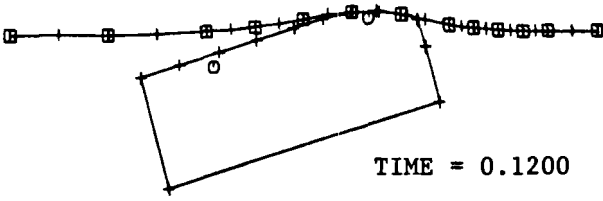
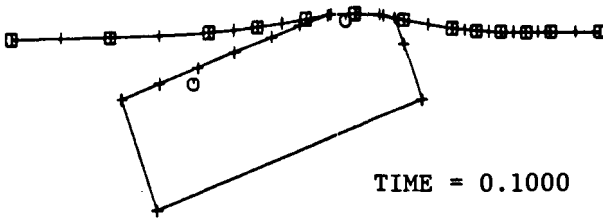
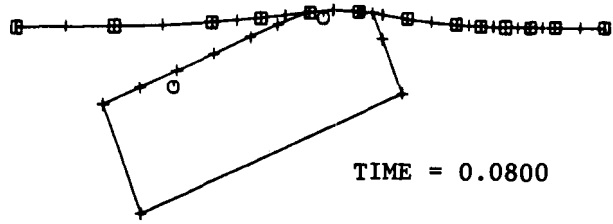
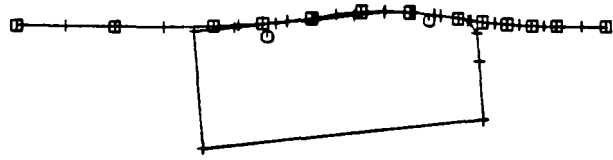
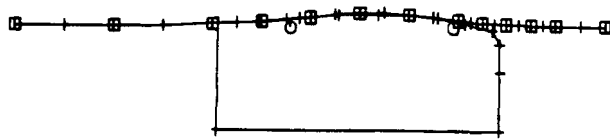


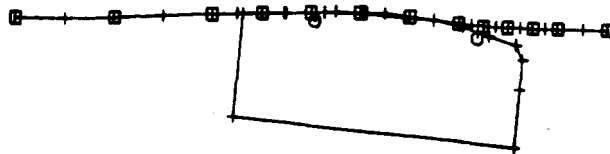
Figure 13. Simulation for impact at 487.5 in (continued).



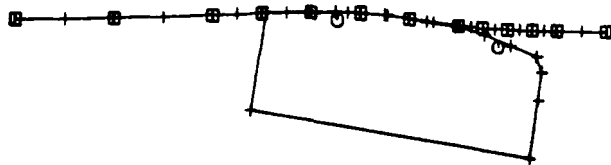
TIME = 0.1600



TIME = 0.1800

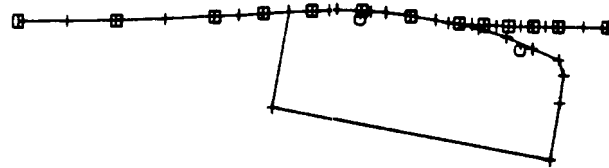


TIME = 0.2000

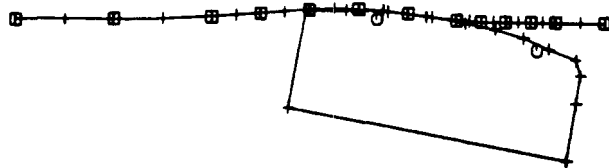


TIME = 0.2200

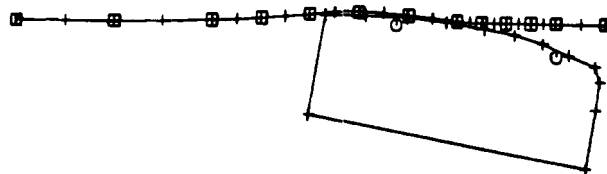
Figure 13. Simulation for impact at 487.5 in (continued).



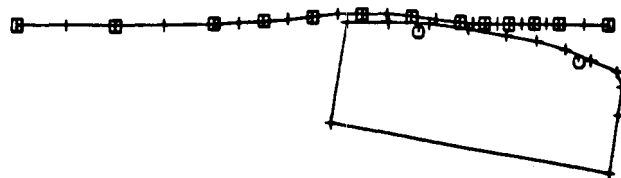
TIME = 0.2400



TIME = 0.2600

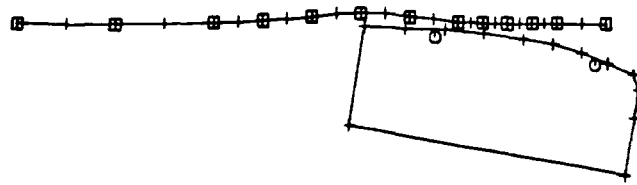


TIME = 0.2800

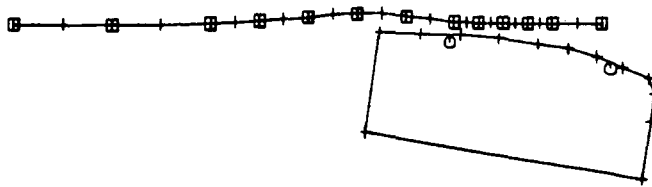


TIME = 0.3000

Figure 13. Simulation for impact at 487.5 in (continued).



TIME = 0.3200



TIME = 0.3400

Figure 13. Simulation for impact at 487.5 in (continued).

Table 10. BARRIER VII results.

Time (sec)	Deflections (in)			
	Impact @ 450 in Node 37	Node 41	Impact @ 487.5 in Node 37	Node 41
0.02	0.14	-0.03	0.43	0.22
0.04	0.94	0.10	1.98	0.96
0.06	3.30	0.72	6.25	3.08
0.08	7.60	2.65	10.91	5.75
0.10	13.21	5.69	13.91*	9.31
0.12	17.28*	9.04	13.55	11.80*
0.14	17.15	11.79*	11.16	11.15
0.16	14.22	11.42	8.27	8.38
0.18	11.37	8.15	7.36	6.45
0.20	10.25	5.59	8.39	6.23
0.22	9.73	4.77	9.02	6.06
0.24	10.00	5.02	9.17	5.91
0.26	9.50	4.72	7.82	4.99
0.28	9.07	4.93	5.88	3.97
0.30	6.09	3.49	5.31	3.82
0.32	4.64	2.41	5.26	3.90
0.34	4.91	2.72	5.25	3.94
0.36	5.51	3.12	5.28	3.99
0.38	5.98	3.38		

* Maximum deflections.

Metric Conversion 1 in = 2.5 cm 1 ft = 30 cm
--

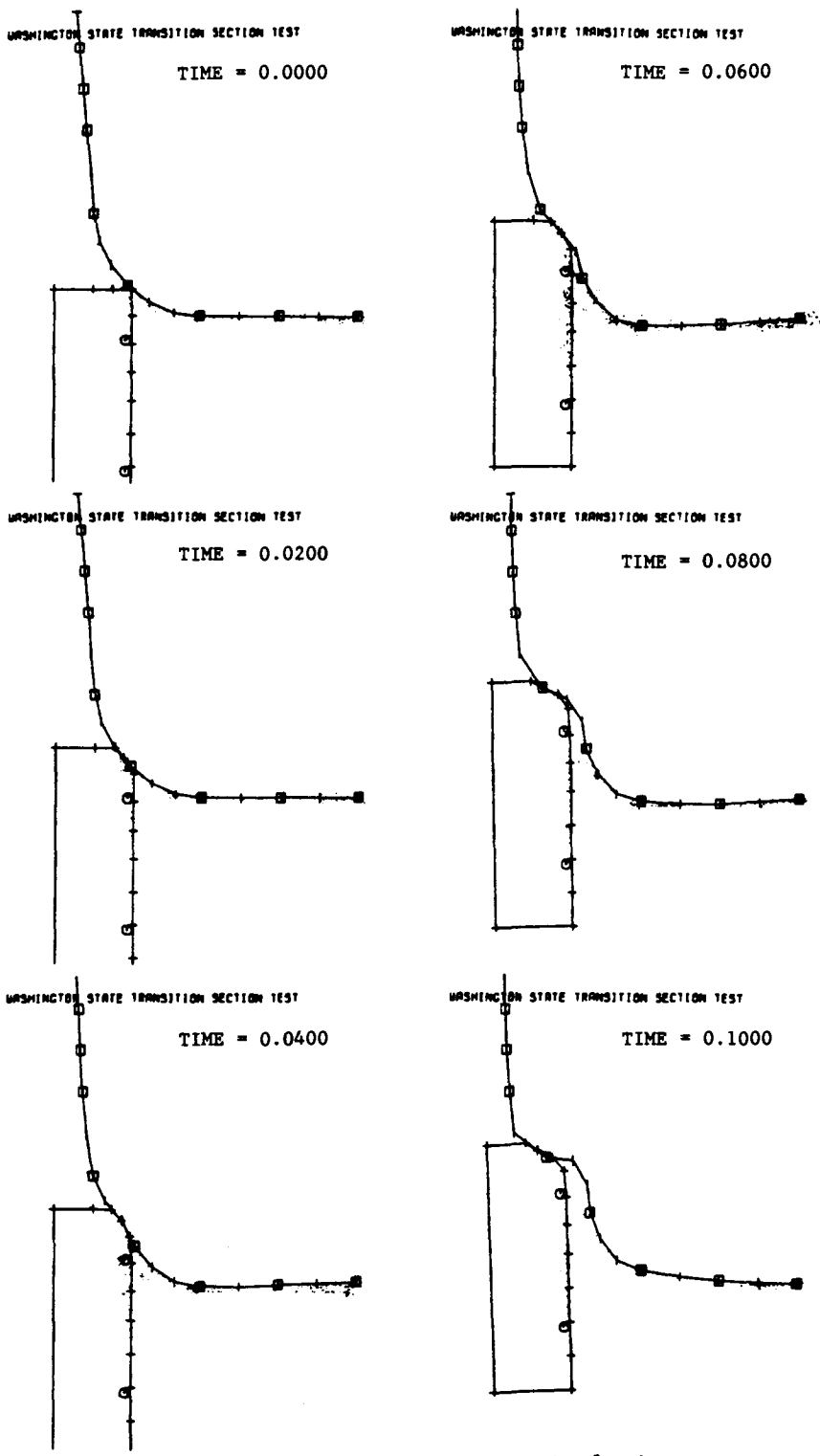


Figure 14. Washington test simulation.

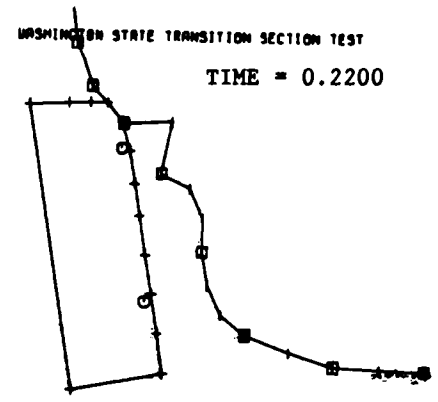
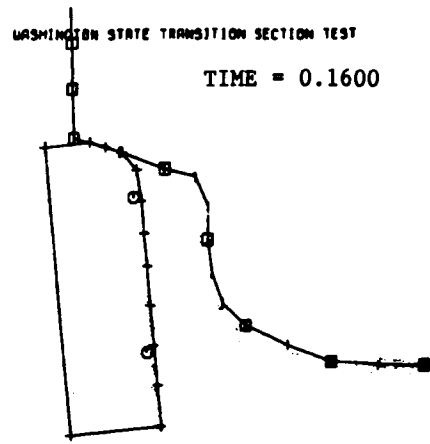
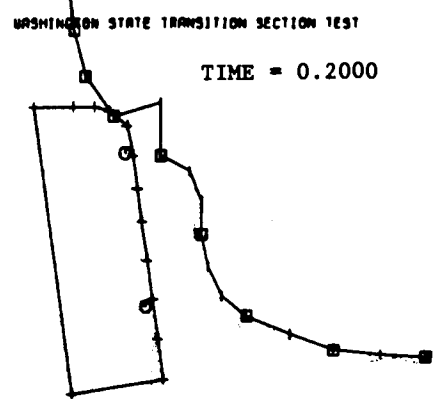
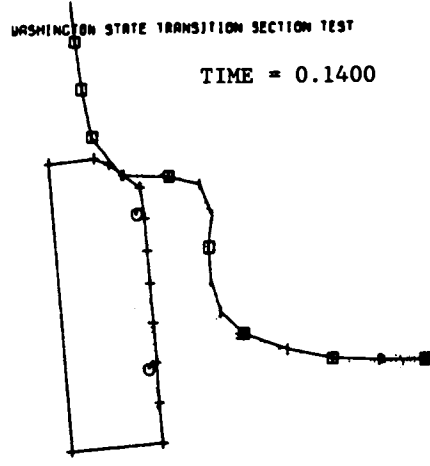
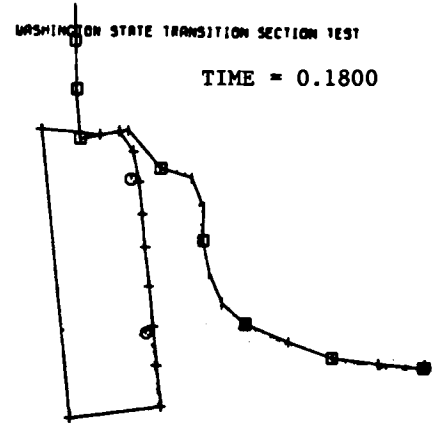
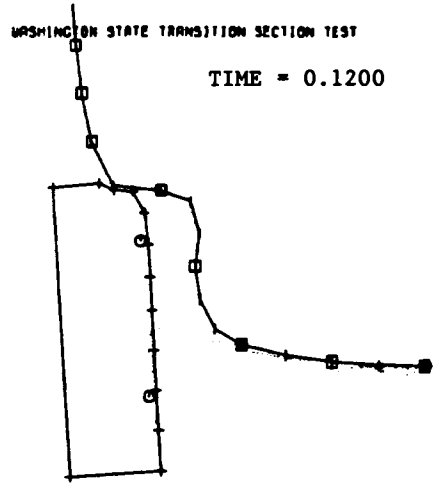


Figure 14. Washington test simulation (continued).

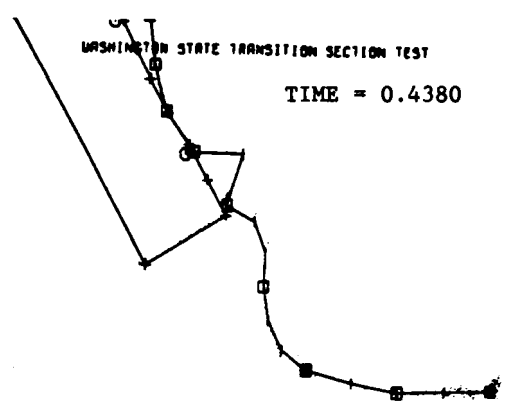
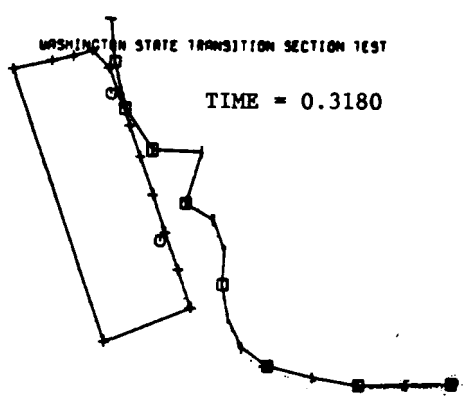
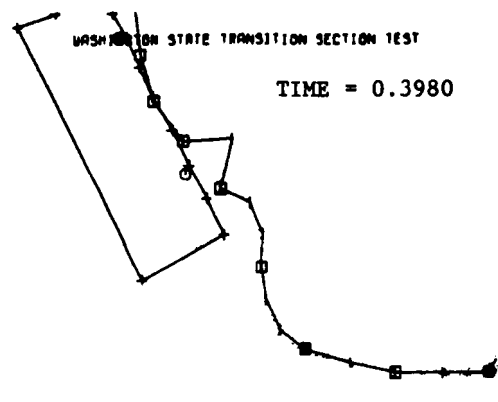
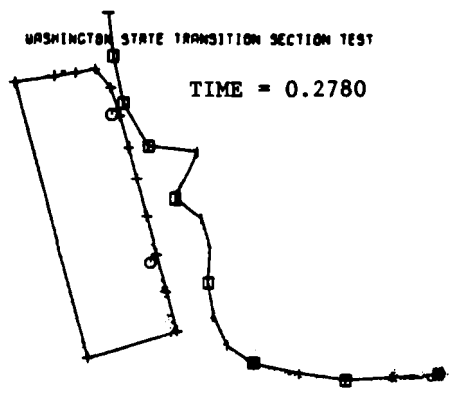
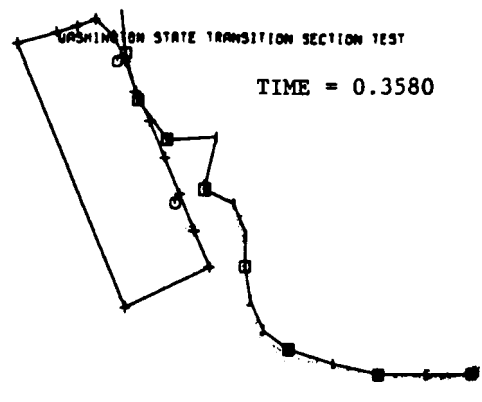
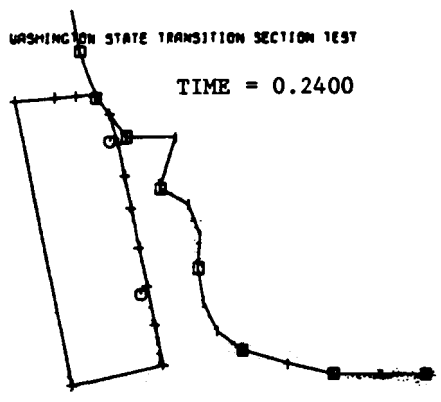


Figure 14. Washington test simulation (continued).

3. Summary of Full-Scale Crash Tests

Crash tests conducted in this project included systems selected as discussed in chapter 2, section b, and modification of these systems. In addition, new designs were conceived and evaluated. The transition systems can be grouped according to the following categories:

- W-beam/wingwall transition
 - straight wingwall
 - tapered wingwall
- Thrie-beam/wingwall transition
 - straight wingwall
 - tapered wingwall
 - modified thrie beam
- W-beam bridge approach at intersecting roadways
- W-beam/independent end block transition
- W-beam bridge approach with tapered curb

Test procedures and test results are briefly described in this section. Detailed information on the test installations and test results is contained in appendix A (Transition Configurations) and appendix B (Full-Scale Crash Test Reports); a summary of the test results is contained in tables 11 through 14.

a. Test Procedures

Except for the test series conducted on the intersecting roadway transition design, all tests were conducted using a 4500-lb (2000-kg) car impacting at 60 mph (95 km/h) and a 25-degree angle. A restrained 50th percentile, Part 572 dummy was placed in the driver seat and a like unrestrained dummy in the right front passenger position of the full-size car. Impact events were recorded from transducers mounted in the dummies

Table 11. Summary of W-beam/wingwall transition tests.

Test No.	LA-1	LA-1M	T-5	NC-1	NC-1M	NC-2M	T-6
Guardrail	G4(2W)	G4(2W)	G4(2W)	G4(1S)	G4(1S)	G4(1S)	G4(1S)
Test Vehicle	1978 Plymouth	1978 Plymouth	1978 Plymouth	1978 Dodge	1978 Dodge	1978 Dodge	1978 Dodge
Gross Vehicle Weight, lb	4635	4737	4700	4642	4630	4572	4655
Impact Speed (film), mph	62.2	60.6	58.9	60	60.4	59.8	61.7
Impact Angle, deg	25.1	25.3	25.8	25	25.9	25.4	25.6
Impact Duration, sec	.40	.27	.35	.43	.35	.53	.43
Maximum Deflection, in							
Dynamic	W-beam separated	6.4	10.9	12.6	7.6	29.1	14.1
Permanent	W-beam separated	6	6.0	8.8	4.4	20.0	7.5
Exit Angle, deg							
Film	Did not exit	-5.5	-8.0	Not Avail.	-10.7	-16.9	-14.7
Yaw Rate Transducer	Did not exit	Not Avail.	-6.8	-9.5	-7.1	Not Avail.	-13.3
Exit Speed, mph							
Film	Did not exit	46.7	40.5	Not Avail.	46.1	34.6	40.0
Accelerometer	Did not exit	Not Avail.	37.7	34.0	42.9	Not Avail.	39.7
Maximum 50 ms Avg Accel (film/accelerometer)							
Longitudinal	-12.9	-7.6/Not Avail.	-5.8/-11.1	Not Avail./-12.8	-6.5/-9.8	-5.4/-7.1	-6.2/-10.9
Lateral	-6.0	-6.6/Not Avail.	6.2/11.9	Not Avail./-11.1	-7.7/12.0	-5.5/-5.9	-7.1/-10.0
NCHRP Report 230 Evaluation							
Structural Adequacy (A,D)	Failed	Passed	Passed	Passed	Passed	Passed	Passed
Occupant Risk (E)	Failed	Passed	Passed	Passed	Passed	Passed	Passed
Vehicle Trajectory (H,I)	Failed	Passed	*, **	*, **	Passed	*, **	*, **
* Exit Angle (60% = 15°)			< 15°	< 15°		> 15°	< 15°
** ΔV (15 mph)			> 15 mph	> 15 mph		> 15 mph	> 15 mph

56

Metric Conversion
1 in = 2.5 cm
1 ft = 30 cm

Table 12. Summary of thrie beam/wingwall transition tests.

Test No.	T-1	T-7	T-2	T-3
Guardrail	G4(2W)	G4(1S)	G4(2W)	G4(2W)
Test Vehicle	1978 Plymouth	1978 Dodge	1978 Plymouth	1978 Plymouth
Gross Vehicle Weight, lb	4658	4675	4650	4580
Impact Speed (film), mph	61.5	58.9	64.0	60.8
Impact Angle, deg	25.2	25.1	25.6	23.8
Impact Duration, sec	.34	.39	.32	.39
Maximum Deflection, in				
Dynamic	9.4	13.9	14.4	11.3
Permanent	5.6	6.4	9.0	7.9
Exit Angle, deg				
Film	-11.2	-5.7	-9.1	-12.1
Yaw Rate Transducer	-5.6	-1.4	-2.0	-9.7
Exit Speed, mph				
Film	43.8	40.2	36.8	43.6
Accelerometer	36.8	42.0	35.8	47.4
Maximum 50 ms Avg Accel (film/accelerometer)				
Longitudinal	-5.8/-9.9	-4.5/-5.2	-7.5/-7.9	-5.1/-5.9
Lateral	7.7/16.6	5.9/7.3	-7.4/-13.4	-7.3/-10.4
NCHRP Report 230 Evaluation				
Structural Adequacy (A,D)	Passed	Passed	Passed	Passed
Occupant Risk (E)	Passed	Passed	Passed	Passed
Vehicle Trajectory (H,I)	*, **	*, **	*, **	*
* Exit Angle (60% = 15°)	< 15°	< 15°	< 15°	< 15°
** ΔV (15 mph)	> 15 mph	> 15 mph	> 15 mph	> 15 mph

57

Metric Conversion
1 in = 2.5 cm
1 ft = 30 cm

Table 13. Summary of W-beam approach at intersecting roadways.

Test No.	WA-1	WA-1M	WA-2M	WA-3M	WA-4M	WA-5M
Barrier	State Design	----- Modified Design -----			---- See Figure 82 ----	
Test Vehicle	1978 Plymouth	1978 Honda	1977 Dodge	1978 Dodge	1978 Plymouth	1978 Plymouth
Gross Vehicle Weight, lb	4520	1903	4789	4640	4650	4640
Impact Speed (film), mph	60.0	60.8	60.6	58.9	58.8	59.0
Impact Angle, deg	0	23.7	13.4	16.6	14.6	-1.1
Impact Duration, sec	.47	Not Avail.	Not Avail.	Not Avail.	Not Avail.	.57
Maximum Deflection, in						
Dynamic	Not Avail.	Not Avail.	Not Avail.	Rail fractured	Barrier on ground	3.5
Permanent	Barrier on ground	153	Barrier on ground	Rail fractured	Barrier on ground	3.0
Exit Angle, deg						
Film	Did not exit	Did not exit	Did not exit	Did not exit	Did not exit	-19.6
Yaw Rate Transducer	Did not exit	Did not exit	Did not exit	Did not exit	Did not exit	-9.6
Exit Speed, mph						
Film	Did not exit	Did not exit	Did not exit	Did not exit	Did not exit	41.6
Accelerometer	Did not exit	Did not exit	Did not exit	Did not exit	Did not exit	40.0
Maximum 50 ms Avg Accel (film/accelerometer)						
Longitudinal	Not Avail.	-11.0/-12.2	-4.3/-6.7	-4.3/Not Avail.	-5.3/-8.3	-2.3/-5.5
Lateral	Not Avail.	5.4/7.4.	-1.7/-1.7	-1.7/Not Avail.	-1.3/-5.4	2.7/4.1
Occupant Risk, NCHRP Report 230 (film/accelerometer)						
ΔV long., fps (30)	Not Avail.	37.9/Not Avail.	19.9/18.9	13.9/Not Avail.	16.7/18.1	16.2/18.0
ΔV lat, fps (20)	Not Avail.	-16.6/Not Avail.	7.5/5.6	7.9/Not Avail.	6.3/6.5	-7.7/-10.5
Ridedown Acceleration, g's (accelerometer)						
Longitudinal (15)	Not Avail.	Not Avail.	-8.8	Not Avail.	-10.5	-7.6
Lateral (15)	Not Avail.	Not Avail.	-4.6	Not Avail.	-7.1	8.0
NCHRP Report 230 Evaluation						
Structural Adequacy (A,D)	Failed	Passed	Failed	Failed	Passed	Passed
Occupant Risk (E,F,G)	Failed (E)	40 < ΔV > 30	Passed	Passed	Passed	Passed
Vehicle Trajectory (H,I)	Failed	Passed	Failed	Failed	Passed	Passed

Metric Conversion
1 in = 2.5 cm
1 ft = 30 cm

Table 14. Summary of W-beam independent block and tapered curb tests.

Test No.	NV-1	IB-1	TC-1
Barrier	State Block	New Block	Tapered Curb
Test Vehicle	1978 Dodge	1978 Plymouth	1978 Dodge
Gross Vehicle Weight, lb	4636	4750	4655
Impact Speed (film), mph	61.3	60.1	60.9
Impact Angle, deg	26.3	24.4	25.0
Impact Duration, sec	.53	.35	.30
Maximum Deflection, in			
Dynamic	16.6	10.5	12.3
Permanent	6.1	5.3	5.4
Exit Angle, deg			
Film	-7.1	-13.4	-3.0
Yaw Rate Transducer	Not Avail.	-11.9	Not Avail.
Exit Speed, mph			
Film	35.1	43.2	41.6
Accelerometer	Not Avail.	44.2	Not Avail.
Maximum 50 ms Avg Accel (film/accelerometer)			
Longitudinal	-6.9/-9.9	-5.4/-10.6	-6.2/Not Avail.
Lateral	-5.4/-7.9	-8.6/-10.2	-8.9/Not Avail.
Occupant Risk, NCHRP <u>Report 230</u> (accelerometer)			
Δv long., fps (30)	24.8/18.0	3.0/19.3	11.1/Not Avail.
Δv lat., fps (20)	17.7/15.8	21.7/21.0	21.8/Not Avail.
Ridedown Acceleration, g's (accelerometer)			
Longitudinal (15)	-4.1 (film)	5.1	-1.9 (film)
Lateral (15)	-5.3 (film)	-18.6	-7.0 (film)
NCHRP <u>Report 230</u> Evaluation			
Structural Adequacy (A,D)	Failed	Passed	Marginal
Occupant Risk (E)	Passed	Passed	Passed
Vehicle Trajectory (H,I)	Passed	Passed	Passed

Metric Conversion
1 in = 2.5 cm
1 ft = 30 cm

and on the vehicle. Extensive film coverage also documented the barrier, vehicle, and dummy behavior.

b. W-Beam/Wingwall Transitions

Straight Wingwall. The most common transition utilized by the States is a W-beam approach to a straight flat concrete wingwall or parapet. Many of the State designs feature a transition from the flat wingwall to a full safety shape.

Test LA-1. This design, as shown in figure 15, features eight 3 ft-1 1/2 in (0.9-m) spaces between posts and wingwall before the typical 6 ft-3 in (3.8-m) post spacing began. All of the transition posts and blocks were 6-in x 8-in (15-cm x 20-cm) timber with a Michigan end shoe providing the connection between the wingwall/parapet and the W-beam approach rail.

After impacting the transition at the third post from the bridge end at nominal 60 mph (95 km/h) and 25 degrees, the vehicle snagged on the wingwall/parapet end and the vehicle was abruptly stopped as shown in figure 16. Longitudinal and lateral translation of the simulated bridge wingwall/parapet occurred during the test and the longitudinal displacement was sufficient to cause tensile failure of the beam. Photographs after the test shown in figure 15 show the extensive vehicle and barrier/wingwall damage.

Test LA-1M. In order to minimize the wheel snagging observed in Test LA-1, a single 12 ft-6 in (3.8-m) W-beam element was added below the beam as shown in figure 17; in addition, two additional posts were added between the first two spaces at the bridge end. Tapered blocks between the lower beam and the posts were used and the lower beam was field bent about the fifth post from the end as shown in figure 17.



Figure 15. Test LA-1 photographs.

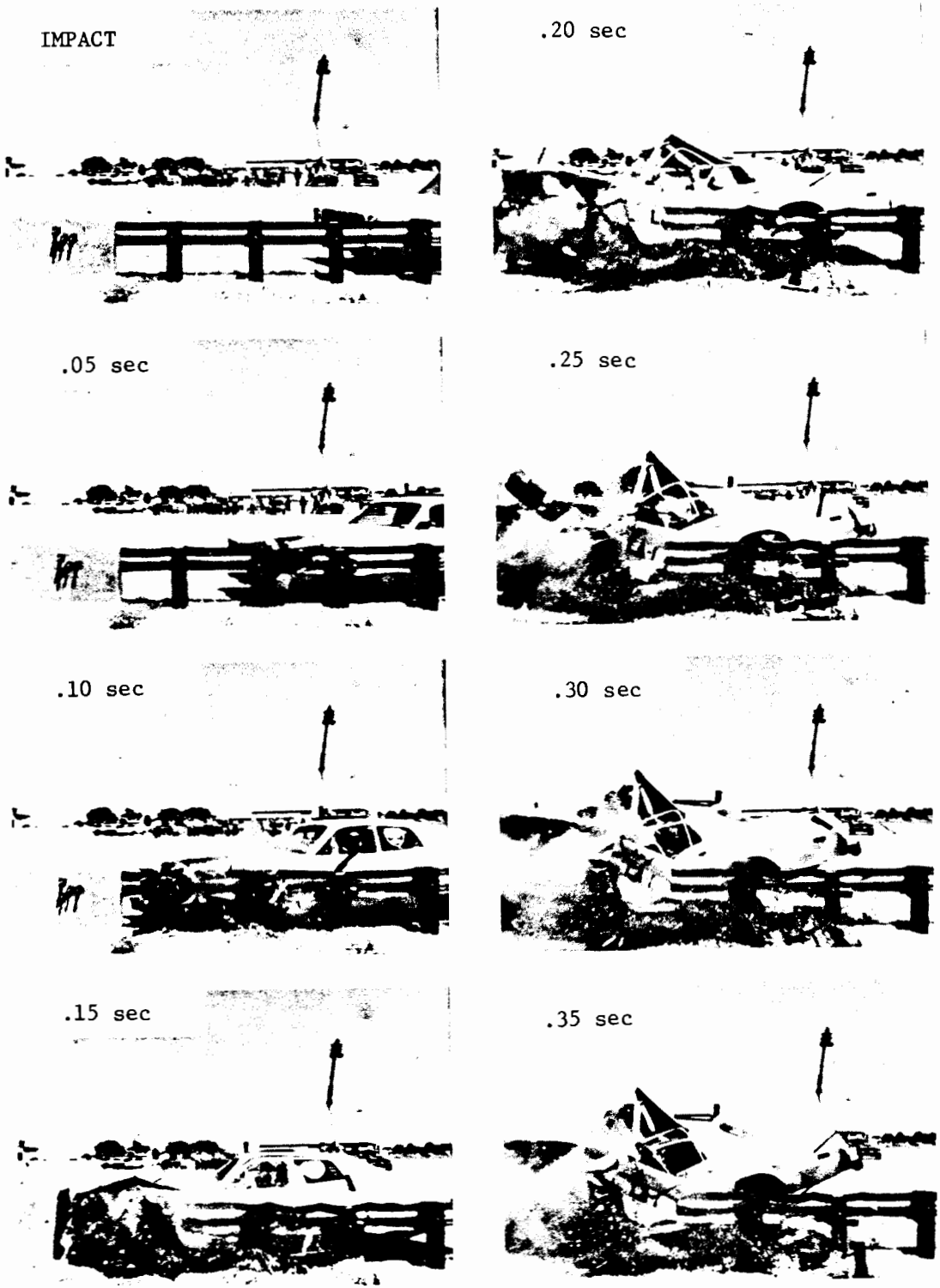


Figure 16. Sequential photographs, Test LA-1.

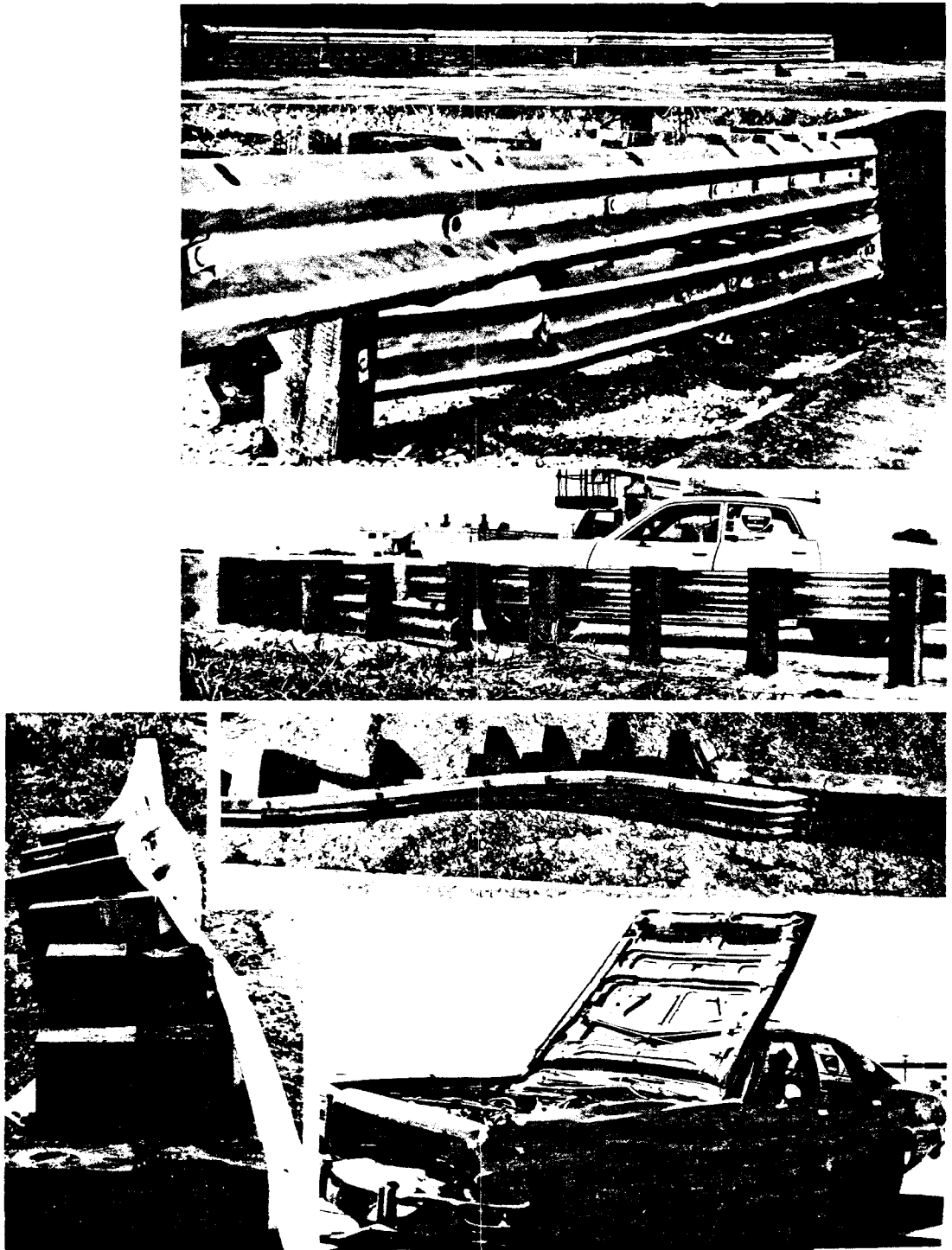


Figure 17. Test LA-1M photographs.

The test vehicle impacted the transition at 60 mph (95 km/h) and 25 degrees and was smoothly redirected as shown in figure 18. There was some rotation of the simulated wingwall/parapet, but no evidence of wheel snagging on the wingwall end. Photographs after the test are shown in figure 17.

Test T-5. Details for this test are identical to Test LA-1M with the exception of the wingwall/parapet. For this test a much larger concrete mass (see figure 19) was used to prevent the wingwall rotation observed during Test LA-1M.

As shown in figure 20, the vehicle impacted the transition at 60 mph (95 km/h) and 25-degree angle. The vehicle was smoothly redirected with no evidence of wheel snagging and negligible rotation of the wingwall end. Photographs after the test are shown in figure 19.

Tapered Wingwall. Included in this test series is an evaluation of the lower beam termination.

Test NC-1. This test evaluated the curved wingwall transition selected as discussed in the previous section. Use of standard steel posts/ block-outs with a post spacing of 1 ft-6 3/4 in (0.5 m) and the tapered wingwall to prevent snagging resulted in a high rating for this design. Photographs of the test installation are shown in figure 21.

The test vehicle impacted the transition at nominal 60-mph (95-km/h) and 25-degree angle conditions and was smoothly redirected as shown in figure 22. There was considerable evidence of wheel snagging on the last post which was pushed against the wall. In addition, some snagging occurred due to local deformation of the beam at the wood block between the beam and concrete wall. Photographs after the test are shown in figure 21.

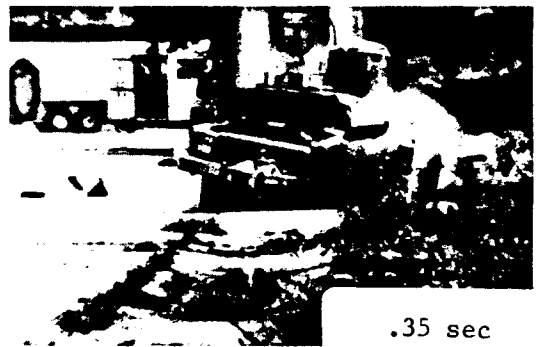
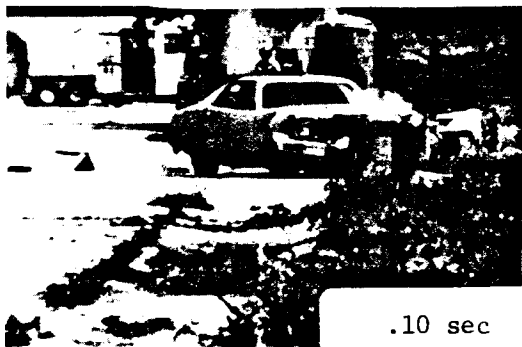


Figure 18. Sequential photographs, Test LA-1M.

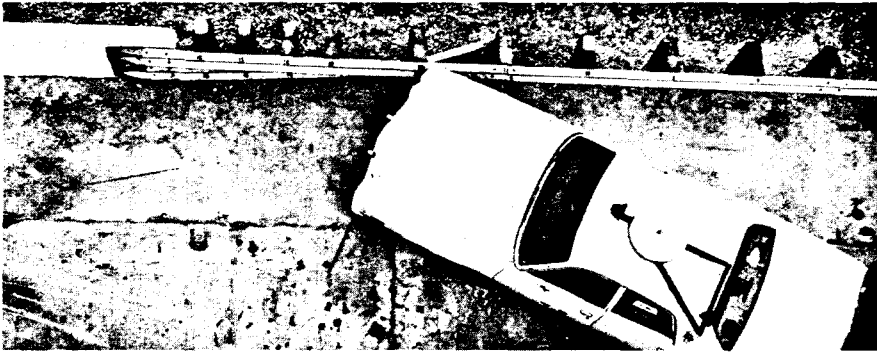
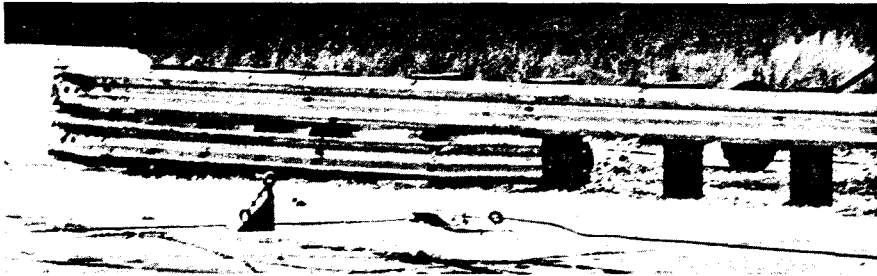


Figure 19. Before and after photographs, Test T-5.



Figure 20. Sequential photographs, Test T-5.



Figure 21. Test NC-1 photographs.



IMPACT



.20 sec



.05 sec



.25 sec



.10 sec



.35 sec



.15 sec



.45 sec

Figure 22. Sequential photographs, Test NC-1.

Test NC-1M. Although the vehicle was smoothly redirected in Test NC-1, the wheel snagging observed in the test was of some concern. Accordingly, a retrofit design using one 12 ft-6 in (3.8-m) panel of W-beam for a lower rail was constructed as shown in figure 23. The lower beam was bolted to all the posts as shown; no attachment of the beam to the wingwall was made as this was considered unnecessary. The flare or taper screens the lower W-beam end from the vehicle impacting from opposing traffic directions.

The test vehicle impacted at the nominal 60-mph (95-km/h), 25-degree angle impact conditions and was smoothly redirected as shown in figure 24. The lower beam element was effective in minimizing wheel snagging. Photographs after test are shown in figure 23.

Test NC-2M. The purpose of this test was to evaluate the potential hazard of the lower beam upstream end in the design evaluated in the previous test. For evaluation purposes, the transition was impacted 3 post spans upstream from the beam end as shown in figure 25 (note position of vehicle before test).

The vehicle impacted the transition at the nominal 60-mph (95-km/h), 25-degree impact angle conditions and was smoothly redirected as shown in figure 26. Photographs after the test are shown in figure 25.

Test T-6. The purpose of this test was to evaluate a straight tapered wingwall; the NC series used a curved wingwall which is considered to be more expensive to form. In addition, a collapsible pipe section was used as an intermediate block-out, as shown in figure 27.

The vehicle impacted at the nominal test condition and was smoothly redirected as shown in figure 28. Figure 27 contains photographs taken after the test.



Figure 23. Test NC-1M photographs.



Impact



.20 sec



.05 sec



.25 sec



.10 sec



.35 sec



.15 sec



.45 sec

Figure 24. Sequential photographs, Test NC-1M.

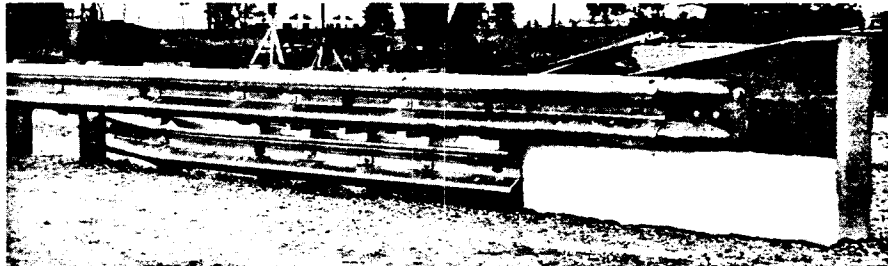


Figure 25. Test NC-2M photographs.

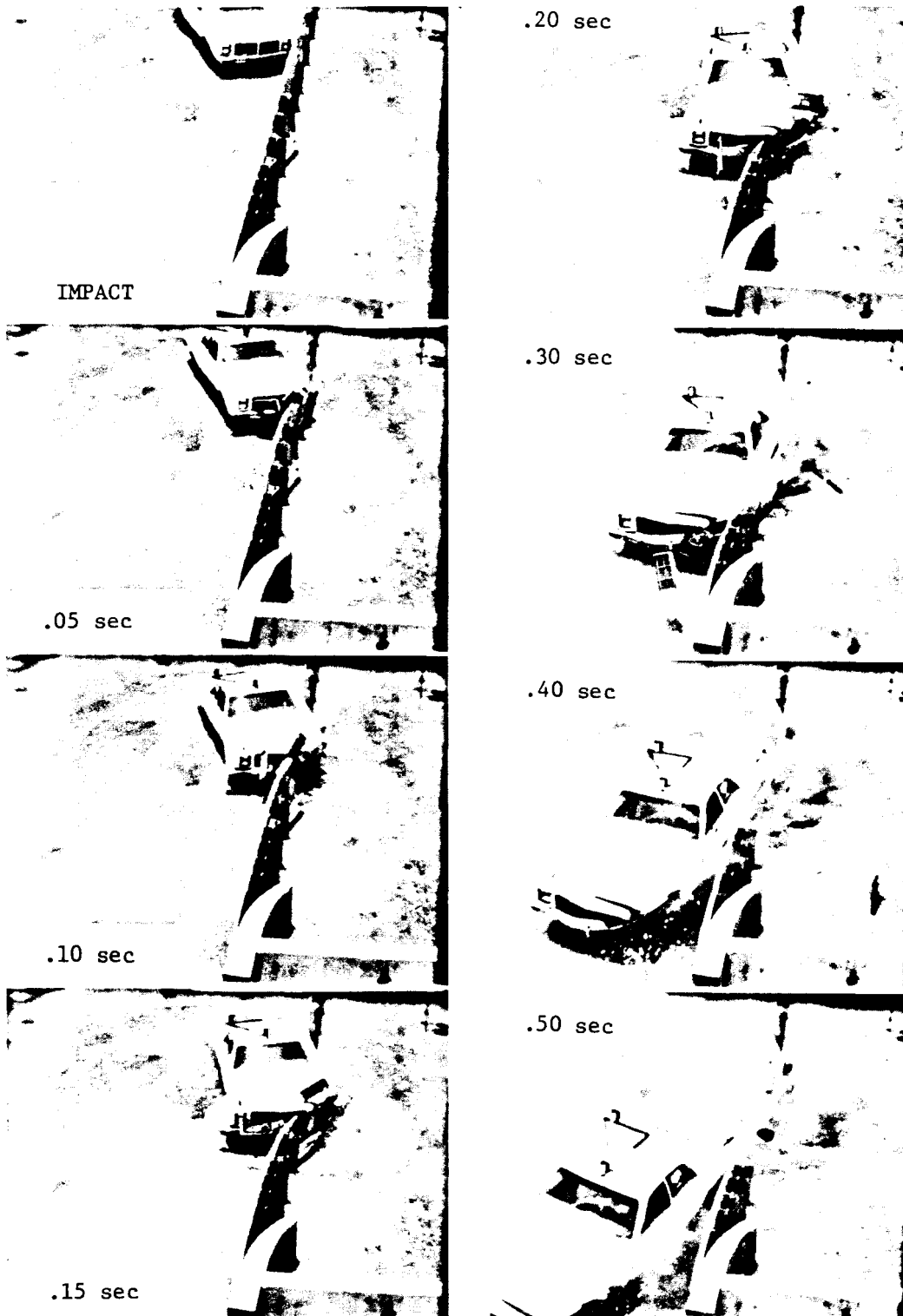


Figure 26. Sequential photographs, Test NC-2M.

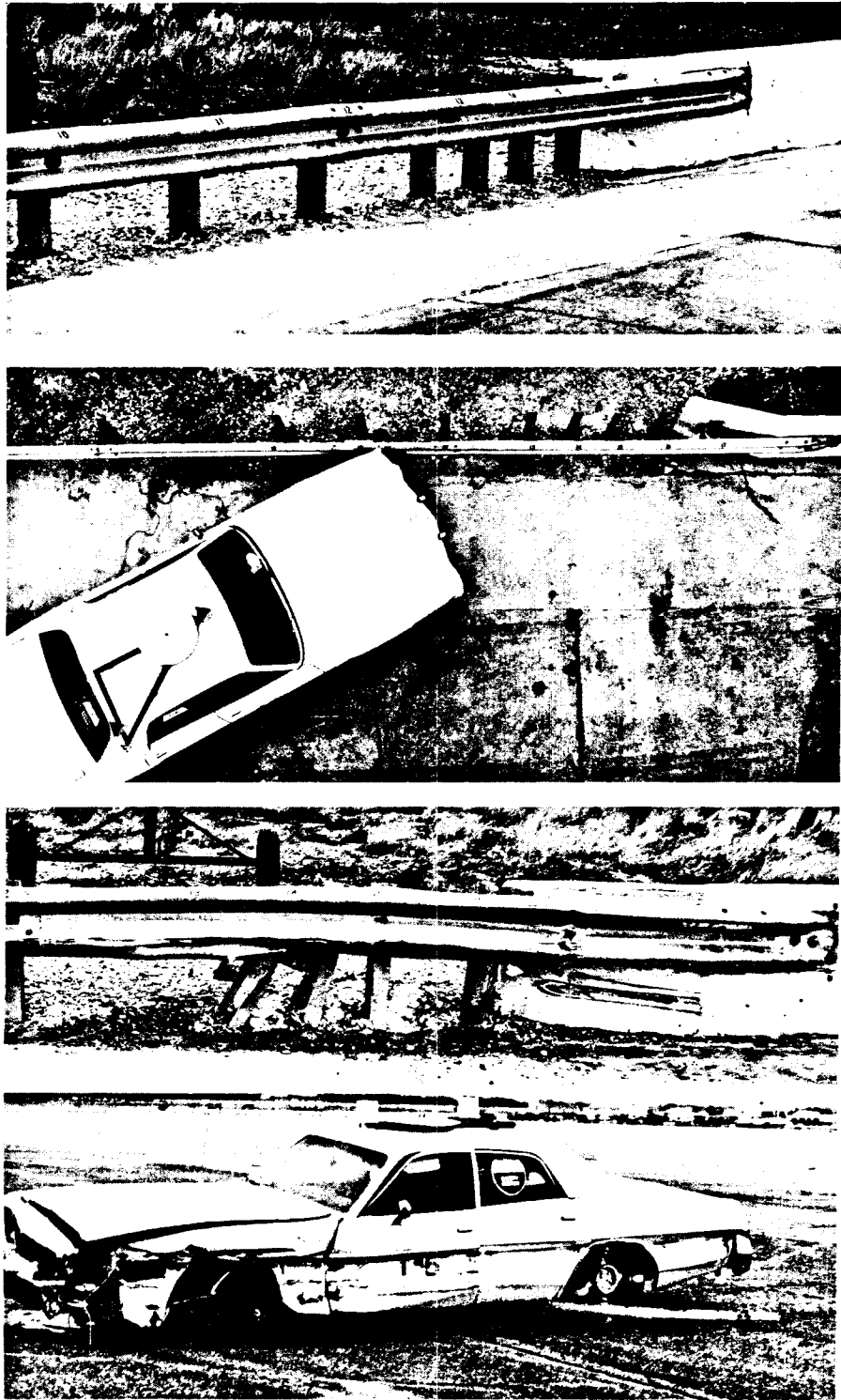


Figure 27. Before and after photographs, Test T-6.



IMPACT



.05 sec



.10 sec



.15 sec



.20 sec



.25 sec



.35 sec



.45 sec

Figure 28. Sequential photographs, Test T-6.

c. Thrie-beam/Wingwall Transitions

Straight Wingwall. Two tests were conducted on straight flat wingwalls that later transition into New Jersey shaped barriers. One transition design used standard wood posts and the other standard steel posts.

Test T-1. This test evaluated a G9 (wood post) transition. As shown in figure 29, there were four 1 ft-6 3/4 in (0.5 m) post spacings near the bridge followed by four 3 ft-1 1/2 in (1.9-m) spaces before the standard 6 ft-3 in (3.8-m) spacing was used.

The vehicle impacted the transition at the nominal 60-mph (95-km/h), 25-degree angle conditions and was smoothly redirected as shown in figure 30. Although no wheel snagging occurred at the wingwall edge there was some wingwall damage indicating that additional reinforcement or wall thickness would be required to eliminate the damage. Photographs after test are shown in figure 29.

Test T-7. This test evaluated the transition from the modified thrie beam⁽¹⁰⁾ using a 14-in (36-cm) blockout to the new G4(1S) transition to a flat wingwall. The initial point of impact was upstream of the third modified thrie beam post.

The test vehicle was smoothly redirected as shown in figure 32. The deflection of the system was as desired as shown in figure 31.

Tapered Wingwall. Two tests were conducted on a straight taper wingwall using one spacer between the last guardrail post and the attachment to the parapet. The taper provided 14 1/2-in (0.4-m) offset of the wall end from the wall face.

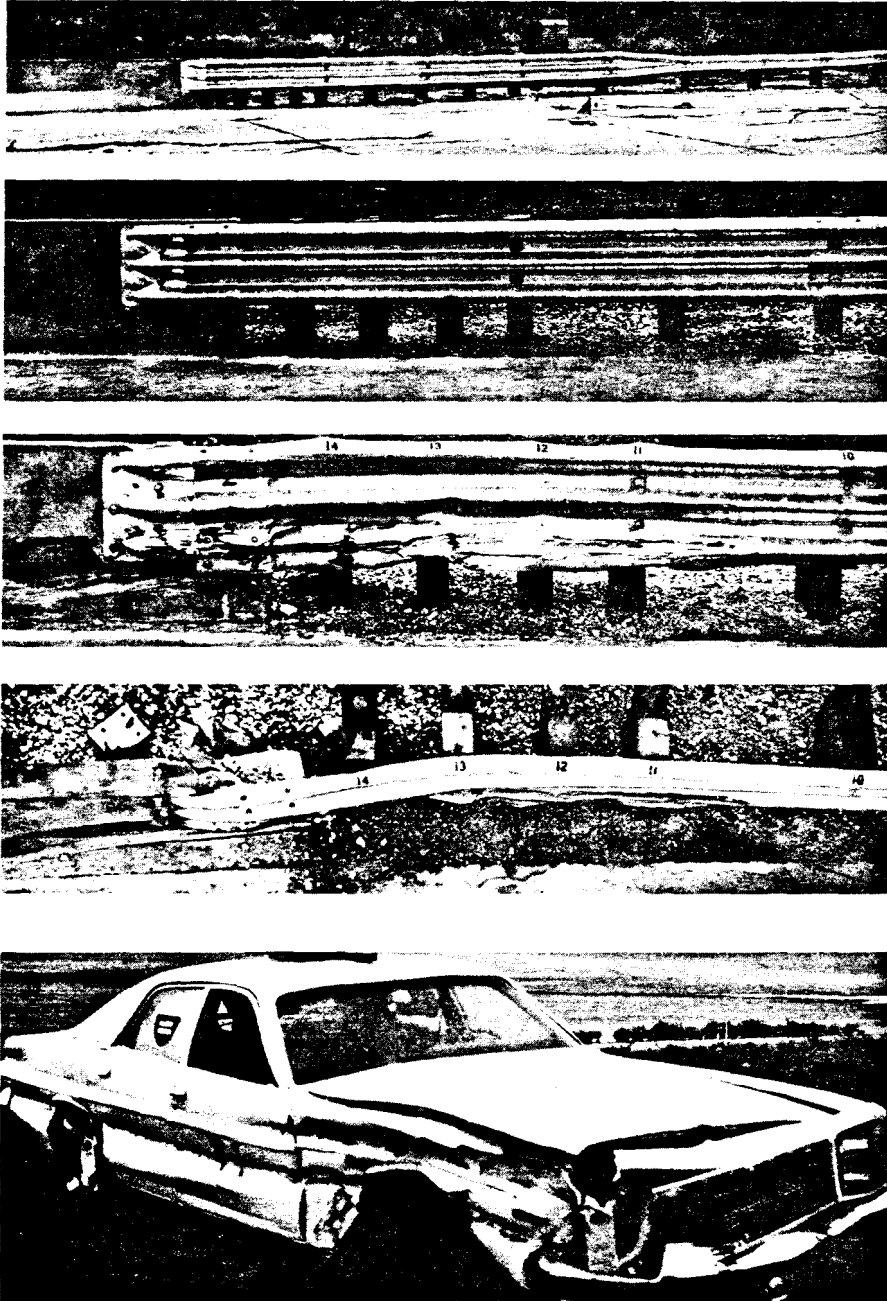


Figure 29. Test T-1 photographs.

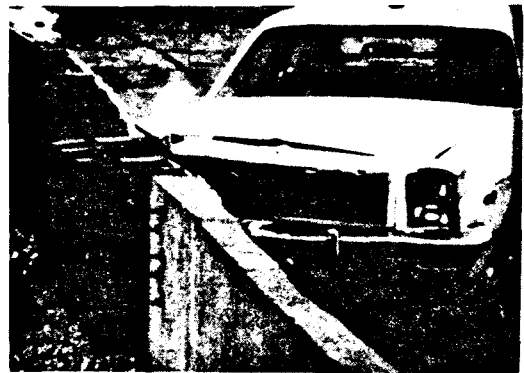
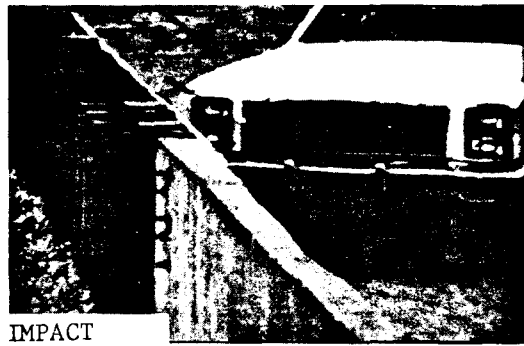


Figure 30. Sequential photographs, Test T-1.

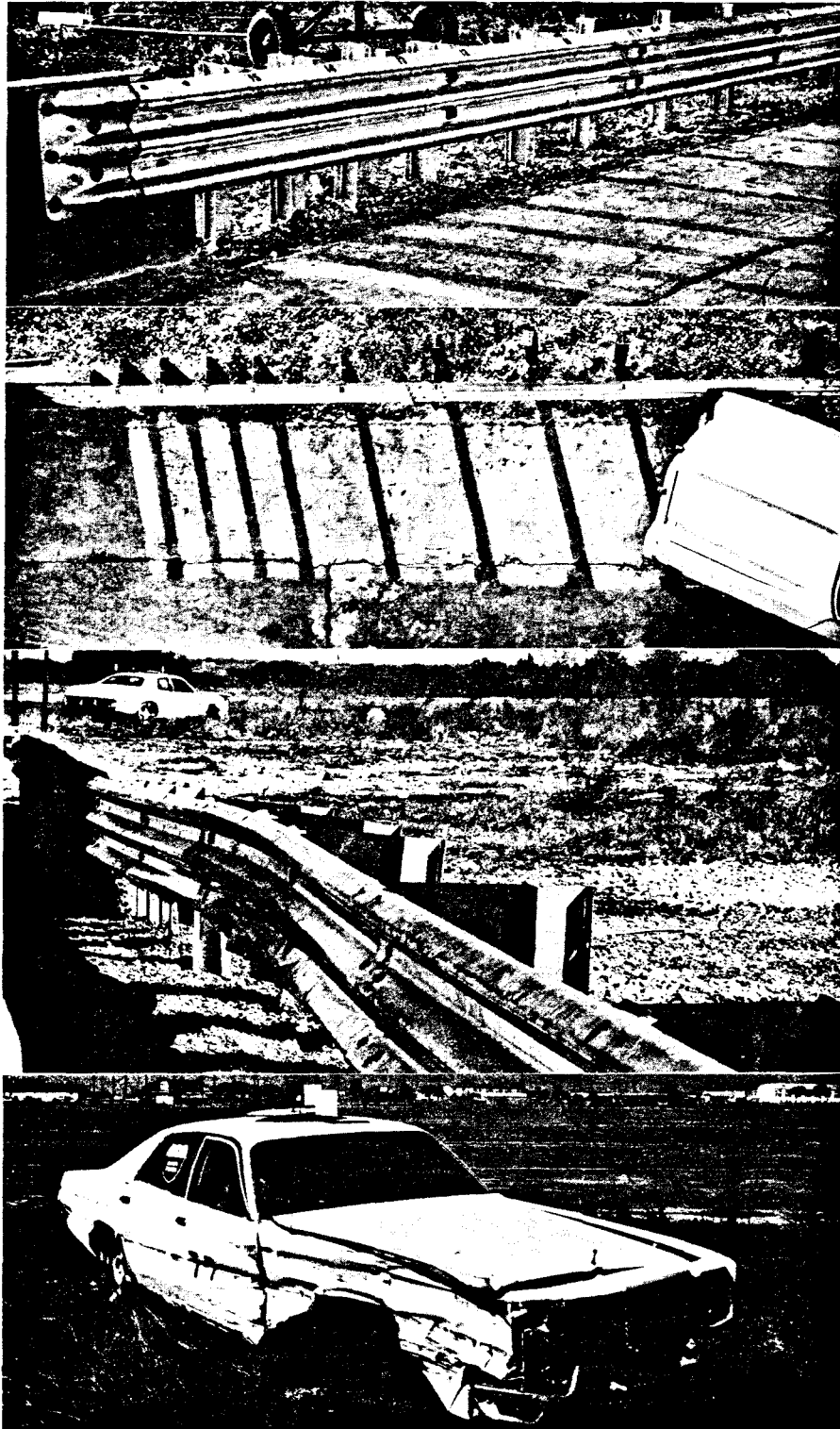


Figure 31. Before and after photographs, Test T-7.



Figure 32. Sequential photographs, Test T-7.

Test T-2. A wood block-out was used between the last guard-rail post and the wall as shown in figure 33. The vehicle impacted the transition and was smoothly redirected as shown in figure 34. There was some evidence of snagging at the wood block-out due to local beam deformation as shown in figure 33.

Test T-3. The performance of the intermediate wood block was not considered to be good in the previous test. A steel pipe section was sized to provide a controlled collapsing spacer between the tapered wall and the beam as shown in figure 35. The spacer was bolted to the beam and a 2-in (5.1-cm) space between the wall and the pipe provided elastic "spring" in this detail. For severe impacts, the pipe collapses under a dynamic load of approximately 10 kips (44.5 kN).

The test vehicle was smoothly redirected as shown in figure 36. There was no evidence of snagging and some permanent deformation of the pipe spacer occurred. This detail performed as desired. Photographs after the test are shown in figure 35.

d. W-Beam Approach at Intersecting Roadways

A common occurrence in many rural and some urban locations is the presence of a secondary road intersecting near a bridge of a higher classification roadway. This intersection provides very little distance for an effective guardrail/bridge rail transition to be installed. A design concept by the State of Washington was evaluated in one test, and based on this and subsequent tests, a design was developed for this situation.

Test WA-1. The test installation as shown in figure 37 included a 12 ft-6 in (3.8 m) tangent section on the intersecting road, an 8.5-ft (2.6-m) radius section, and 25-ft (7.6-m) tangent transition section leading up the bridge. As shown in figure 37, a shallow angle, 60-mph

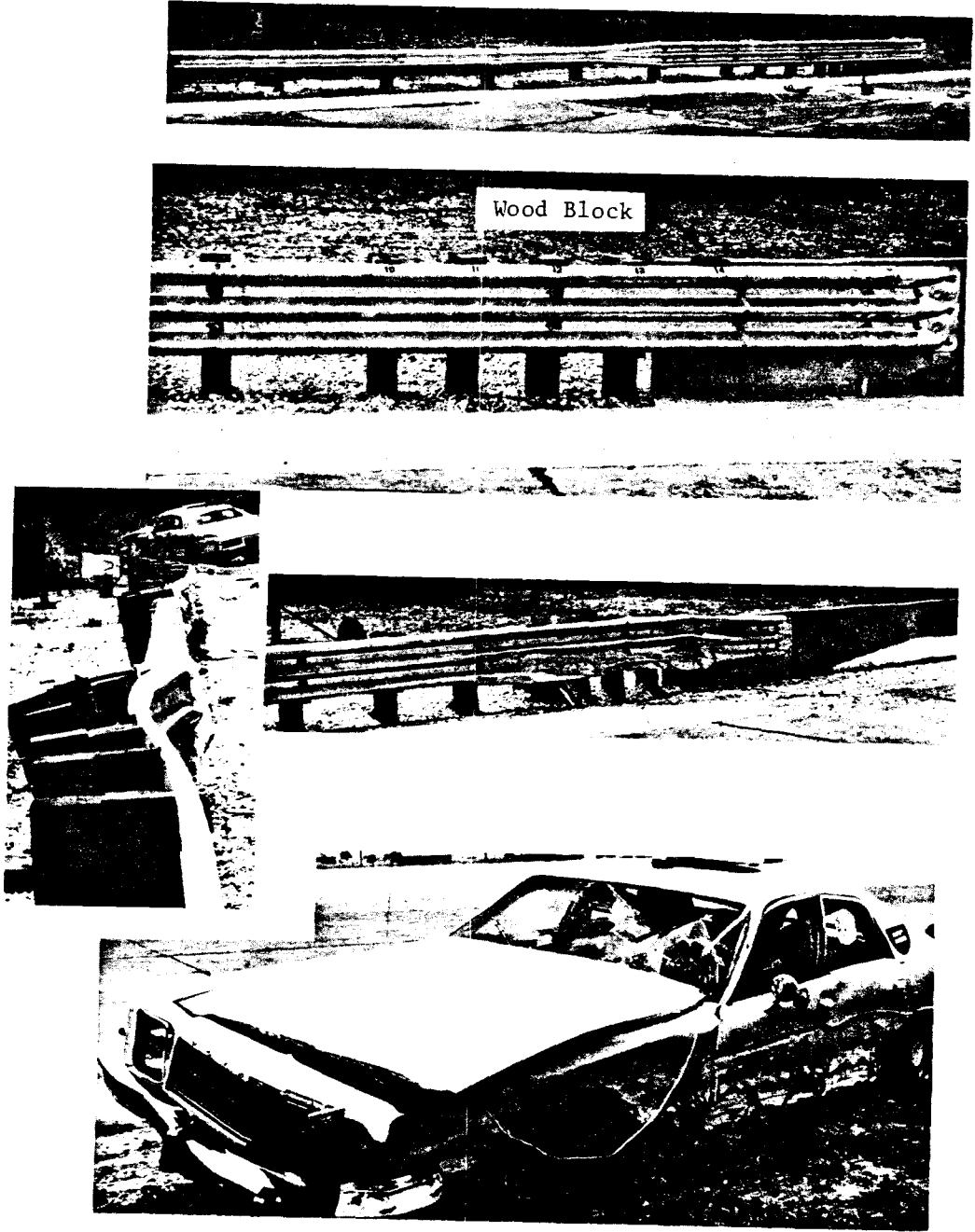
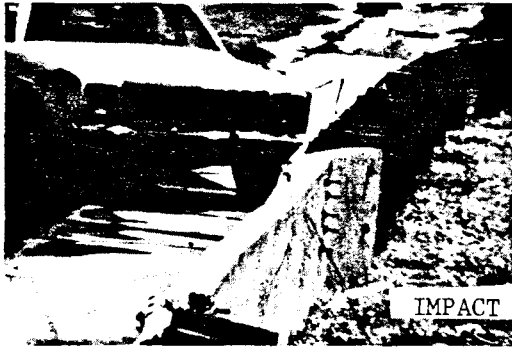
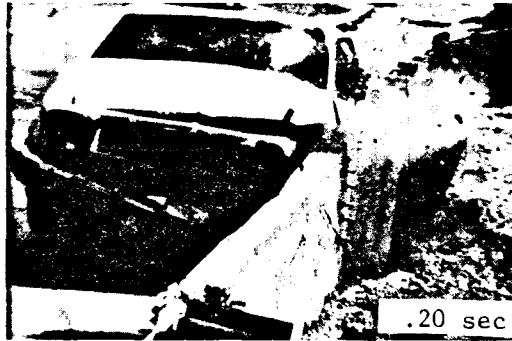


Figure 33. Test T-2 photographs.



.05 sec



.25 sec



.15 sec



.35 sec



.35 sec



.40 sec



Figure 34. Sequential photographs, Test T-2.



Figure 35. Test T-3 photographs.

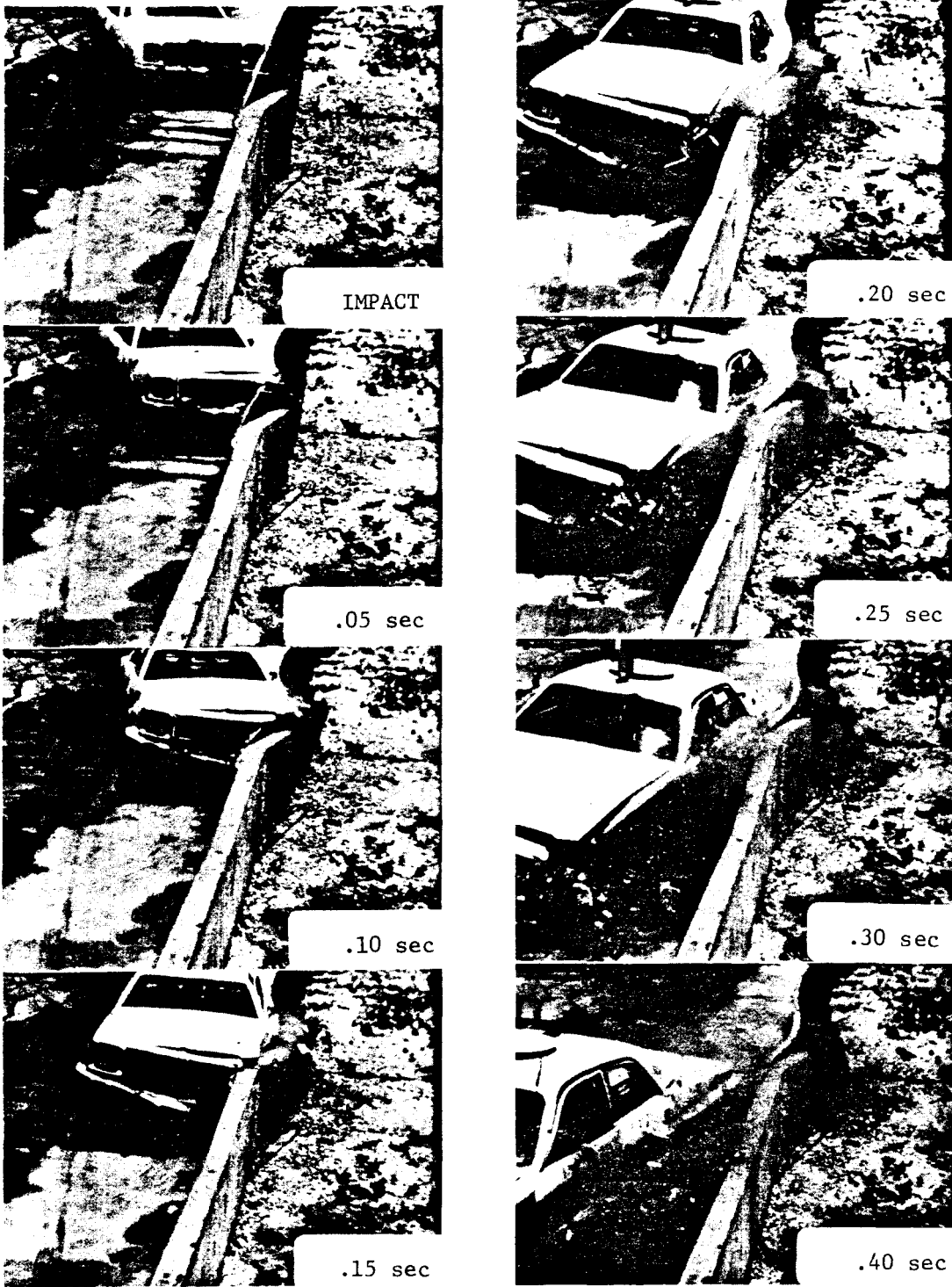


Figure 36. Sequential photographs, Test T-3.

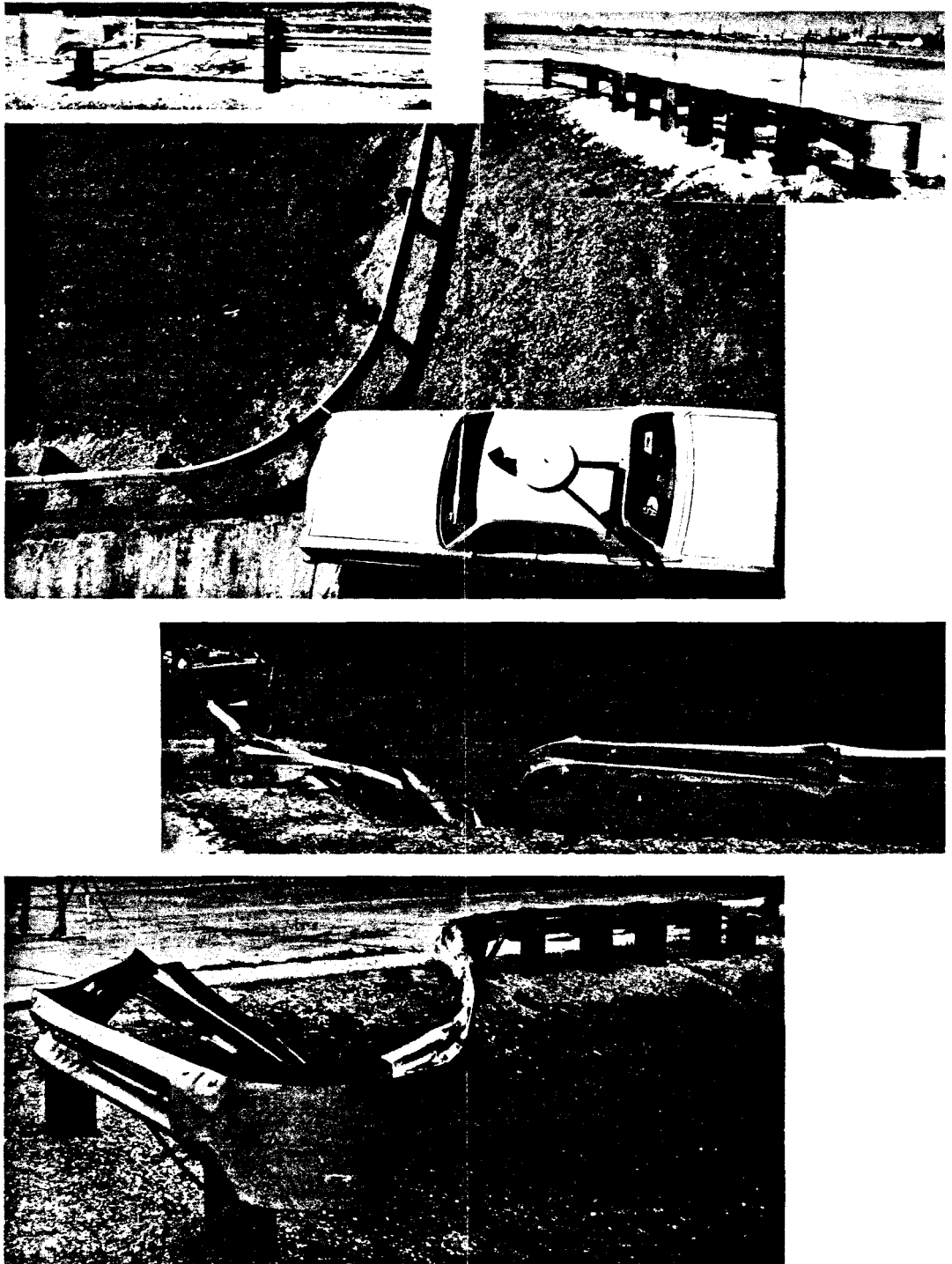


Figure 37. Test WA-1 photographs.

(95-km/h) impact was selected for the first test of the system. A steep 2:1 embankment was simulated by excavating behind the installation.

As shown in figure 38, the vehicle impacted the transition, fractured several wood posts, and was then launched into a rollover-tumbling mode by the system. Pocketing in the system and the leaning of posts in the soil contributed to the launching of the vehicle.

Test WA-1M. Some changes in the posts and beam anchorage details were made in the previous test installation as shown in figure 39. A pipe section used at the end anchorage post permits the beam to rotate about the end post without applying torsion to the post. In addition, breakaway posts were substituted in the curved beam area.

Impact conditions selected for this test were 60 mph (95 km/h) and 25-degree angle with an 1800-lb (800-kg) car. The purpose of this test was to examine the containment capacity of the modified design and determine the occupant risk values. The vehicle was contained as shown in figure 40 by the system although the 37 ft/s (11.3 m/s) longitudinal ΔV value exceeded the recommended value of 30 ft/s (9 m/s) of NCHRP Report 230.⁽⁴⁾

Test WA-2M. Based on the results of the previous test, it was obvious that the containment capacity of the system would not be sufficient to restrain a 4500-lb (2000-kg) car impacting at 60 mph (95 km/h). Accordingly, an additional 12.5 ft (3.8 m) of beam was added to the secondary roadside to give the system more "stroke" as shown in figure 41. Conditions for this test included a 4500-lb (2000-kg) car impacting the nose of the system at 60 mph (95 km/h) and 15-degree angle. As shown in figure 42, all of the posts on the secondary roadside were fractured during the impact. Due to the length of the simulated embankment, the vehicle was partially stopped by the slope of the downstream end of the excavation as shown in figure 41.

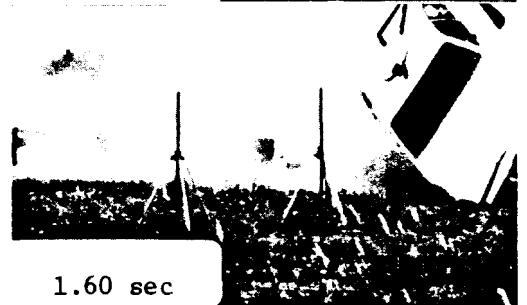
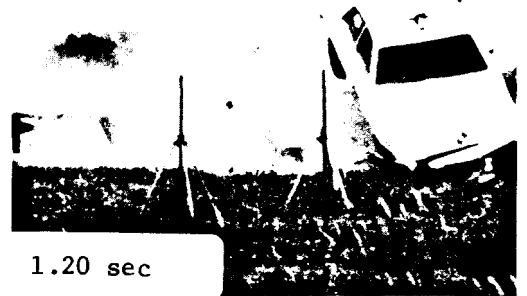
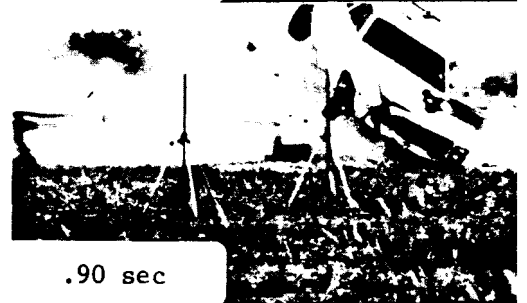
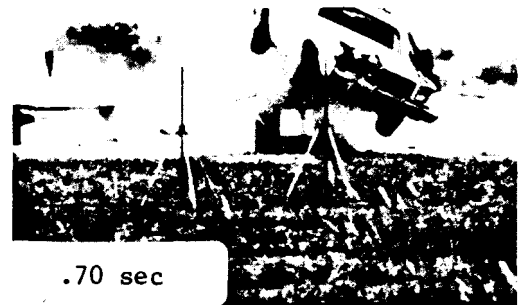
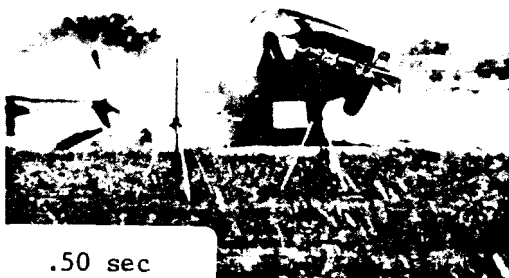
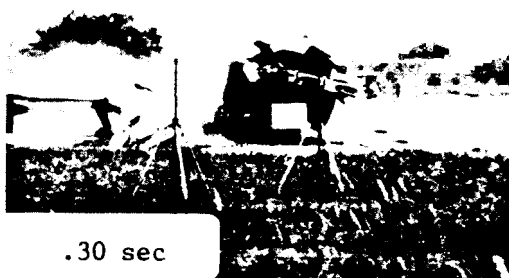
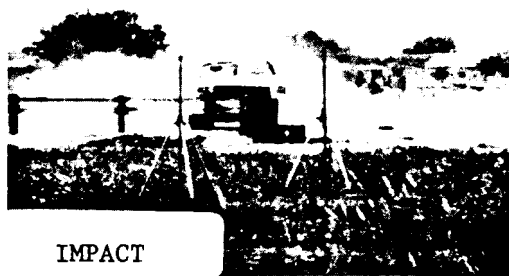


Figure 38. Sequential photographs, Test WA-1.

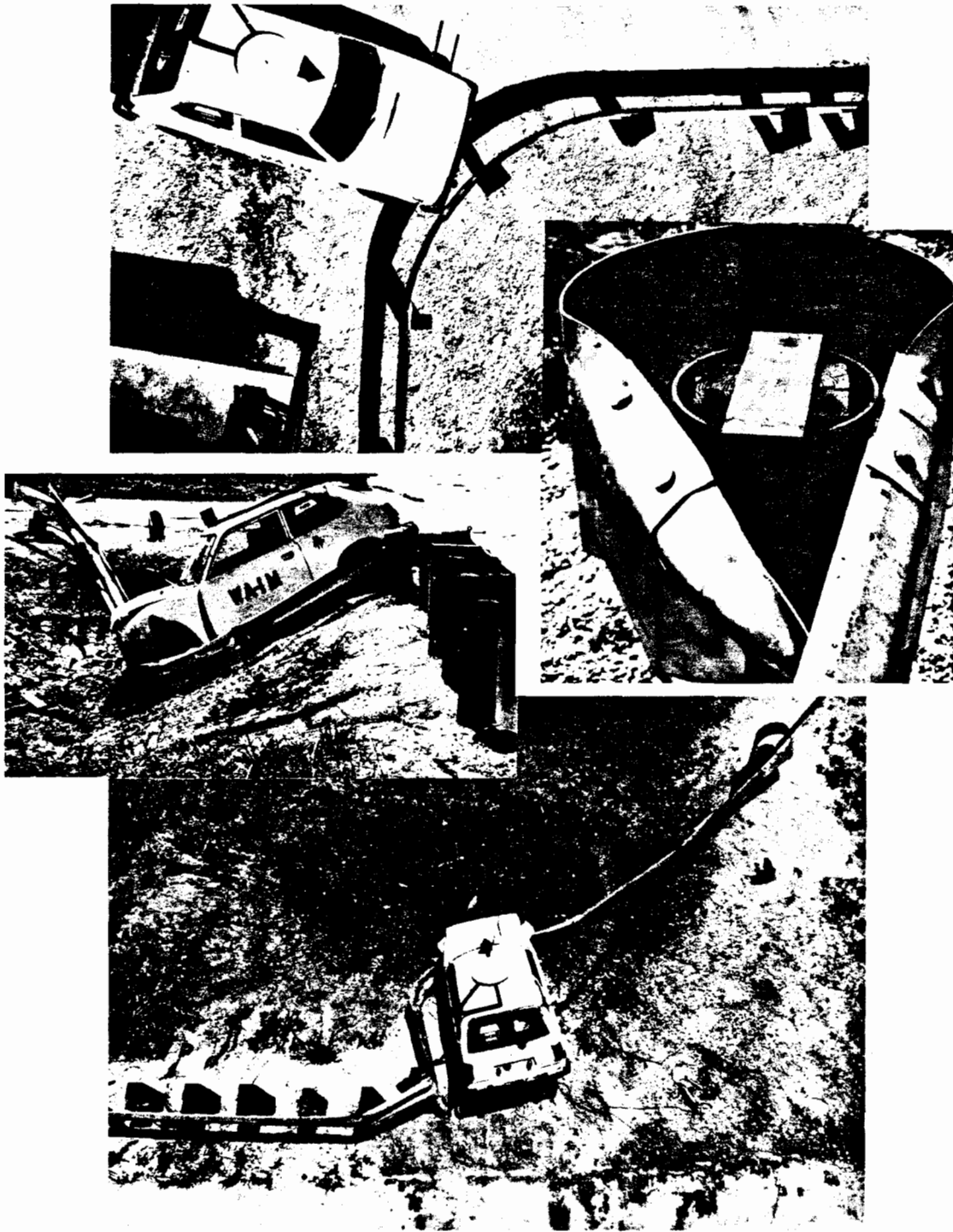


Figure 39. Test WA-1M photographs.

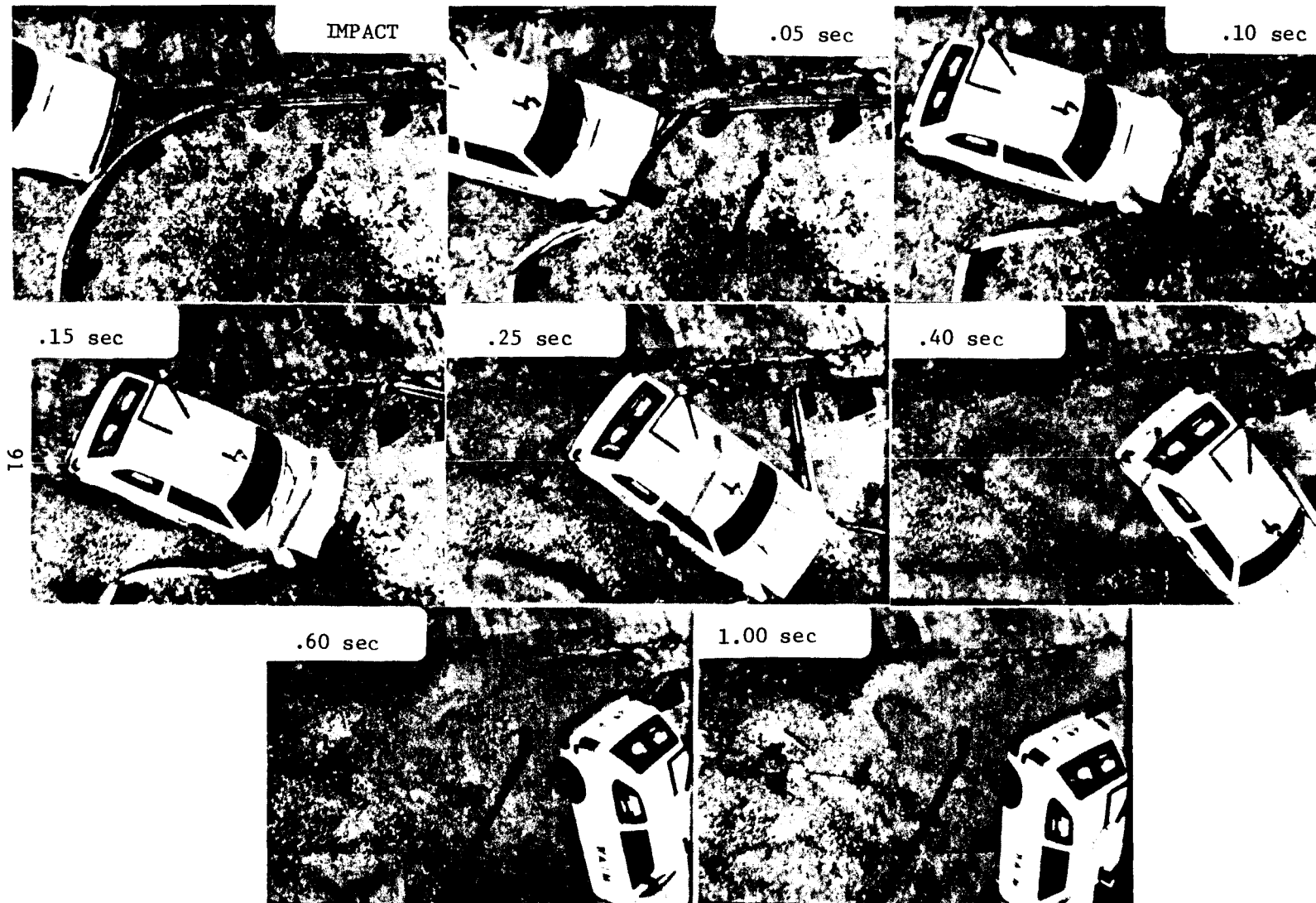


Figure 40. Sequential photographs, Test WA-1M.

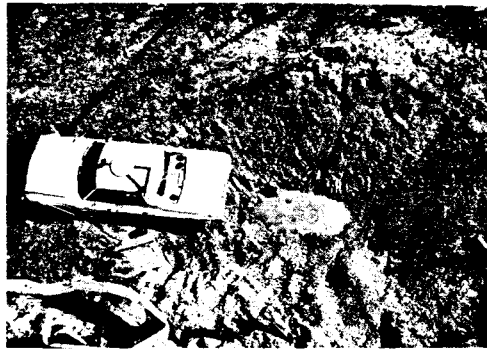
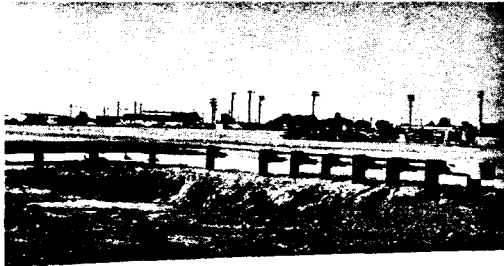


Figure 41. Test WA-2M photographs.

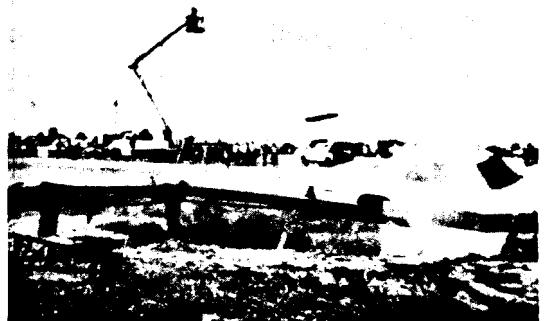
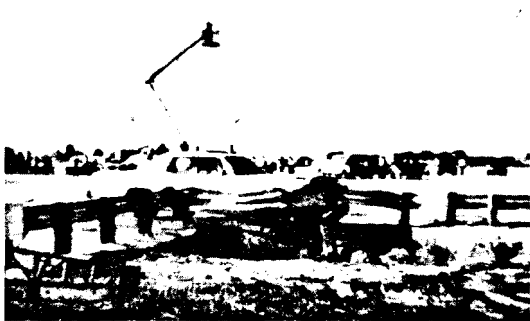
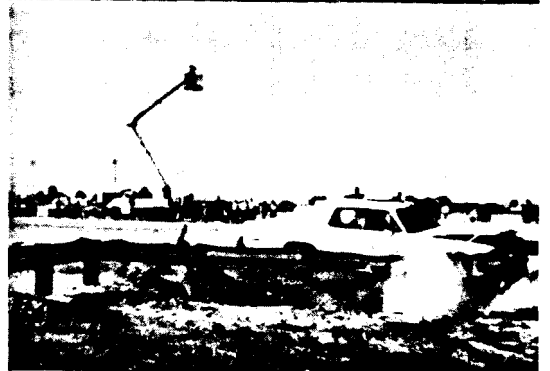
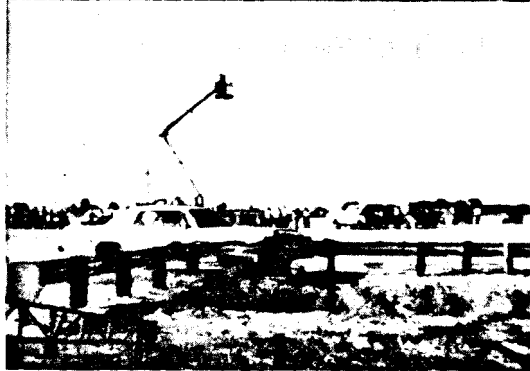
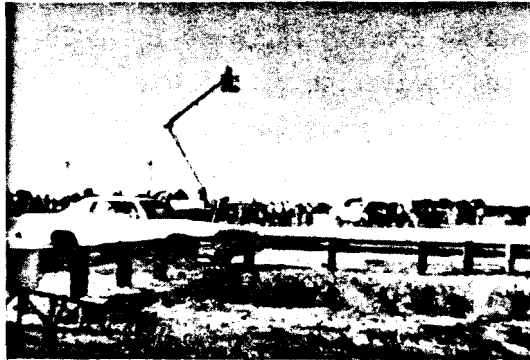


Figure 42. Sequential photographs, Test WA-2M.

Test WA-3M. Based on the results of the previous test, it was concluded that additional anchorage was needed to contain the 4500-lb (2000-kg) vehicle. In addition, the length of the excavation behind the installation was increased to allow the vehicle to continue down the ditch.

An anchorage system was installed that used a second cable attached to the end anchor cable and a second post foundation as shown in figure 43. The attachment to the second post foundation is not "breakaway" and thus provides a positive anchor after all of the secondary road posts have failed. Failure of the end post releases the first cable as designed for end-on impacts from the secondary roadside.

Test conditions were the same as the previous test. As shown in figure 44, the vehicle broke through the railing early in the event due to beam failure at the first impacted post. The failure of this beam was attributed to snagging of the bolt head in the slot of the beam which initiated tearing.

Test WA-4M. Due to the beam tearing that occurred in Test WA-3M, the bolt was omitted at Post 6 where the beam tearing occurred in that test. This bolt is not required for support of the beam and based on Tests WA-1M and WA-2M, the beam tearing was considered to be a freak occurrence that could only be attributed to the bolt. All other details were identical to the previous test.

The vehicle impacted the barrier with the same conditions as the two previous tests and was contained by the system. The vehicle began a clockwise (looking down) yaw during the event as shown in figure 45 and the rear end eventually yawed over the barrier before coming to rest as shown in figure 46 with approximately one-third of the vehicle protruding beyond the end of the bridge. The beam and anchorage system remained intact and successful containment of the vehicle was achieved.

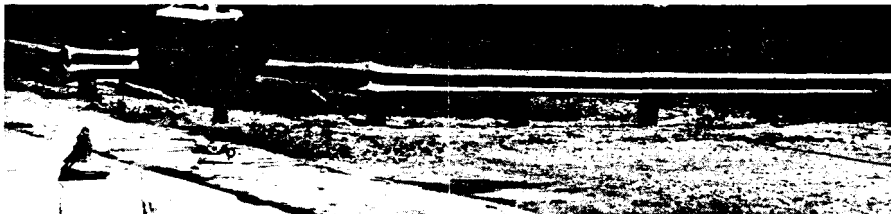
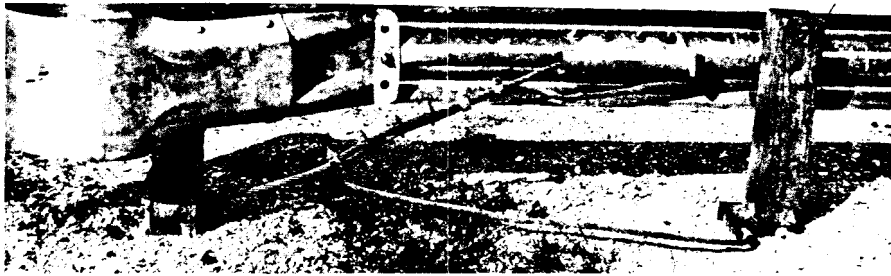
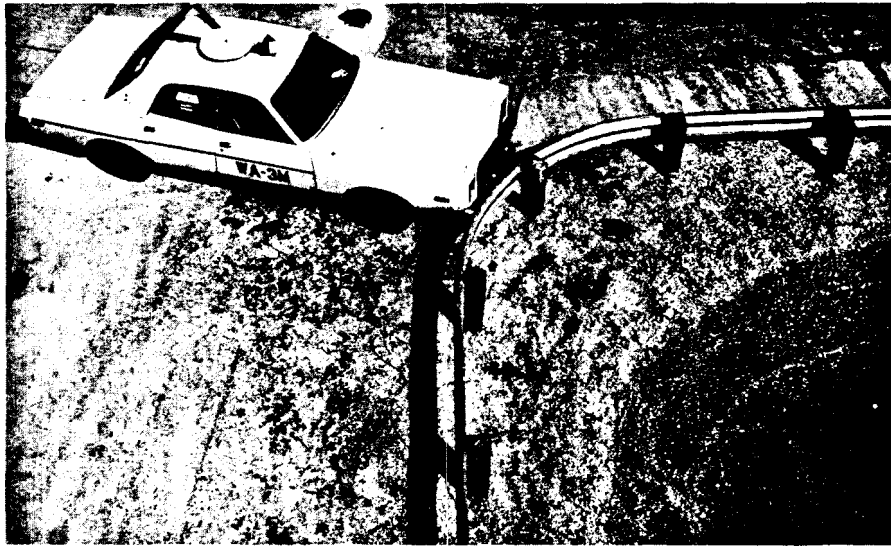


Figure 43. Test WA-3M photographs.

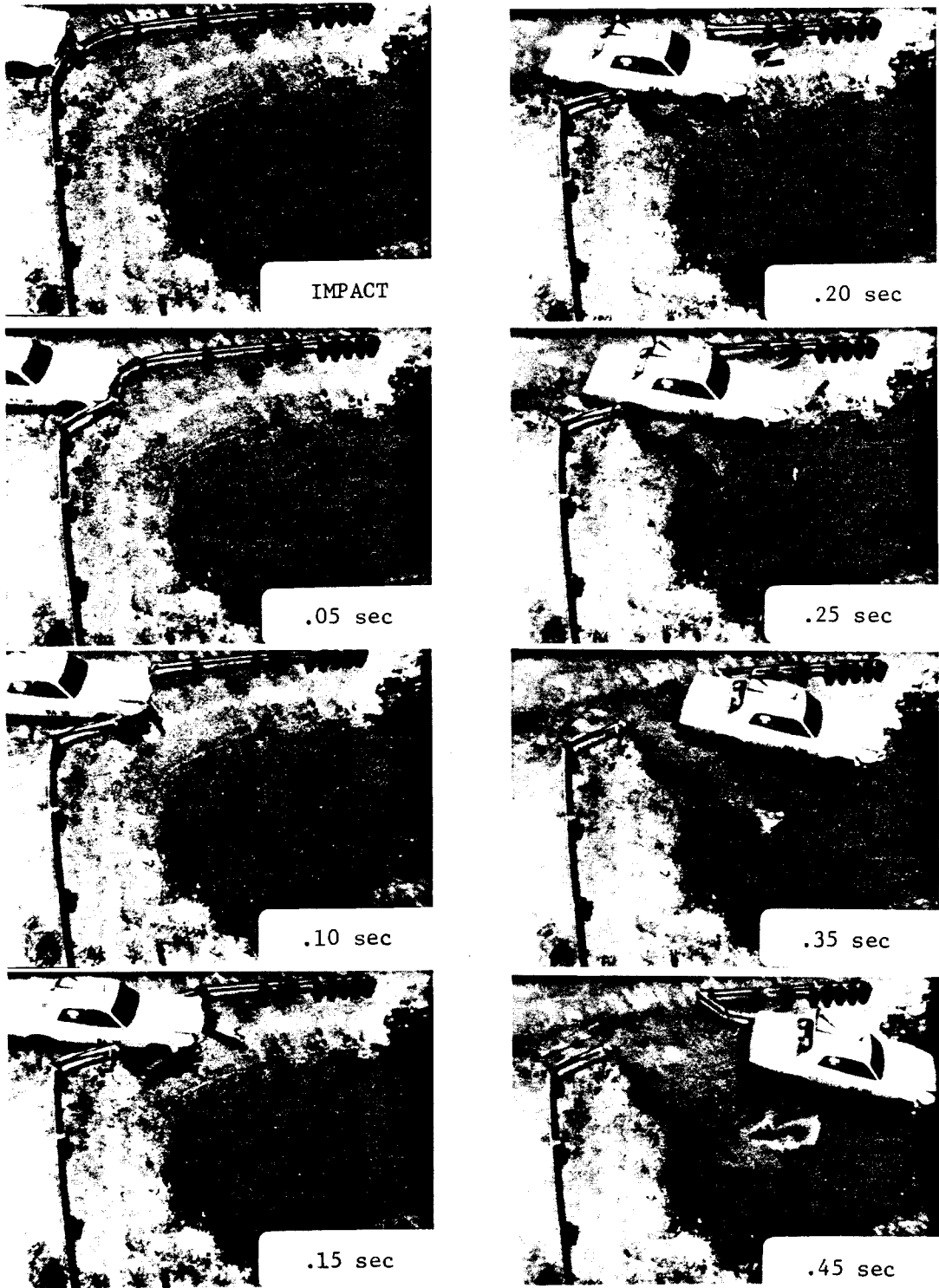


Figure 44. Sequential photographs, Test WA-3M.

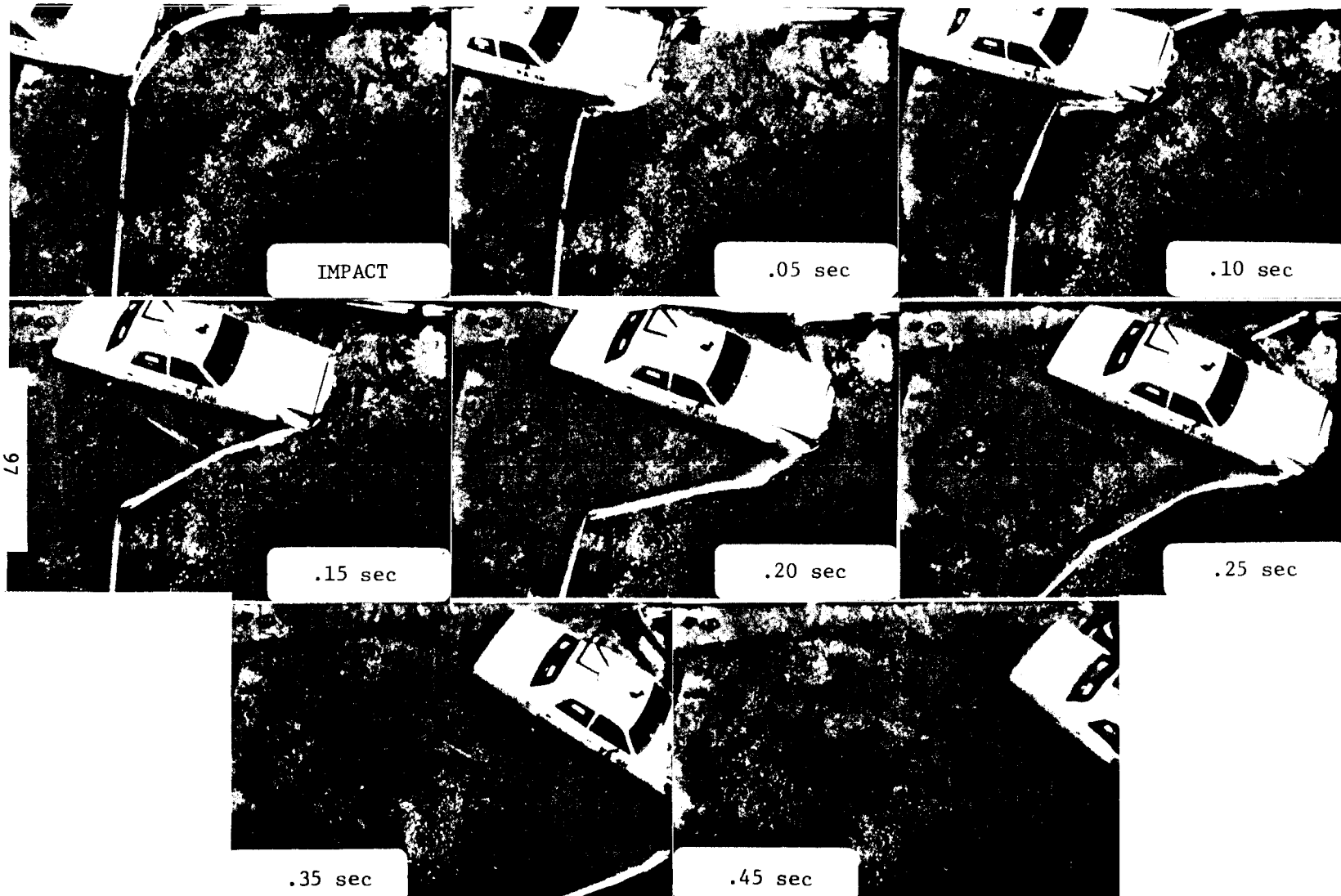


Figure 45. Sequential photographs, Test WA-4M.



Figure 46. Test WA-4M photographs.

Test WA-5M. This test repeated the test conditions of the first test on the Washington design (WA-1). The installation was identical to the previous test as shown in figure 47.

The vehicle impacted the barrier as shown in figure 48 and was smoothly redirected. All elements of the barrier performed as designed.

e. W-Beam/Independent Block

Use of an independent block at bridge approaches has one significant advantage; i.e., it provides an opportunity to have the approach guardrail independent of the bridge structure which is desirable at significant expansion joints. In addition, an independent end block provides a ready retrofit requiring no physical connection to the bridge rail.

Two independent end blocks were tested in this project. One was a State standard and the other was designed using the criteria described in the next section. Unsuccessful results were obtained in the State standard, but the independent block design using the project criteria performed as desired.

Test NV-1. This test evaluated the transition for a G4(2W) guardrail system to an 18-ft (5.5-m) long concrete end block embedded 10 in (25 cm) in the ground. The end block transitioned from a relatively flat wall at one end to the New Jersey safety shape at the other end as shown in figure 49. Steel box spacers between the W-beam and flat wall portion were used to block-out the beam. The transition included six 3 ft-1 1/2 in (1.0-m) post spacings and use of 10x10 posts adjacent to the block end.

The 4500-lb (2000-kg) test vehicle impacted the transition upstream of the block end as shown in figure 50 and was redirected. Significant vehicle snagging occurred at the block end and first steel spacer. Considerable roll of the block occurred which is undesirable due to

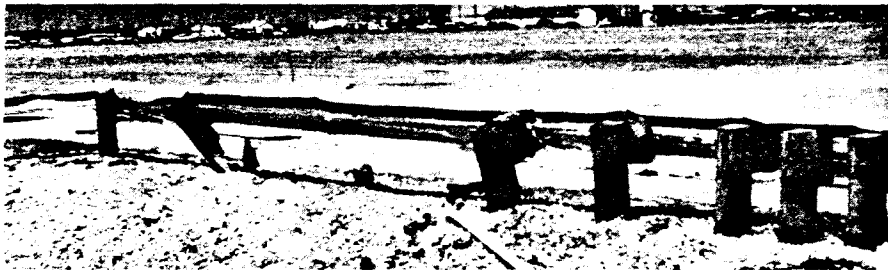
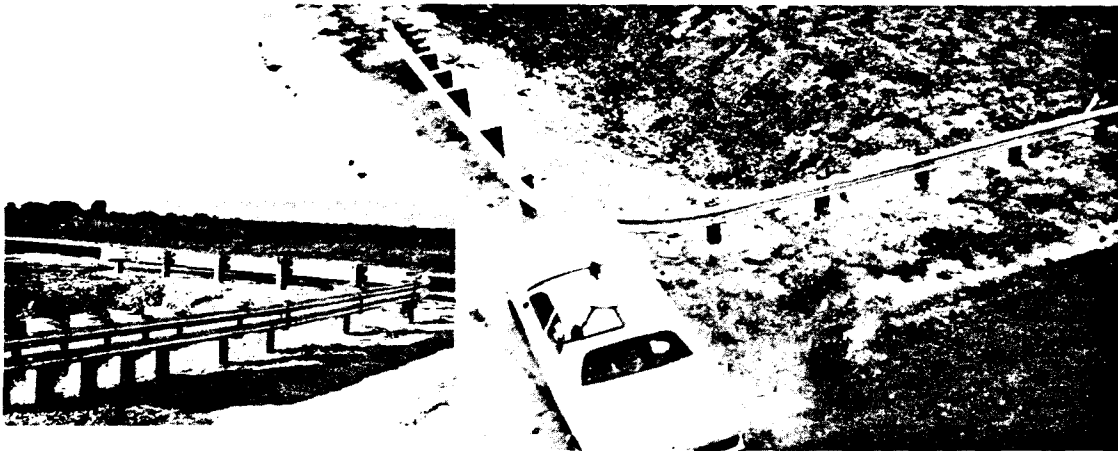


Figure 47. Test WA-5M photographs.

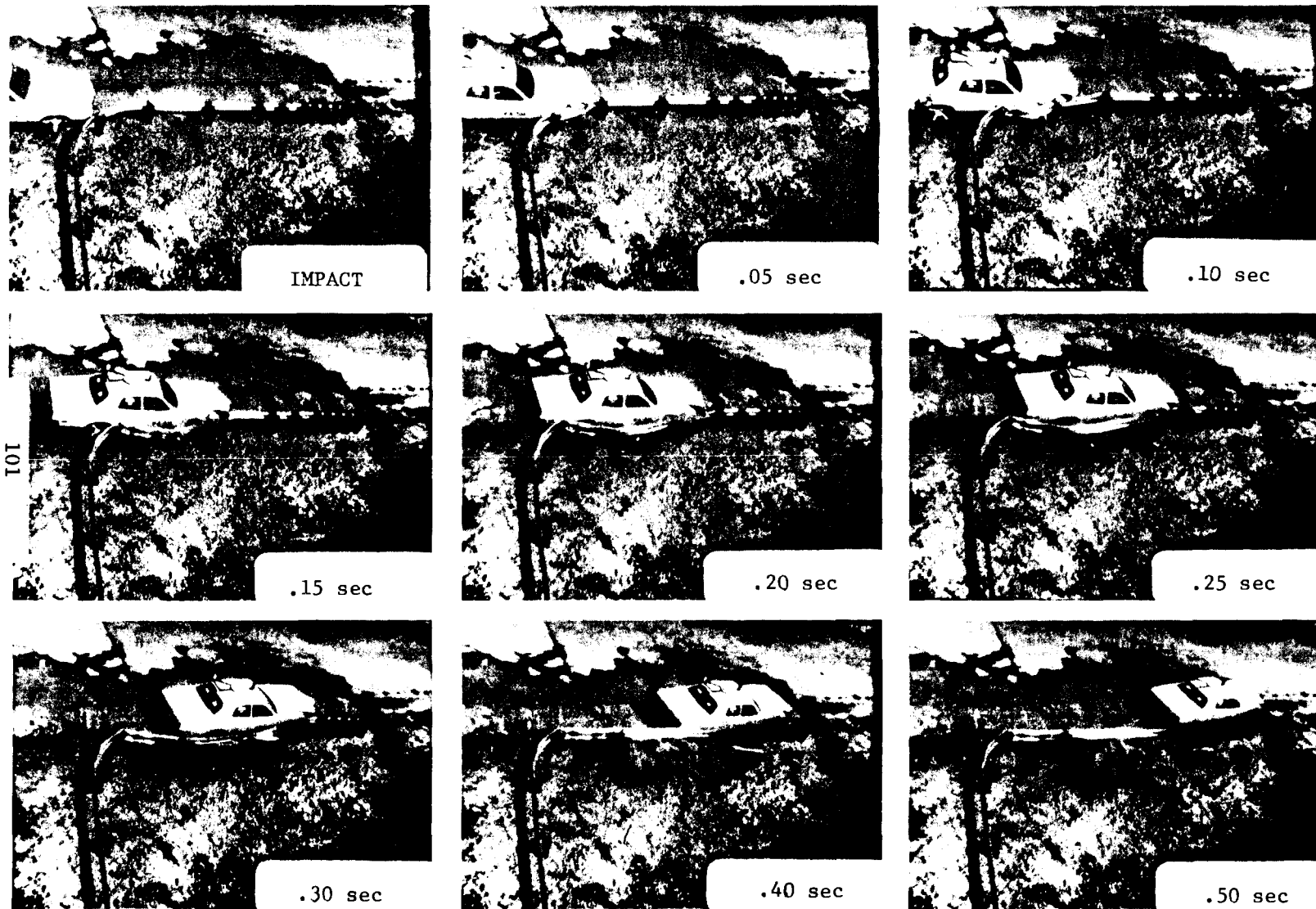


Figure 48. Sequential photographs, Test WA-5M.

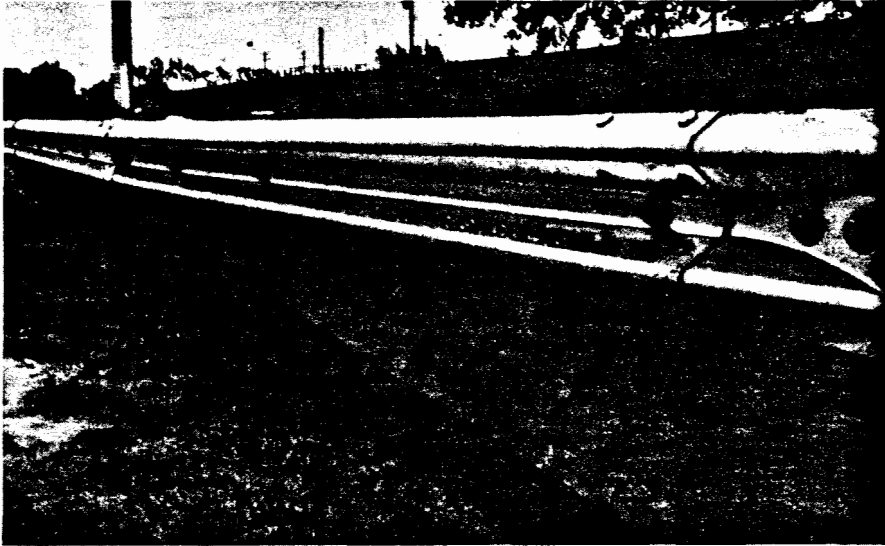


Figure 49. Test NV-1 photographs.

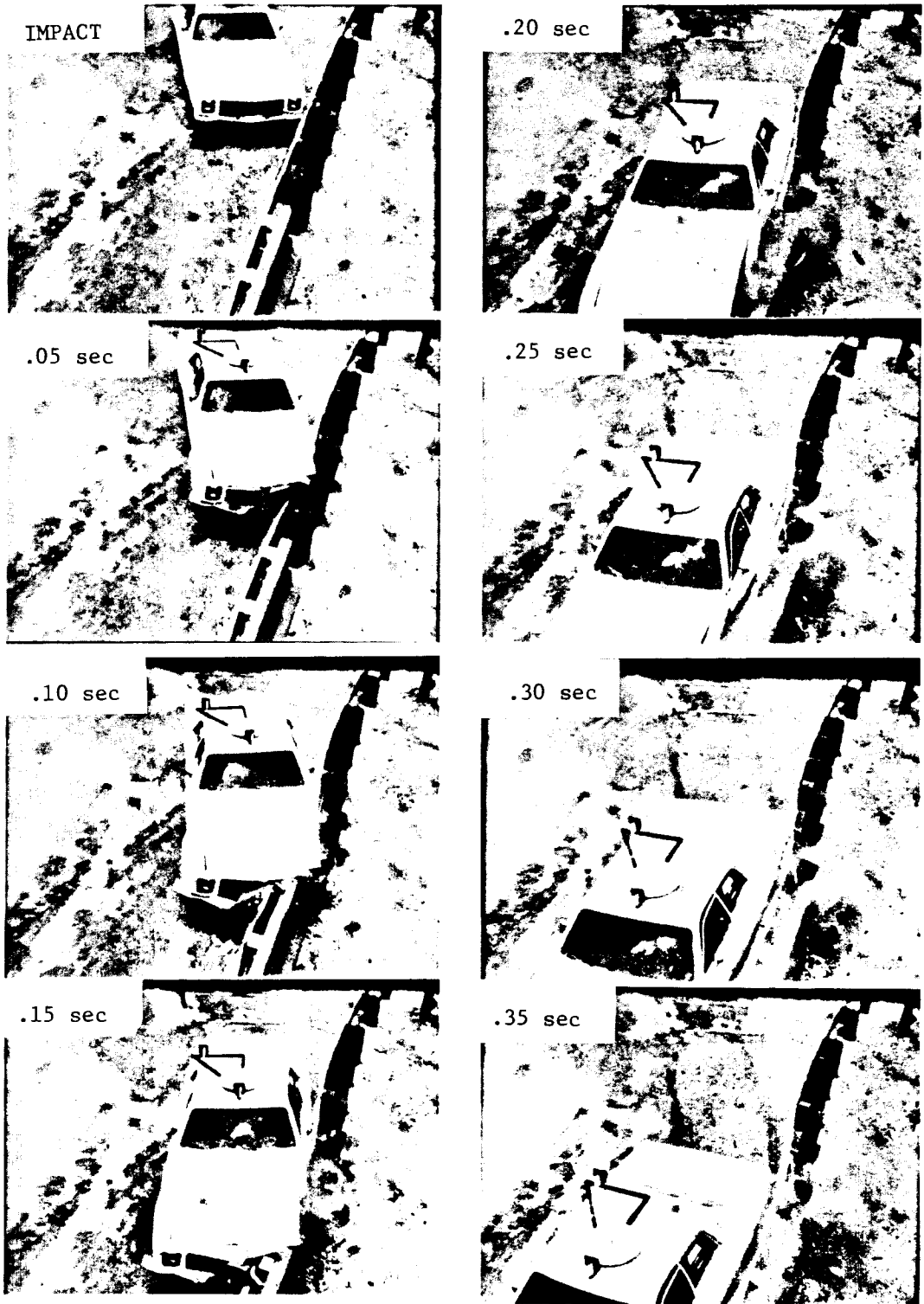


Figure 50. Sequential photographs, Test NV-1.

potential for exposing the bridge end to impacting vehicles. There was significant fracturing of the end block as shown in figure 49. Results of the test were considered to be unsatisfactory due to the rolling of the barrier and the snagging that occurred.

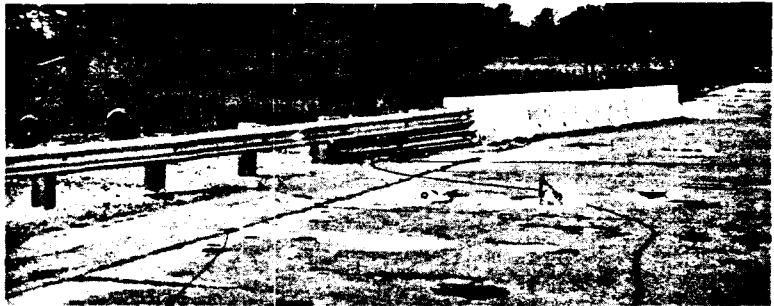
Test IB-1. This test evaluated a 10-ft (3.0-m) long independent block that used the same flat wall to safety shape transition geometry as a current State standard. The block was embedded 2 ft-6 in (0.8-m) below grade. The standard practice developed previously in this project was used in this test; i.e., reduced post spacings of 1 ft-6 3/4 in (0.5-m) and 3 ft-1 1/2 in (1.0-m) near the block end, a double W-beam at the end and a single 12 ft-6 in (3.8-m) W-beam rub rail at the end as shown in figure 51.

The 4500-lb (2000-kg) test vehicle was smoothly redirected as shown in figure 52. No significant movement of the end block was noted.

f. W-Beam/Tapered Curb

Use of a tapered curb to transition from the lower segment of a concrete safety shape to a 5 in (13 cm) high bituminous (or other material) curb was evaluated in this test. A current State standard was modified based on experience gained in this project. The reduced post spacing concept identified in previous testing and a double W-beam at the end were features that were included along with the details of the State standard as shown in figure 53.

Test TC-1. The tapered curb detail was impacted with the full-size car and redirected although wheel snagging on the exposed edge of the concrete safety shape occurred due to translation of the tapered curb. Although the vehicle was redirected as shown in figure 54, improved performance would have resulted from a more substantial anchoring of the tapered curb.



It should be noted that the damage to the top of the vehicle was caused by a secondary impact with a tree.

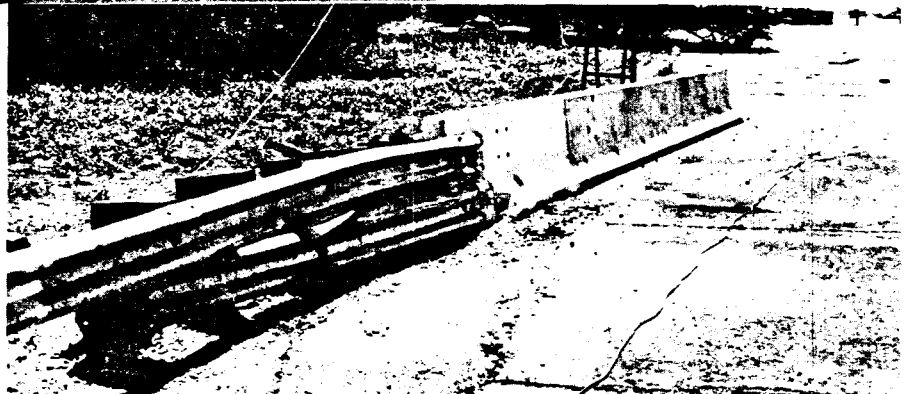


Figure 51. Before and after photographs, Test IB-1.

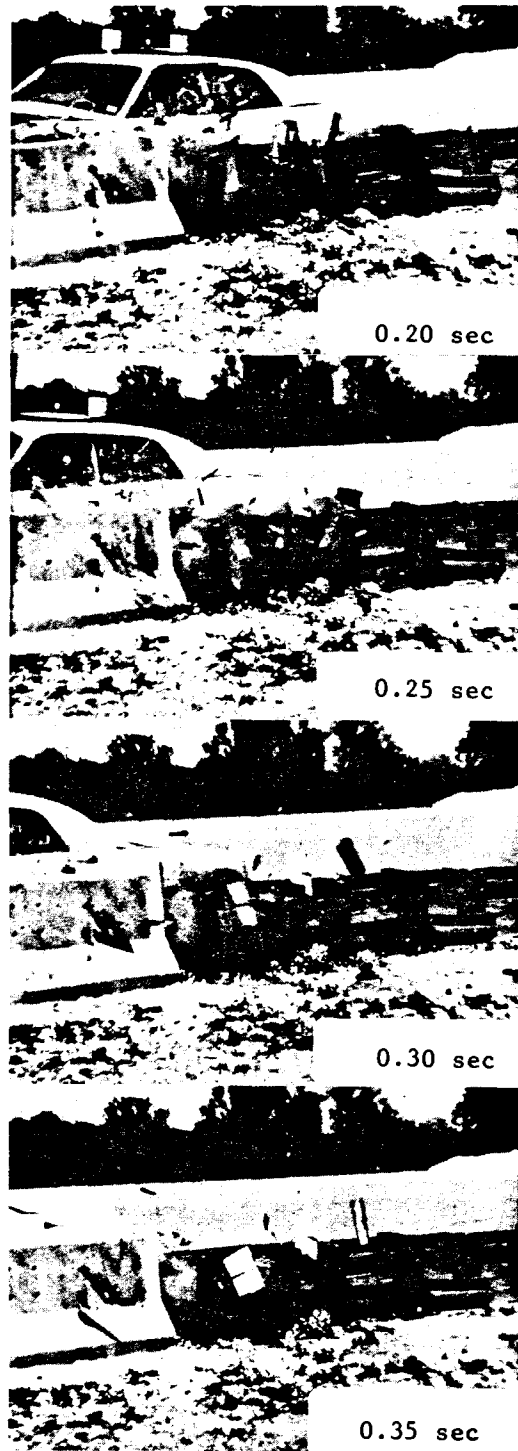
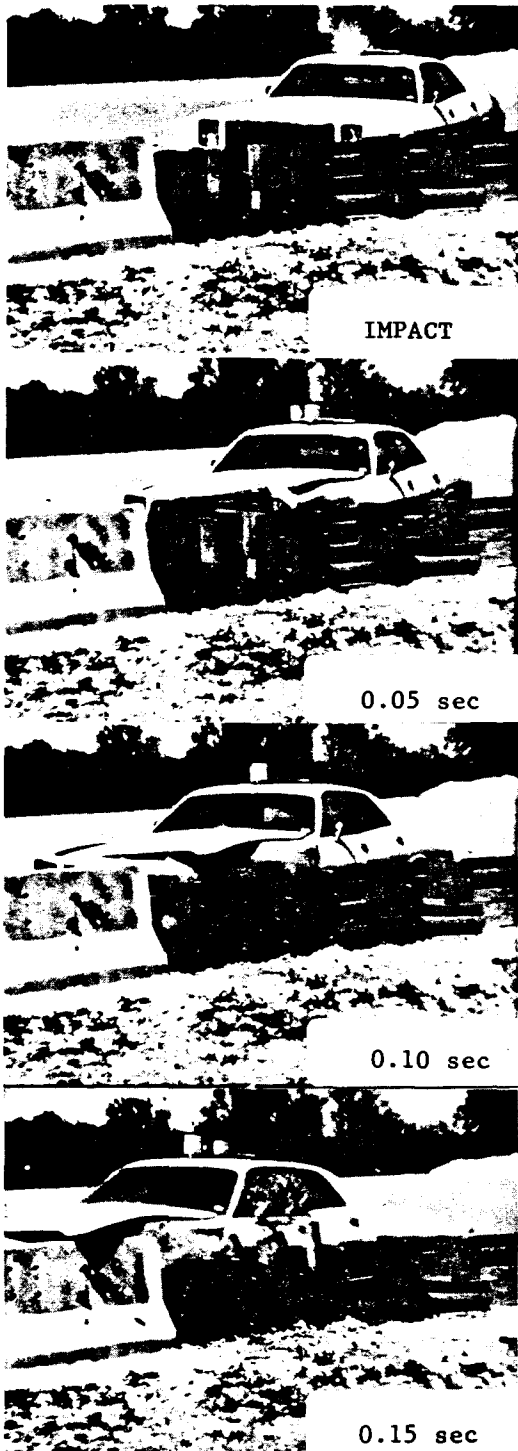


Figure 52. Sequential photographs, Test IB-1.

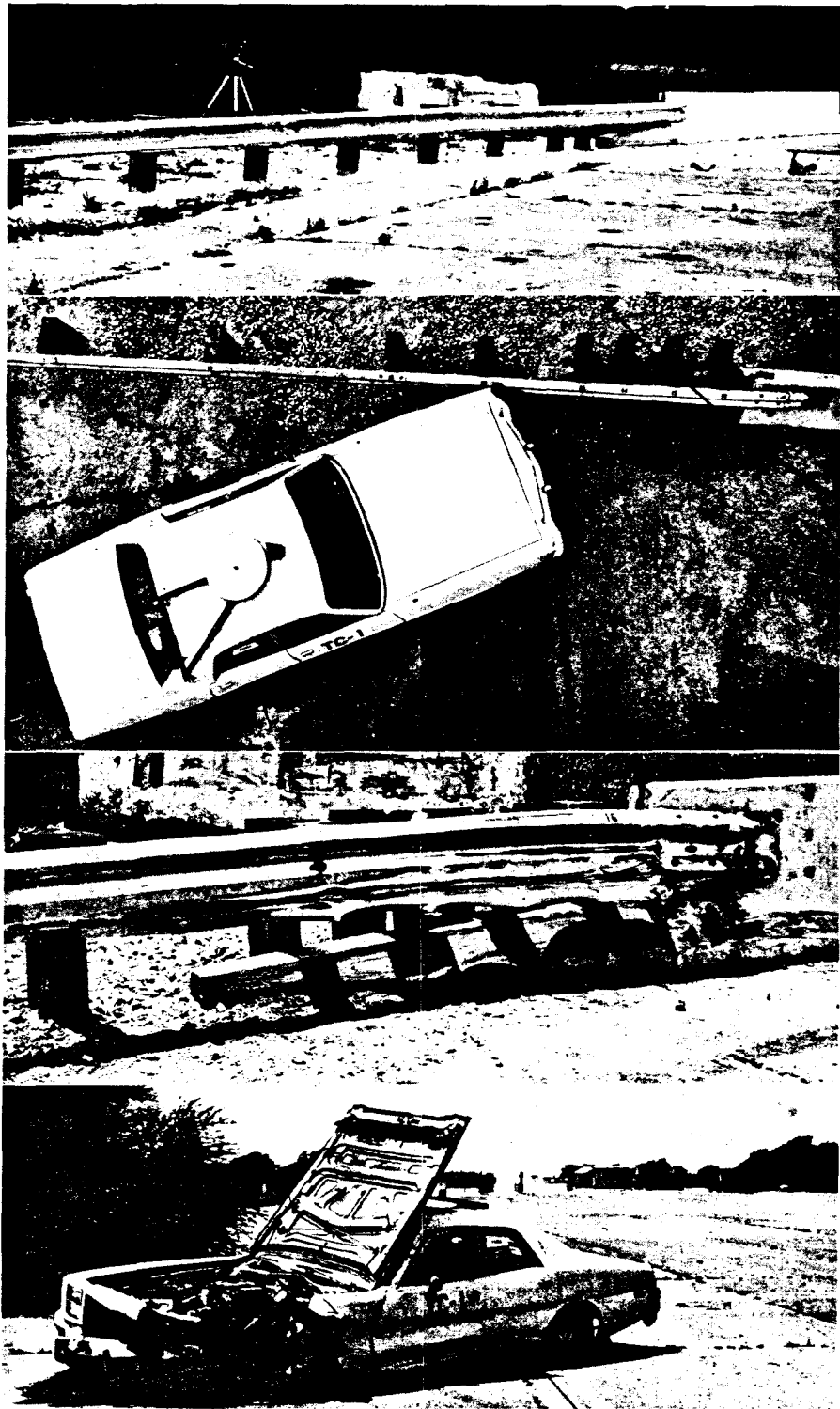


Figure 53. Before and after photographs, Test TC-1.

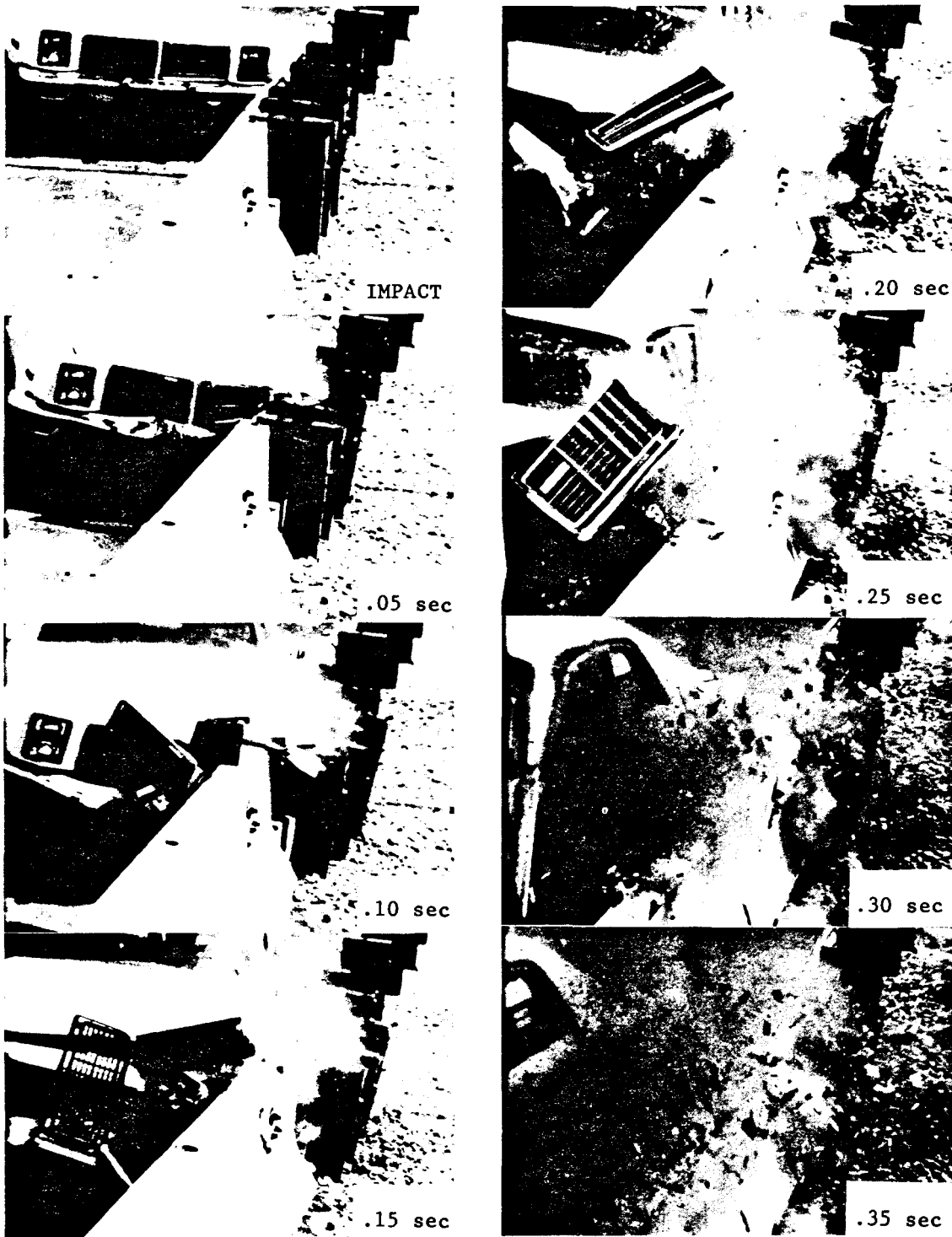


Figure 54. Sequential photographs, Test TC-1.

4. Design of Independent Anchor Blocks

a. Introduction

An independent anchor block is a structure whose purpose is to provide a nearly rigid fixed support for an approach guardrail. In most instances, this is accomplished by using a very large mass to anchor the guardrail system. The following sections discuss a simple method for analyzing and designing independent anchor blocks.

There are two distinct types of loadings which typically occur during a vehicle impact with an anchored approach guardrail; these two scenarios are shown in figure 55. Load case no. 1 represents a significant loading condition where lateral overturning forces are transmitted to the anchor block in addition to the longitudinal sliding forces. In this case, the block will rotate, causing a shear failure behind the anchor as the base of the block "kicks" out of the soil. In load case no. 2, where the vehicle strikes downstream of the anchorage, the anchor block must resist the tensile force transmitted by the guardrail beam. This force will cause the block to slide through the soil, causing shear failure on the soil's bearing surface.

A force-time history of an independent anchor block derived from the BARRIER VII simulation program is shown in figure 56. The solid lines represent an idealized force-time history and the data points are the BARRIER VII estimates at each time step. These data are used to represent both W-beam and thrie beam transitions to concrete end blocks. On using these idealized force-time histories and the two worst-case scenarios depicted in figure 55, the following sections will present a simplified independent anchor block analysis procedure and a set of design curves to be used for selecting the footing width, embedment depth, and wall length required to ensure adequate anchor performance.

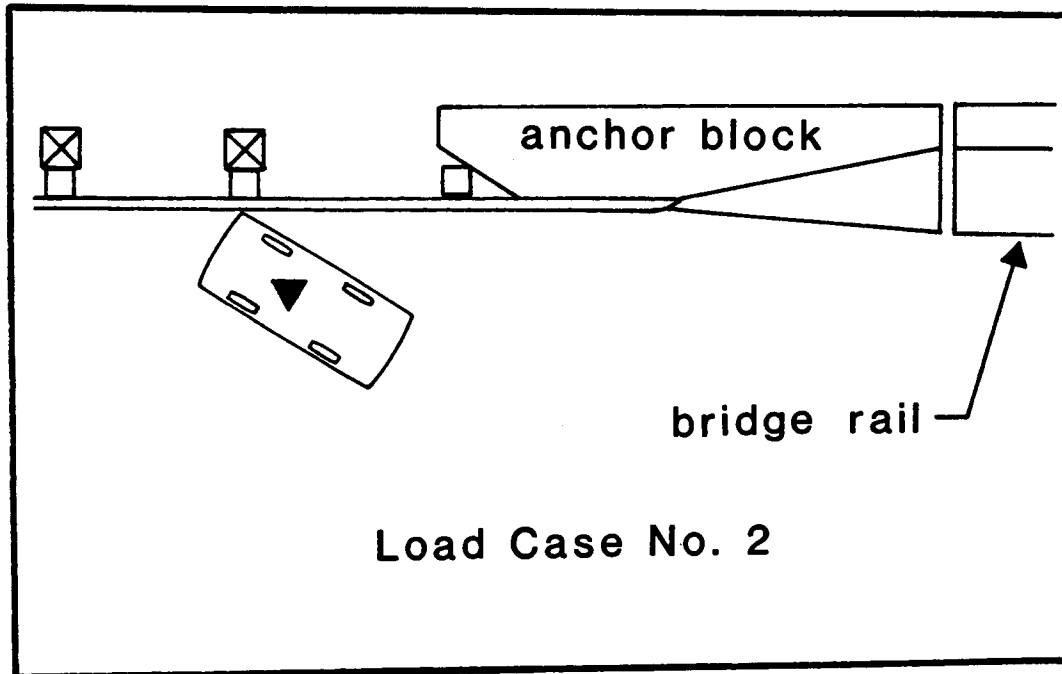
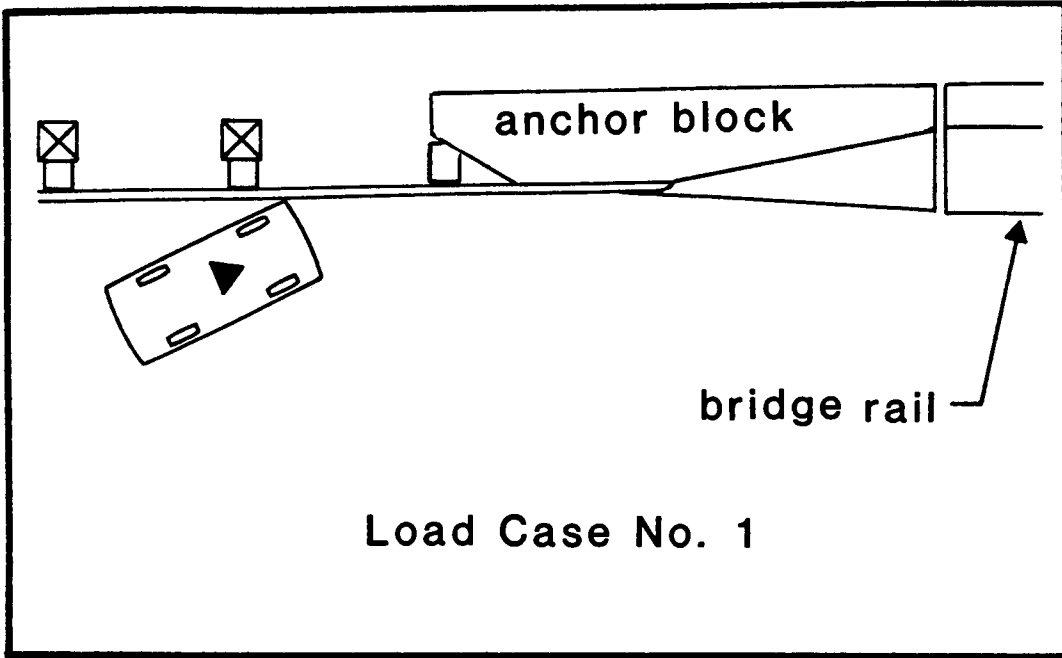


Figure 55. Critical load case for an independent anchor block.

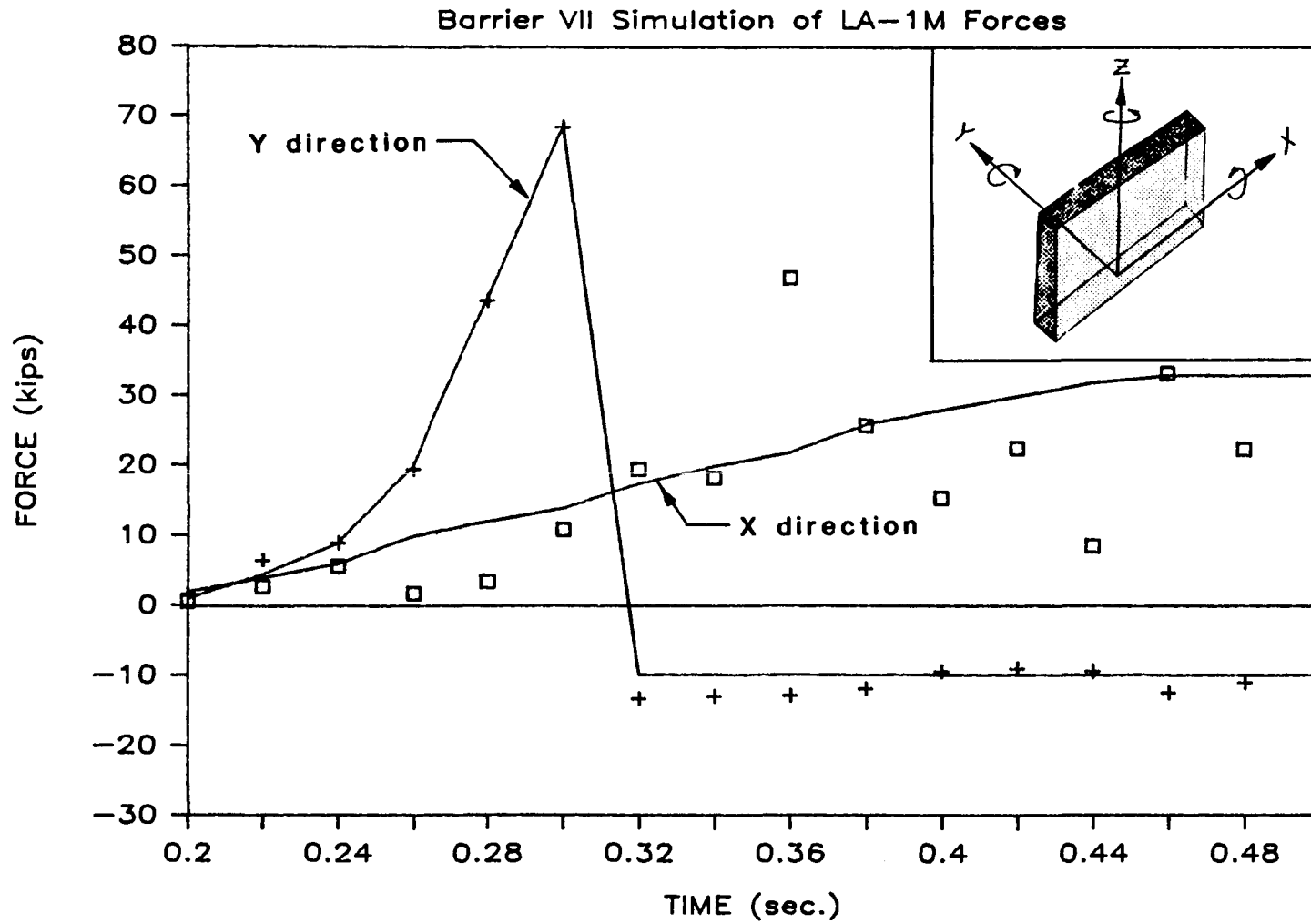


Figure 56. Idealized wall-force/time history.

b. Ultimate Strength of Soils

The behavior of soils during dynamic large deflection events is very difficult to model. Soil is a highly non-linear material, it is not homogenous, and its strength depends on many factors for which the designer has no knowledge or control. Except under very small deflections, soils behave plastically and not elastically. There is, therefore, some ultimate plastic load with which the soil will resist motion regardless of the magnitude of the deflection. Figure 57 shows a force-deflection plot of a guardrail post which illustrates the plastic behavior of soils when subjected to large dynamic forces.⁽⁵⁾ For both rotational and translational deflections, the soil behaves elastically for only 10 percent of the total deflection; the remaining 90 percent of the deflection exhibits plastic behavior.

The force drops below the ultimate value for several reasons in figure 57. First, as the post rotates, it is also being pulled from the ground, leaving less soil in contact with the post. Secondly, according to the Coulomb earth pressure theory,⁽⁶⁾ the lateral earth pressure decreases as the rotation increases. If rotations, in the case of figure 57, are less than 20 degrees, the idealized constant ultimate load will provide a good estimate of the soil strength. Since the purpose of the following procedure is to assist designers of independent blocks, the idealized ultimate soil resistance was used since the deflections cannot be excessive. In the range of deflections which will be acceptable to the designer, the ultimate resistance is nearly constant.

The assumption that the soil's ultimate load is perfectly plastic greatly simplifies developing equations of motion for the anchor block. The anchor block must satisfy dynamic equilibrium at each time step; the sum of the applied forces, resisting forces, and acceleration forces must all sum to zero. The acceleration acting on the block during any time step is therefore merely the sum of the resisting and applied forces divided by

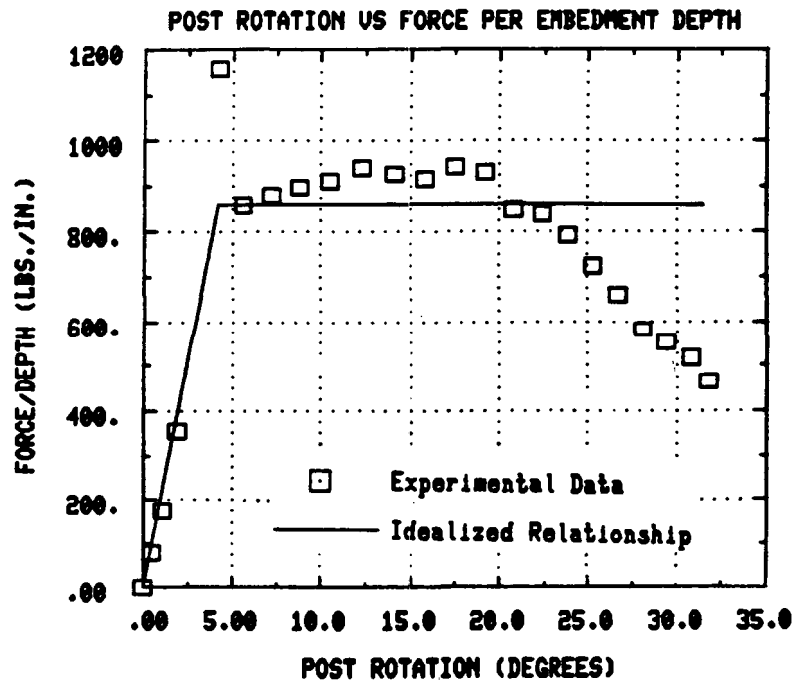
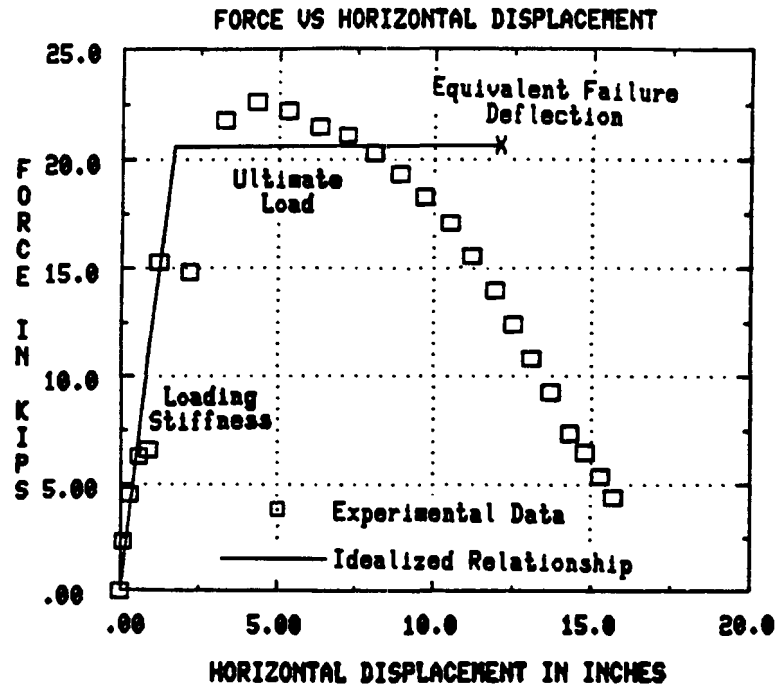


Figure 57. Force-displacement behavior of a dynamically loaded guardrail post. (5)

the mass property of the block. The equations of motion will be developed fully in the next subsection.

Determining the lateral earth pressure coefficient is a critical factor in determining the strength of soils. Terzaghi presents the following expression for lateral earth pressure:⁽⁷⁾

$$P_d = \gamma d (K_p - K_a) \quad (1)$$

where P_d = lateral earth pressure
 γ = unit weight of soil
 d = depth of interest
 K_p = passive earth pressure
 K_a = active earth pressure.

The Coulomb formulation of the active and passive earth pressures was used because it incorporates the rotation of the wall as well as the angle of internal friction, angle of wall-soil friction, and the slope of the backfill. For soils with large values of ϕ , the angle of internal friction, the passive pressure is much larger than the active pressure.⁽⁶⁾ Well graded base materials that are typically used as the foundation for road surfaces generally have values of ϕ between 40 and 53 degrees. The term K_a , therefore, can be neglected because it is very small compared to K_p . The Coulomb formulation of the passive pressure is given by:

$$K_p = \frac{\sin^2 (\alpha + \phi)}{\sin^2 \alpha \sin (\alpha + \delta) \left[1 - \sqrt{\frac{\sin (\phi + \beta) \sin (\phi + \delta)}{\sin (\alpha + \beta) \sin (\alpha + \delta)}} \right]^2} \quad (2)$$

where K_p = passive earth pressure coefficient
 α = wall rotation
 δ = angle of wall-soil friction
 ϕ = angle of internal friction
 β = slope of the backfill.

Unfortunately, the soil strength estimated using this form of K_p is much too low for dynamically loaded soils. When subjected to dynamic loads, soil exhibits much greater strength for several reasons. First, because the event happens very quickly, the soil moisture has no time to drain. This hydrodynamic resistance arises because the water cannot be pushed through the soil pores quickly enough; the end effect is to create miniature hydraulic cylinders which resist the applied load. A more important effect, especially in well-drained soils where there is little water present, is the inter-particle friction. In static tests, the particles will align themselves and flow slowly. During dynamic events, the particles are not aligned and cannot flow as quickly because of higher inter-particle friction. One reason for specifying well-graded base material is to provide a wide range of particle sizes which will ensure a high degree of inter-particle friction.

Although rationalizing the soil behavior is easily done, it is far more difficult to quantify its effects. Dewey et al⁽⁸⁾ reported on a number of static and dynamic tests of guardrail posts embedded in soil. By comparing the magnitudes of the ultimate loads observed in static and dynamic tests, it was determined that soils, or at least well-graded crushed stone, were approximately 5 times stronger during dynamic events than during static events. The lateral passive earth pressure coefficient in the following analysis was therefore multiplied by this factor of 5 to provide a more realistic estimate of the lateral soil strength.

The final and perhaps most critical factor in estimating lateral soil strength is the shape of the soil pressure distribution. Figure 58 shows a distribution empirically derived by Seiler⁽⁹⁾ for laterally loaded timber poles. The choice of the shape of the pressure distributions will define the point of rotation.

Using the rationale outlined above, equations for soil resistance were developed and are presented in the following section.

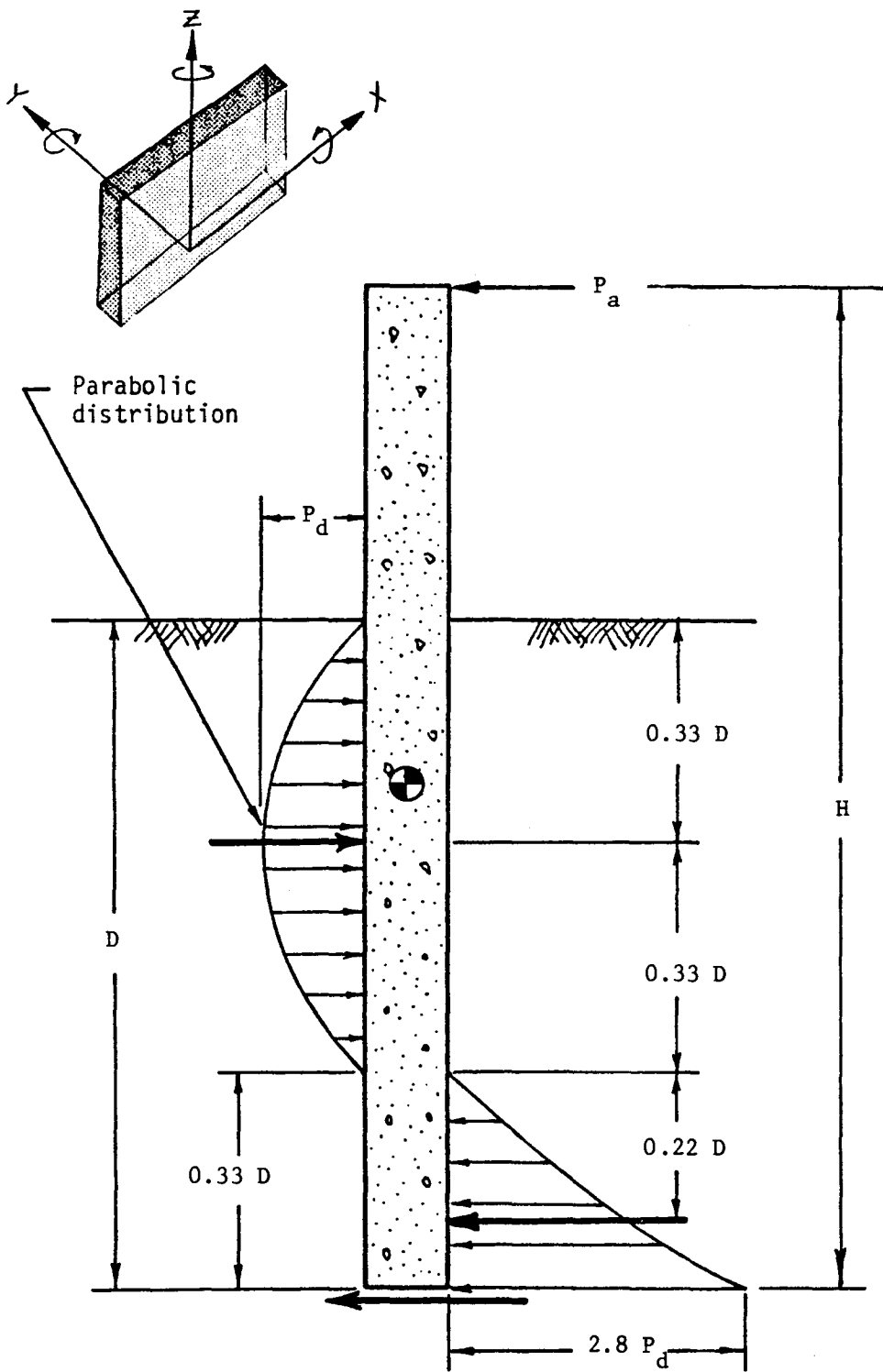


Figure 58. Seiler's lateral post soil pressure distribution. (8)

c. Analysis of the Independent Block

Since dynamic equilibrium must be satisfied at each time step, a short 200 line BASIC program called IBAP (Independent Block Analysis Program) was written to solve the large number of repetitive equations quickly. The following sections present the derivation of the equations used in the analysis program.

The first step in writing equations of motion for the independent block is to calculate the resultant acceleration for each degree of freedom. At each time step, the sum of the applied and resisting forces must be equal to the acceleration of the block for dynamic equilibrium, or:

$$P_{an} + P_{rn} = \frac{A_n}{I_n} \quad (3)$$

where P_{an} = applied load in the degree of freedom n direction
 P_{rn} = resistance in the degree of freedom n direction
 A_n = acceleration in the degree of freedom n direction
 I_n = inertial property of the block for the nth degree of freedom
 n = degree of freedom number, from 1 through 6.

x and y Translation

On referring to Seiler's pressure distribution shown in figure 58, the following equations can be written for the x and y translational degrees of freedom:

$$A_x M = P_{ax} - R_{1x} + R_{2x} - \mu W_b \tan \phi$$

where A_x = resulting acceleration in the x direction
 M = mass of the block
 μ = coefficient of soil-block friction
 W_b = weight of the anchor block
 P_{ax} = applied load in the x direction.

The last term represents the contribution of base friction to the total resistance. On recognizing that the distribution in figure 58 is parabolic, expressions for R_1 and R_2 can be rewritten as:

$$R_1 = \frac{4}{3} \frac{D}{3} P_d = \frac{4DBP_d}{3}$$

$$R_2 = \frac{1}{3} \frac{D}{3} 2.8 P_d = \frac{BDP_d}{3.22}$$

where B = width of block
 D = embedment depth.

Using equation (1) to calculate P_d at a depth of $D/3$ yields the following:

$$P_d = 0.333 \gamma DK_p$$

$$R_1 = 0.148 \gamma D^2 BK_p \quad (4)$$

$$R_2 = 0.104 \gamma D^2 BK_p$$

The x-direction and the analogous y-direction resistances to translation are therefore found to be:

$$A_x M = P_{ax} - .0442 \gamma D^2 BK_p - \mu W_b \tan \phi \quad (5)$$

$$A_y M = P_{ay} - .0442 \gamma D^2 LK_p + \mu W_b \tan \phi$$

where L = block length.

The sign of the base friction term in equations (5) is due to an assumption about how the block is likely to deflect. Since the length will be much greater than the block's width, friction will have the same sense as the applied load for the y direction because base friction will resist

overturning, and the opposite sign for the x direction since pitch rotation is unlikely and friction will oppose the x displacements.

Rotations About the x and y Axes

Rotation about the x axis is called roll and rotation about the y axis is called pitch. Again, the equations are analogous for both x and y rotations. Figure 58 shows the forces which resist rotations of the anchor block.

$$A_{\text{roll}} I_{xx} = \frac{1}{2} P_{ay} H + R_1 \left(\frac{H}{2} - \frac{2D}{3} \right) - R_2 \left(\frac{H}{2} - \frac{D}{4.5} \right) - \mu W_b \tan \phi \left(\frac{H}{2} \right)$$

Substituting equations (4) into the above expression and simplifying yield:

$$A_{\text{roll}} I_{xx} = \frac{1}{2} P_{ay} H + \gamma D^2 L K_p [.0221H - .0756D] - \frac{1}{2} W_b H \mu \tan \phi \quad (6)$$

$$A_{\text{pitch}} I_{yy} = \frac{1}{2} P_{ax} H + \gamma D^2 B K_p [.0221H - .0756D] - \frac{1}{2} W_b H \mu \tan \phi$$

Rotations About the z Axis

The remaining degrees of freedom are the yaw rotations about the z axis and displacement in the z direction. It was assumed that displacement in the z direction was negligible. The acceleration, therefore, in the z direction was always set to zero.

Yaw is not a primary mode of displacement since the overturning and sliding strength are generally much less. In loading case 2, yaw rotation is ignored since the guardrail beam is attached very near the y-z center of gravity, and the moment arm is therefore very small. For load case 2, yaw is more likely to occur although it will generally not be significant since yaw rotation will reduce the potential for snagging since the bridge rail end of the anchor block will rotate into the traveled way where it will shield the vehicle from snagging on the bridge rail.

Yaw resistance arises mainly from frictional forces acting on the bearing surfaces of the block. On referring to figure 59, the resisting force and the applied force produce the following acceleration.

$$A_{\text{yaw}} I_{zz} = \frac{P_{ax} B}{2} - \frac{P_{ay} L}{2} - \frac{\gamma D^2 K_{BL}}{4} \quad (7)$$

Equation (7) illustrates an area where care should be exercised in applying these equations; if $P_{ay}L$ is larger than $P_{ax}B$, then the resistance acts in the opposite direction. When solving these equations by hand, one must ensure that the resistive forces always oppose the motion of the block. The anchor block program automatically checks the applied loads, resisting loads, and displacements to ensure that the resistance always opposes the block's motion.

Equations of Motion

With the foregoing equations representing the block's acceleration at any time step, the derivation of the block's equations of motion is very straightforward. At each time increment, the applied load is read from an external file and the acceleration terms are calculated using equations (5)-(7). The velocity and displacement of each degree of freedom are given by the following equations:

$$V_{i,n} = V_{i-1,n} + A_{i,n} \Delta t \quad (8)$$

$$\Delta_{i,n} = \Delta_{i-1,n} + 0.5 (V_{i-1,n} + V_{i,n}) \Delta t \quad (9)$$

where $V_{i,n}$ = velocity of block at time i for degree of freedom n
 $A_{i,n}$ = acceleration of block at time i for degree of freedom n
 Δ_{in} = displacement of block at time i and degree of freedom n
 Δt = time increment
 i = time step number
 n = degree of freedom, 1 through 6.

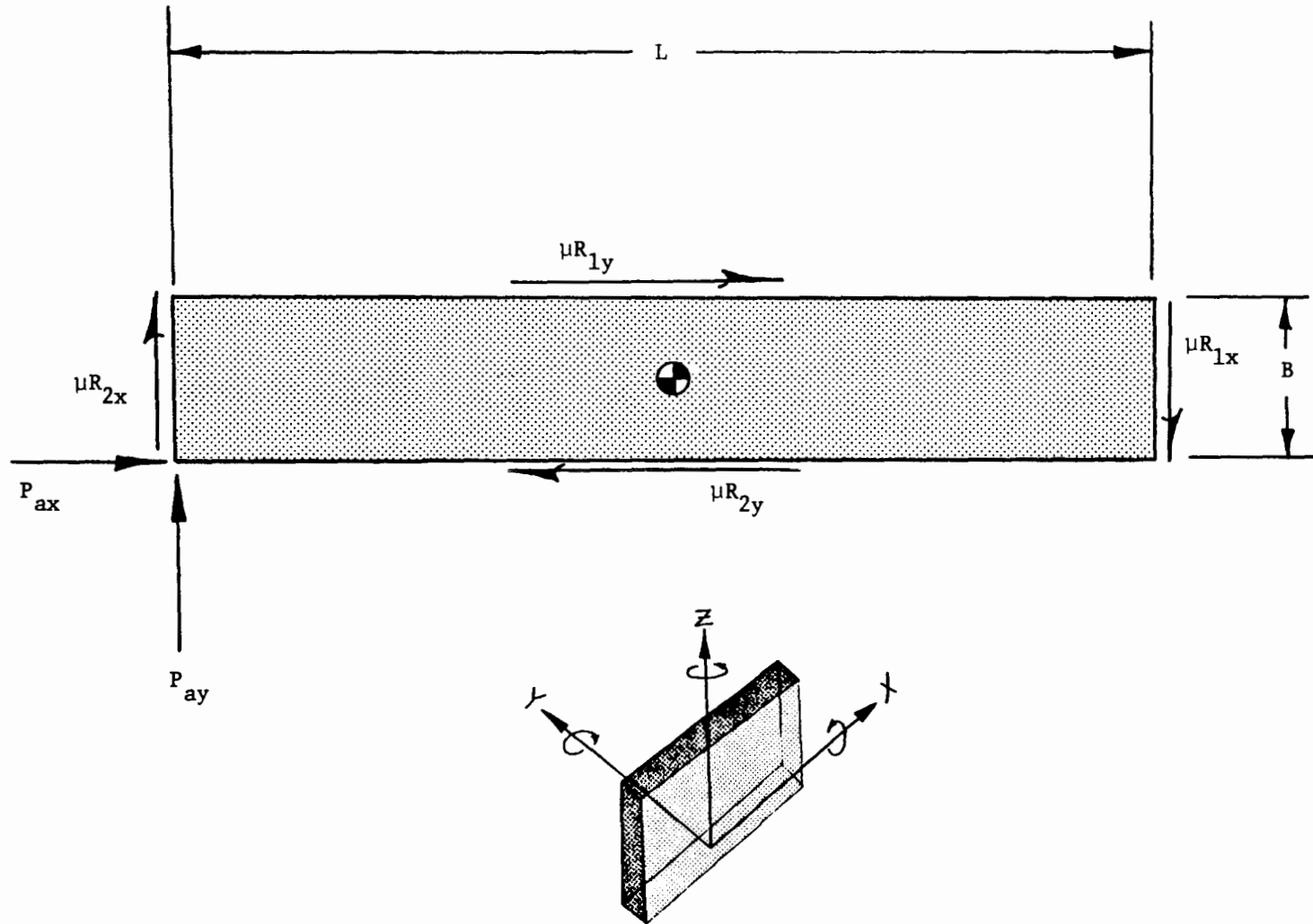


Figure 59. Forces resisting yaw rotation.

The acceleration, velocity, and displacement of each of the block's degrees of freedom can be easily calculated starting at time zero and working incrementally through the last time step.

d. Independent Block Analysis Program

The preceding analysis method was implemented using a short BASIC program written on the IBM PC-XT; the entire program is shown in figure 60. The program is completely interactive, querying the user for the geometry of interest. A sample of the input screen and one of the output options are shown in figures 61 and 62, respectively. The following soil parameters, typical of flexible base materials, were used:

ϕ = angle of internal friction = 45 degrees

μ = coefficient of soil-block friction = 1

δ = angle of soil-block friction = 0 degrees

γ = soil density (if not specified) = 120 lb/ft³ (1922 kg/m³).

e. Design of Independent Anchor Blocks

Using the analysis method presented in the previous section as implemented in the program IBAP, a set of curves was formulated to assist the designer in quickly selecting the wall length, footing width, and embedment depth required. The idealized loading shown in figure 56 was used to simulate case 1 and case 2 loadings.

In order to develop strength, soils must experience some deformation. The curves of figures 63 and 64 were derived by finding the footing width required to prevent an excessive deflection for a given wall length and embedment depth. A width was deemed adequate when the deflection at the point of load application was less than 1 in (2.54 cm). For case 1, the critical deflection would be a y displacement of 1 in (2.54 cm), whereas for case 2, it would be an x displacement. One inch (2.54 cm) was


```

10 '*****
20 '          ANCHOR BLOCK ANALYSIS PROGRAM
30 'The following program calculates the kinematics of an anchor
40 'block subjected to an external loading.
50 '*****
60 '
70 DIM BMASS(6),DISP(20,6),PA(20,6)
80 DIM ACC(20,6),VEL(20,6),DISPA(20,2)
90 DIM VERT%(120)
100 DIM INTENS(1000)
110 NCHOICE = 0
120 SCREEN 2
140   FOR M = 1 TO 6
150     ACC(1,M)=0!
160     VEL(1,M)=0
170     DISP(1,M)=0!
190   NEXT M
210 TEST$="INDEPENDENT BLOCK ANALYSIS PROGRAM"
220 CLS
230 '
240 '***** GEOMETRY INPUT *****
250 '
260 CLS
270 LINE (310,100)-(620,160),,B
280 LOCATE 14,42:PRINT USING "Length      = ##.## ft.";OLDL
290 LOCATE 15,42:PRINT USING "Width      = ##.## ft.";OLDW
300 LOCATE 16,42:PRINT USING "Total Height = ##.## ft.";OLDH
310 LOCATE 17,42:PRINT USING "Embedment Depth = ##.## ft.";OLDD
320 LOCATE 18,42:PRINT USING "Weight      = ##### lbs.";OLDMAS
330 IF NCHOICE = 6 THEN GOTO 580
340 LOCATE 1,22:PRINT TEST$
350 LOCATE 3,6:PRINT "ANCHOR BLOCK GEOMETRY"
360 LOCATE 4,6:PRINT "-----"
370 LINE (10,10)-(290,90),,B
380 LOCATE 5,6:INPUT "LENGTH      (ft.)";XLENG
390 LOCATE 6,6:INPUT "WIDTH      (ft.)";YLENG
400 LOCATE 7,6:INPUT "TOTAL HEIGHT (ft.)";ZLENG
410 LOCATE 8,6:INPUT "EMBEDMENT DEPTH (ft.)";DEPTH
420 LOCATE 9,6:INPUT "WEIGHT      (lbs.)";WEIGHT
430 IF XLENG = 0 THEN XLENG = OLDL
440 IF YLENG = 0 THEN YLENG = OLDW
450 IF ZLENG = 0 THEN ZLENG = OLDH
460 IF DEPTH = 0 THEN DEPTH = OLDD
470 IF WEIGHT = 0 THEN WEIGHT = 140*XLENG*(1.668+(YLENG*DEPTH))
480 '
490 '***** CALCULATE THE BLOCK'S MASS PROPERTIES *****
500 '
520 BMASS(1) = WEIGHT/32.2
530 BMASS(2) = WEIGHT/32.2
540 BMASS(3) = WEIGHT/32.2
550 BMASS(4) = ((ZLENG*ZLENG)+(YLENG*YLENG))*BMASS(1)/12
560 BMASS(5) = ((ZLENG*ZLENG)+(XLENG*XLENG))*BMASS(1)/12
570 BMASS(6) = ((YLENG*YLENG)+(XLENG*XLENG))*BMASS(1)/12
580 LINE (10,100)-(290,160),,B
590 LOCATE 14,10:PRINT "BLOCK MASS PROPERITES"
600 LOCATE 15,10:PRINT "-----"
610 LOCATE 16,10:PRINT USING "Mass = ###. slugs";BMASS(1)
620 LOCATE 17,10:PRINT USING "Ixx = #####. ft^4";BMASS(4)
630 LOCATE 18,10:PRINT USING "Iyy = #####. ft^4";BMASS(5)
640 LOCATE 19,10:PRINT USING "Izz = #####. ft^4";BMASS(6)
650 '
660 '***** ASSIGN SOIL PROPERTIES *****
670 '
680 U=1

```

Figure 60. Independent block analysis program.

```

690 PHI = .785
710 DELTA=0
720 LINE (310,10)-(820,90),,B
730 LOCATE 3,42:PRINT "SOIL PROPERTIES"
740 LOCATE 4,42:PRINT "-----"
750 IF NCHOICE <> 6 THEN LOCATE 5,42:INPUT          "EFFECTIVE SOIL DENSITY      ";
GAMMA
760 IF NCHOICE = 6 THEN LOCATE 5,42:PRINT USING "EFFECTIVE SOIL DENSITY      = ###
";GAMMA
761 IF GAMMA=0 THEN GAMMA=120
762 IF GAMMA<70 THEN U = .333
770 LOCATE 7,42:PRINT USING "SOIL-BLOCK FRICTION COEFF. = #.### ";U
780 LOCATE 8,42:PRINT USING "ANGLE OF INTERNAL FRICTION = #. ";(PHI/.0175)
790 IF NCHOICE <> 6 THEN LOCATE 9,42:INPUT "LOAD CASE TYPE";NCASE
791 IF NCASE=0 THEN NCASE=1
792 IF NCASE=1 THEN OPEN "LOADS.LAT" FOR INPUT AS 1
793 IF NCASE=2 THEN OPEN "LOADS.LNG" FOR INPUT AS 1
800 IF NCHOICE = 6 THEN LOCATE 10,42:INPUT "CONTINUE";CR$
810 IF NCHOICE = 6 GOTO 1290
820 INPUT #1,NSTEPS,TSTEP
860 CLS
870 LOCATE 10,20:PRINT "*** SOLVING THE EQUATIONS OF MOTION ***"
880 ' ***** LOOP FOR EACH TIME STEP *****
890   FOR I = 2 TO (NSTEPS+1)
940     INPUT #1,PA(I,1),PA(I,2),XA,YA,ZA
950     PA(I,3)=-WEIGHT
960     PA(I,4)=PA(I,2)*ZA
970     PA(I,5)=PA(I,1)*ZA
980     PA(I,6)=PA(I,2)*XA-PA(I,1)*YA
981     FOR L=1 TO 2
982       ALPHA=1.5708-DISP(I-1,L+3)
983       RAD=(1-SQR(.651/(SIN(ALPHA)*SIN(ALPHA+DELTA))))^2
984       EPP(L)=5*(SIN(ALPHA-.7854)^2)/((SIN(ALPHA)^2)*SIN(ALPHA+DELTA)*RAD)
985     NEXT L
1000 ' CALCULATE THE ACCELERATIONS ACTING ON THE BLOCK
1002 R1=(DEPTH^2)*GAMMA*EPP(1)
1003 R2=(DEPTH^2)*GAMMA*EPP(2)
1025 ACC(I,1)=(PA(I,1)-.0442*R2*YLENG-U*WEIGHT)/BMASS(1)
1040 ACC(I,2)=(PA(I,2)-.0442*R1*XLENG-U*WEIGHT)/BMASS(2)
1050 ACC(I,3)=0
1078 TERM1=R1*XLENG*(.0756*DEPTH-.0221*ZLENG)
1080 TERM2=U*WEIGHT*ZLENG/2
1085 TERM3=.333*GAMMA*(DEPTH^2)*XLENG*(YLENG+DEPTH)
1110 ACC(I,4)=(PA(I,4)-TERM1-TERM2-TERM3)/BMASS(4)
1120 ACC(I,5)=(PA(I,5)-R2*YLENG*(.0756*DEPTH-.0221*ZLENG)-U*WEIGHT*ZLENG/2)/BMAS
S(5)
1122 IF NCASE=1 THEN ACC(I,1)=0
1123 IF NCASE=1 THEN ACC(I,5)=0
1130 ACC(I,6)=(PA(I,6)-1.9*XLENG*YLENG*(R1+R2)-WEIGHT*XLENG/4)/BMASS(6)
1131 IF NCASE=1 THEN ACC(I,6)=0
1140 ' SOLVE FOR THE KINEMATIC VALUES
1150   FOR N = 1 TO 6
1160     VEL(I,N)=(ACC(I,N)*TSTEP)+VEL(I-1,N)
1170     IF VEL(I,N) < 0 THEN VEL(I,N)=0
1180     DISP(I,N)=DISP(I-1,N)+(.5*(VEL(I-1,N)+VEL(I,N))*TSTEP)
1182     IF DISP(I,N) < 0 THEN DISP(I,N)=0
1190   NEXT N
1200   DISPA(I,1)=(DISP(I,1)-(YA*SIN(DISP(I,6)))-(ZA*SIN(DISP(I,5))))
1210   DISPA(I,2)=(DISP(I,2)+(XA*SIN(DISP(I,6)))+(ZA*SIN(DISP(I,4))))
1220   NEXT I
1230 OLDL = XLENG
1240 OLDW = YLENG
1250 OLDH = ZLENG
1280 OLDD = DEPTH

```

Figure 60. Independent block analysis program (continued).

```

1270 OLDMAS = WEIGHT
1280 CLOSE #1
1290 CLS
1300 LOCATE 10,20:PRINT "SELECT THE OUTPUT TYPE:"
1310 LOCATE 11,20:PRINT " <1> FOR DISPLACEMENTS OF THE C.G."
1320 LOCATE 12,20:PRINT " <2> FOR VELOCITY OF THE C.G."
1330 LOCATE 13,20:PRINT " <3> FOR ACCELERATIONS OF THE C.G."
1340 LOCATE 14,20:PRINT " <4> FOR DISPLACEMENTS AT LOAD APPLICATION"
1350 LOCATE 15,20:PRINT " <5> TO RERUN THE PROGRAM"
1360 LOCATE 16,20:PRINT " <6> VIEW INPUT"
1370 LOCATE 17,20:PRINT " <7> TO EXIT THE PROGRAM"
1380 LOCATE 18,20:INPUT "YOUR CHOICE";NCHOICE
1390 IF (NCHOICE = 2) GOTO 1670
1400 IF (NCHOICE = 3) GOTO 1880
1410 IF (NCHOICE = 4) GOTO 2090
1420 IF (NCHOICE = 5) GOTO 140
1430 IF (NCHOICE = 6) GOTO 280
1440 IF (NCHOICE = 7) GOTO 2270
1450 '***** OUTPUT THE DISPLACEMENTS OF THE C.G. *****
1460 CLS
1470 LOCATE 1,22:PRINT TEST$
1480 LOCATE 6,10:PRINT "TIME"
1490 LOCATE 6,22:PRINT "X"
1500 LOCATE 6,32:PRINT "Y"
1510 LOCATE 6,42:PRINT "Z"
1520 LOCATE 6,50:PRINT "ROLL"
1530 LOCATE 6,60:PRINT "PITCH"
1540 LOCATE 6,70:PRINT " YAW"
1550 LOCATE 3,27:PRINT "DISPLACEMENTS OF THE C.G."
1560 LOCATE 4,27:PRINT " inches and degrees"
1570 FOR L = 1 TO (NSTEPS+1)
1580 LOCATE (L+7),10:PRINT USING "#.###";((L-1)*TSTEP)
1590 FOR N = 1 TO 6
1600 IF N > 3 THEN UNITS = 1/.0175
1610 IF N < 4 THEN UNITS = 12!
1620 LOCATE (L+7),((N+1)*10):PRINT USING "###.##";(DISP(L,N)*UNITS)
1630 NEXT N
1640 NEXT L
1650 LOCATE 25,30:INPUT "CONTINUE";CR$
1660 GOTO 1290
1670 CLS
1680 LOCATE 1,22:PRINT TEST$
1690 LOCATE 3,27:PRINT "VELOCITY OF THE C.G."
1700 LOCATE 4,28:PRINT "in feet per second"
1710 LOCATE 6,10:PRINT "TIME"
1720 LOCATE 6,22:PRINT "X"
1730 LOCATE 6,32:PRINT "Y"
1740 LOCATE 6,42:PRINT "Z"
1750 LOCATE 6,50:PRINT "ROLL"
1760 LOCATE 6,60:PRINT "PITCH"
1770 LOCATE 6,70:PRINT " YAW"
1780 FOR L = 1 TO (NSTEPS+1)
1790 LOCATE (L+7),10:PRINT USING "#.###";((L-1)*TSTEP)
1800 FOR N = 1 TO 6
1810 IF N > 3 THEN UNITS = 1/.0175
1820 IF N < 4 THEN UNITS = 1!
1830 LOCATE (L+7),((N+1)*10):PRINT USING "###.##";(VEL(L,N)*UNITS)
1840 NEXT N
1850 NEXT L
1860 LOCATE 25,30:INPUT "CONTINUE";CR$
1870 GOTO 1290
1880 CLS
1890 LOCATE 1,22:PRINT TEST$
1900 LOCATE 3,27:PRINT "ACCELERATIONS OF THE C.G."

```

Figure 60. Independent block analysis program (continued).

```

1910 LOCATE 4,25:PRINT "units = feet, seconds, and lbs"
1920 LOCATE 6,10:PRINT "TIME"
1930 LOCATE 6,22:PRINT "X"
1940 LOCATE 6,32:PRINT "Y"
1950 LOCATE 6,42:PRINT "Z"
1960 LOCATE 6,50:PRINT "ROLL"
1970 LOCATE 6,60:PRINT "PITCH"
1980 LOCATE 6,70:PRINT " YAW"
1990 FOR L = 1 TO (NSTEPS+1)
2000 LOCATE (L+7),10:PRINT USING "#.###";((L-1)*TSTEP)
2010 FOR N = 1 TO 6
2020 IF N > 3 THEN UNITS = 1/.0175
2030 IF N < 4 THEN UNITS = 1!
2040 LOCATE (L+7),((N+1)*10):PRINT USING "#####";(ACC(L,N)*UNITS)
2050 NEXT N
2060 NEXT L
2070 LOCATE 25,30:INPUT "CONTINUE";CR$
2080 GOTO 1290
2090 CLS
2100 LOCATE 1,22:PRINT TEST$
2110 LOCATE 3,18:PRINT "DISPLACEMENTS AT POINT OF LOAD APPLICATION"
2120 LOCATE 4,18:PRINT "          units = inches, degrees, and lbs."
2130 LOCATE 6,15:PRINT "TIME"
2140 LOCATE 6,27:PRINT "X"
2150 LOCATE 6,37:PRINT "Y"
2160 LOCATE 6,45:PRINT "X LOAD"
2170 LOCATE 6,55:PRINT "Y LOAD"
2180 FOR M = 1 TO (NSTEPS+1)
2190 LOCATE (M+6),15:PRINT USING "#.###";((M-1)*TSTEP)
2200 LOCATE (M+6),25:PRINT USING "##.##";(DISPA(M,1)*12)
2210 LOCATE (M+6),35:PRINT USING "##.##";(DISPA(M,2)*12)
2220 LOCATE (6+M),45:PRINT USING "#####";PA(M,1)
2230 LOCATE (6+M),55:PRINT USING "#####";PA(M,2)
2240 NEXT M
2250 LOCATE 25,30:INPUT "CONTINUE";CR$
2260 GOTO 1290
2270 END

```

Figure 60. Independent block analysis program (continued).

INDEPENDENT BLOCK ANALYSIS PROGRAM

ANCHOR BLOCK GEOMETRY

LENGTH (ft.)? 18
WIDTH (ft.)? 1.3
TOTAL HEIGHT (ft.)? 4.5
EMBEDMENT DEPTH (ft.)? 1.8
WEIGHT (lbs.)? 12500

SOIL PROPERTIES

EFFECTIVE SOIL DENSITY ? 120
SOIL-BLOCK FRICTION COEFF. = 1.000
ANGLE OF INTERNAL FRICTION = 45
LOAD CASE TYPE? 1

BLOCK MASS PROPERTIES

Mass = 388 slugs
Ixx = 710 ft⁴
Iyy = 11136 ft⁴
Izz = 10536 ft⁴

Length = 18.00 ft.
Width = 1.30 ft.
Total Height = 4.50 ft.
Embedment Depth = 1.80 ft.
Weight = 12500 lbs.

Metric Conversion

1 in = 2.5 cm

1 ft = 30 cm

Figure 61. Independent block analysis program sample input screen.

INDEPENDENT BLOCK ANALYSIS PROGRAM

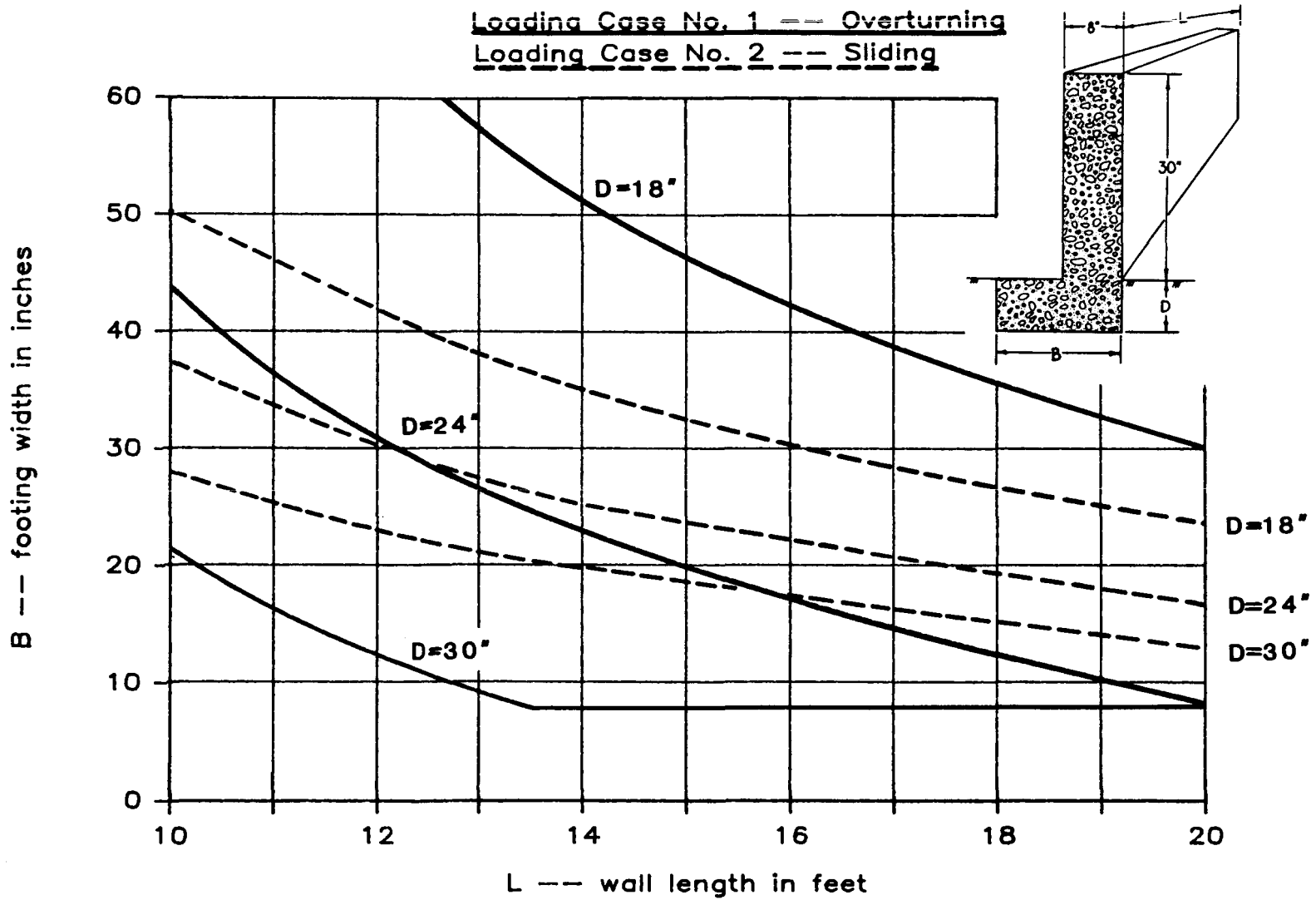
DISPLACEMENTS OF THE C.G. inches and degrees

TIME	X	Y	Z	ROLL	PITCH	YAW
0.000	0.00	0.00	0.00	0.00	0.00	0.00
0.010	0.00	0.00	0.00	0.00	0.00	0.00
0.020	0.00	0.00	0.00	0.00	0.00	0.00
0.030	0.00	0.00	0.00	0.00	0.00	0.00
0.040	0.00	0.00	0.00	0.00	0.00	0.00
0.050	0.00	0.00	0.00	0.00	0.00	0.00
0.060	0.00	0.00	0.00	0.00	0.00	0.00
0.070	0.00	0.00	0.00	0.00	0.00	0.00
0.080	0.00	0.00	0.00	0.00	0.00	0.00
0.090	0.00	0.02	0.00	0.06	0.00	0.00
0.100	0.00	0.09	0.00	0.33	0.00	0.00
0.110	0.00	0.24	0.00	0.95	0.00	0.00
0.120	0.00	0.39	0.00	1.51	0.00	0.00
0.130	0.00	0.43	0.00	1.66	0.00	0.00
0.140	0.00	0.43	0.00	1.66	0.00	0.00
0.150	0.00	0.43	0.00	1.66	0.00	0.00

128

Metric Conversion
1 in = 2.5 cm
1 ft = 30 cm

Figure 62. Independent block analysis program sample output.



Metric Conversion
 1 in = 2.5 cm
 1 ft = 30 cm

Figure 63. Design curves for load cases nos. 1 and 2.

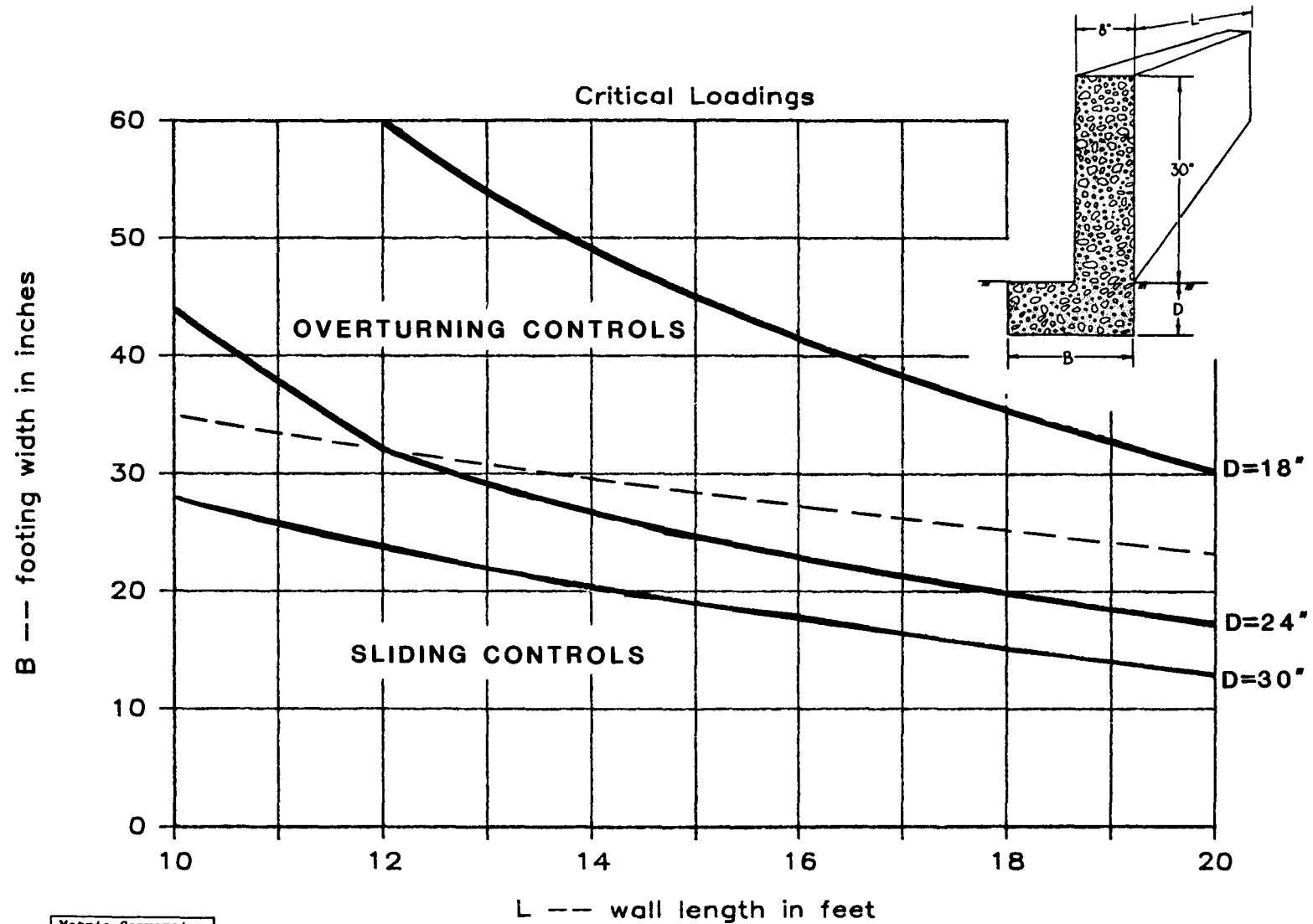


Figure 64. Design curves for the critical load case.

chosen as a critical displacement because deflections of more than 1 in (2.54 cm) could produce snag points since faces of the wingwall anchor block and bridge structure would not be aligned. The vehicle, after rotating the wall, could then snag on the end of the nearly rigid bridge rail.

In order to generate fairly generic design curves, it was necessary to assume some typical or at least conservative geometry. The geometry chosen is shown in the inset portion of figures 63 and 64. Most typical wingwalls would perform somewhat better because they use a sloped wall which adds more weight.

The solid lines in figure 63 show the family of curves for load case 1, the case where the anchor block is more likely to overturn. Each curve corresponds to a particular embedment depth and can be used to select the most appropriate footing width. For example, if an anchor wall 18 ft (54.8 m) long with a footing width of 20 in (50.8 cm) is to be used, figure 63 indicates that the embedment depth must be at least 24 in (61 cm) to prevent excessive roll rotation.

Load case 2, where the anchor block slides in the x direction, is represented in figure 64. As in figure 63, each curve represents a particular embedment depth. For example, the 18-ft long 20-in (50.8-cm) wide wall which was adequate for case 1 is only marginally adequate for this loading.

If the solid and dashed lines in figure 63 are compared, it becomes apparent that load cases 1 and 2 can both be critical for different geometries. Figure 64 is a set of curves which show only the critical values. In the portion of figure 64 below the dashed line, the sliding stability dominates and load case 2 controls. In the area above the dashed line, overturning stability is critical and load case 1 controls. With figure 64, the designer merely needs to select the embedment depth represented by

the line just below the plotted point defined by the wall length and footing width.

f. Summary

When using conventional soil-strength analysis, the geometries required to provide adequate support against displacements of the anchor wall are far too conservative in comparison with designs which have been shown to perform well in full-scale crash tests. The previous sections have outlined a simple method of modifying traditional soil-strength analysis techniques which will produce far more realistic designs. The first modification required was to account for the increased strength of soils under dynamic loadings. This was done by multiplying the usual Coulomb passive earth pressure coefficient by an empirically observed factor of 5. A second modification was to enforce dynamic instead of static equilibrium in calculating the forces acting on the block. Using an incremental time step and an assumed force-time history allowed the calculation of the acceleration, velocity, and displacement of the block at each time step. Using these modifications, the designer can determine the geometry required to ensure good performance of independent anchor blocks.

5. Conclusions and Recommendations

In this project a large number of current State guardrail/bridge rail transition designs were evaluated using a system developed for the project. Certain of these designs were selected for crash test evaluation and redesign as required. New designs were also formulated for evaluation.

a. Conclusions

1. State-of-the-Practice. Most of the designs submitted to FHWA by the States featured a standard G4(1S) or G4(2W) W-beam guardrail approach to a concrete safety shape bridge parapet or wingwall using a Michigan end shoe for attachment of the beam to the wall. Variations in these transition details included the following:

- Transition post spacing.
- Use of larger posts or standard posts.
- Soil plates or concrete footings for posts.
- Double beam used in some designs.
- Transition from safety shape parapets.
- Beam block-outs at parapet or wingwall.
- Straight parapet/wingwall or tapered wall.
- Use of rub rail near bridge.
- Beam attachment to bridge parapet/wingwall.
- Independent end blocks.
- Tapered curb transition to safety shape.

2. Desirable Transition Characteristics. Based on the findings of this project, certain desirable characteristics were identified for optimum guardrail/bridge rail transition designs. The characteristics apply to W-beam and thrie beam systems attached to concrete parapets/wingwalls.

- Posts. Standard guardrail posts have been shown to be effective with proper spacing. Use of standard posts eliminates the need for stockpiling non-standard posts. Use of soil plates or concrete footings is also considered to be unnecessarily costly.

- Transition from Safety Shape Parapets. It is considered to be hazardous to mount a W or thrie beam on the upper face of a safety shape as shown in figure 65(a). A preferable treatment is to transition from a flat wall to a safety shape as shown in figure 65(b).

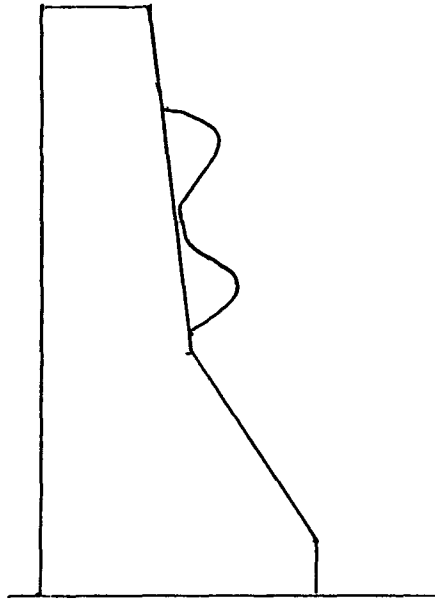
- Beam Block-outs at Parapets/Wingwalls. An effective alternative to the lower rub rail adjacent to the bridge is the use of block-outs to minimize wheel snagging on the end. For roadways with 2-way traffic, it is necessary to flare or taper the beam back to a flush position with the upper wall face to avoid snagging opposing traffic.

- Beam Attachment. Michigan end shoes for both W and thrie beams proved to be effective attachments using 7/8 in (2.2 cm) diameter bolts through the concrete walls.

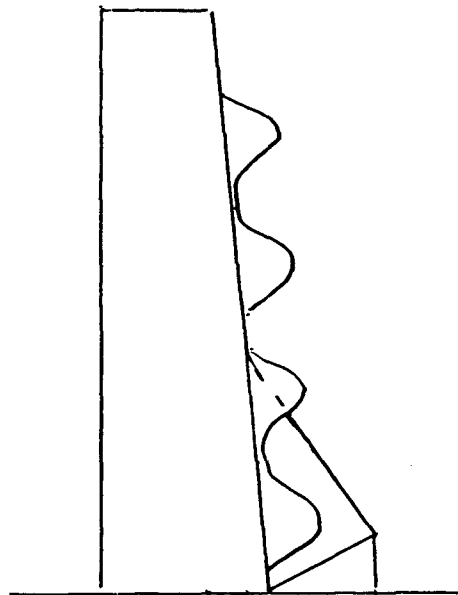
- Post Spacing. Based on computer simulations verified by crash tests, four spacers at 1 ft-6 3/4 in (0.5 m) adjacent to the parapet/wingwall followed by adjacent spaces at 3 ft-1 1/2 in (1.0 m) provide an acceptable transition for both W-beam and thrie beam approach guardrail systems.

- Parapet/Wingwall Geometry. For straight parapet/wingwalls, a lower W-beam element is required adjacent to the bridge to prevent wheel snagging on the exposed wall edge. The thrie beam mounted at 31-32 in (0.8 m) does not require a lower beam or rub rail.

A tapered wingwall/parapet is an effective means of preventing wheel snagging at the bridge end. Both curved and straight



(a) Safety shape - no transition



(b) Transition from safety shape to flat wall

Figure 65. Safety shape parapet end consideration.

tapered wingwalls were evaluated in this project and the effectiveness of treatments was demonstrated.

- Double Beam Designs. An effective treatment for the beam element adjacent to the bridge is to double or nest a W or thrie beam at this location. For the steel post systems, this eliminates a larger number of 12 in (0.3 m) long back-up plates required at each post where a splice does not occur.

- Modified Thrie Beam. A transition from the modified thrie beam system to a standard thrie beam/wingwall bridge approach transition was successfully evaluated. The modified thrie beam is a high performance barrier system capable of redirecting heavy buses and trucks. (10)

- Transitions at Intersecting Roadways. Design details were finalized and crash test performance demonstrated for a given intersection geometry. Based on the results of the finalized design tests, a satisfactory treatment of this difficult problem was demonstrated.

- Independent End Blocks. The function of independent end blocks was defined and design guidelines produced based on the crash test condition defined by a 4500 lb (2000-kg) car impacting at 60 mph (95 km/h) and angle of 25 degrees. Using these guidelines, the designer can select from a range of foundation widths and depths.

- Transitions with Curbs. One test was conducted on a modified State design employing a tapered curb in the transition zone. Results of the test were not completely satisfactory and recommendations for improving the performance are made in the next section.

b. Recommendations

1. General. Using computer simulation and full-scale crash test evaluations, a number of effective guardrail/bridge rail transition designs were developed in this project. These designs are characterized by the following:

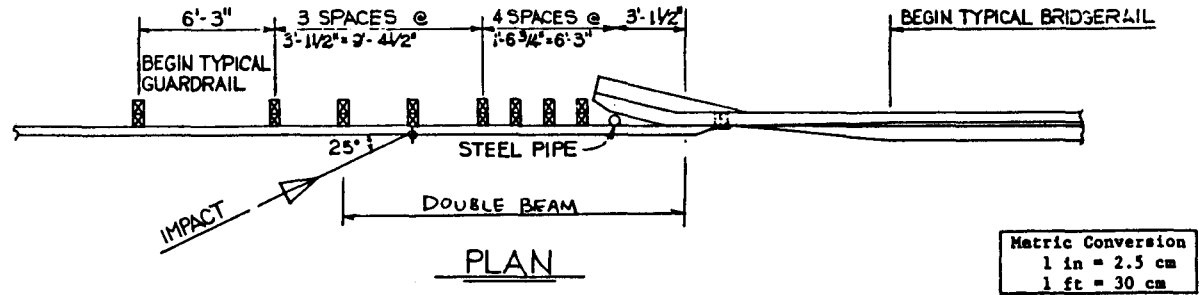
- Standard guardrail posts and blocks with 2 sets of spacing near the bridge end.
- 3 ft-1 1/2 in and 1 ft-6 3/4 in
Note: Use of larger posts near the bridge end was not as effective as reducing spacing of standard posts.
- One W-beam panel (12 ft-6 in) as a lower rub rail on straight wingwall or parapets.
- W-beam with single collapsing tube when attached to a tapered wingwall or parapet.
- Thrie beam on both straight and tapered wingwalls.
- The upper W-beam rail and thrie beam rail panel at the bridge end is doubled to reduce local deformations.

The designs shown in figures 66, 74 and 79 have not been crash tested. Other designs using these details which have been successfully tested for the 4500-lb car, 60 mph, 25-degree angle impact are shown in figures 66 through 81. Figure 71 is the only existing State standard that was successfully evaluated in the project.

2. Transition at Intersecting Roadways. Figure 82 describes the geometrical layout and design details of the system evaluated in this project. These details are recommended based on these evaluations.

3. -Independent End Block. The independent end block successfully evaluated in this project was based on a State standard. The depth of embedment was increased based on the design criteria of chapter 4. The drawing of this detail is shown in figure 83.

Barrier components with F, P, and RE prefixes are found in latest edition of "A Guide to Standardized Highway Barrier Rail Hardware," a report prepared and approved by the AASHTO-ACC-ARTBA Joint Cooperative Committee.



138

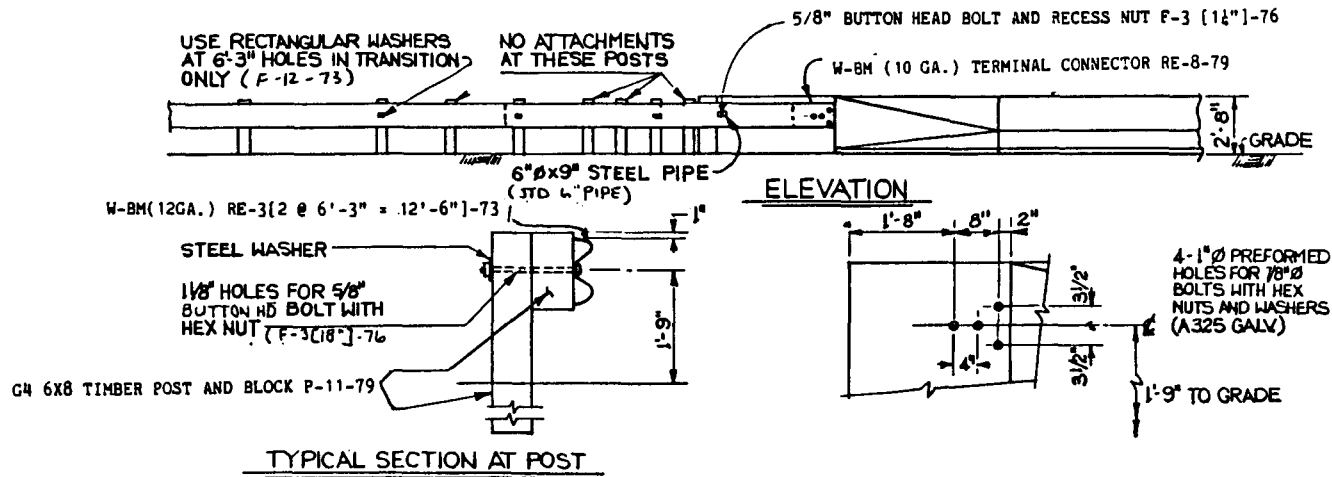


Figure 66. G4(2W) W-beam transition - tapered wingwall.

Barrier components with F, P, and RE prefixes are found in latest edition of "A Guide to Standardized Highway Barrier Rail Hardware," a report prepared and approved by the AASHTO-AGC-ARTEA Joint Cooperative Committee.

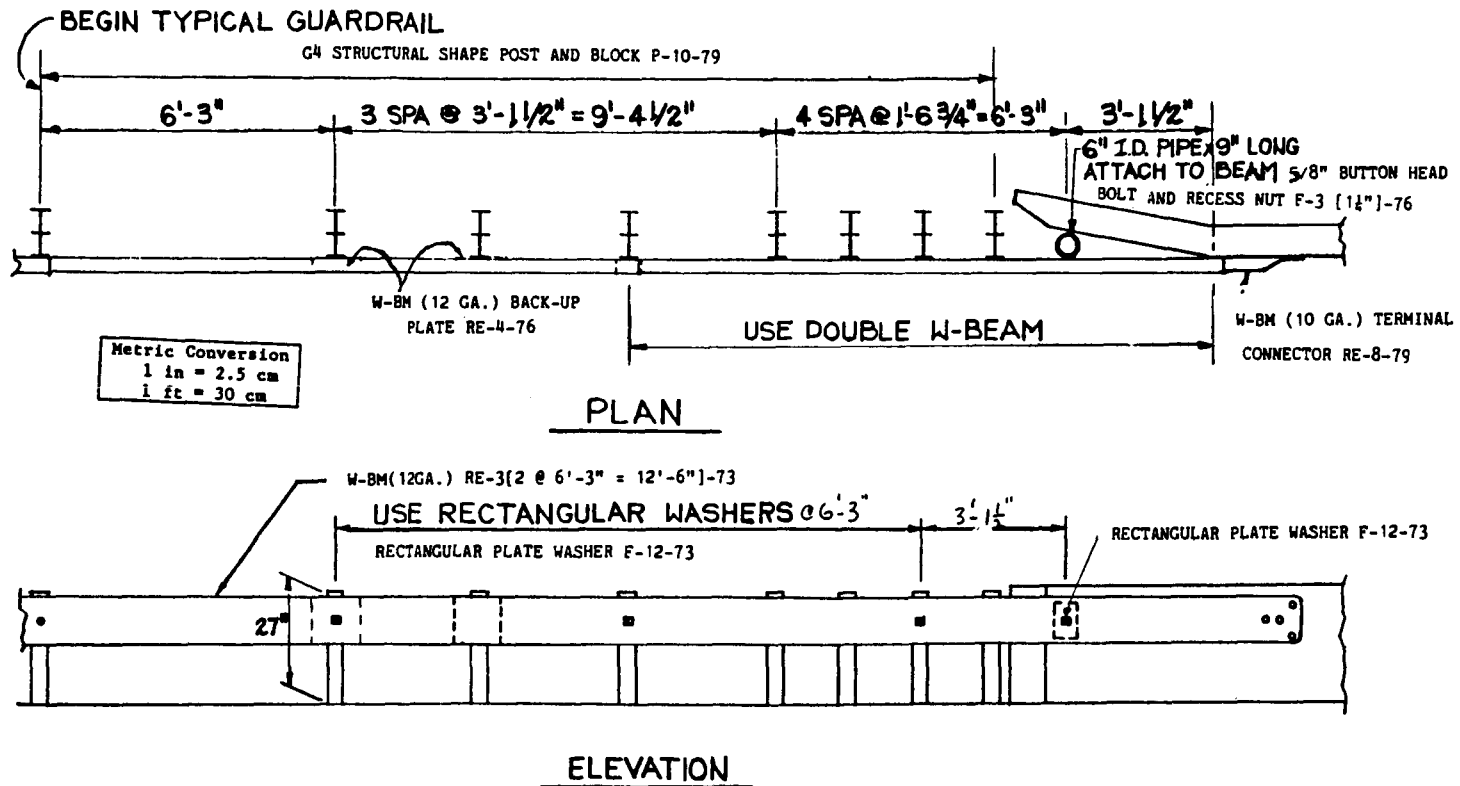
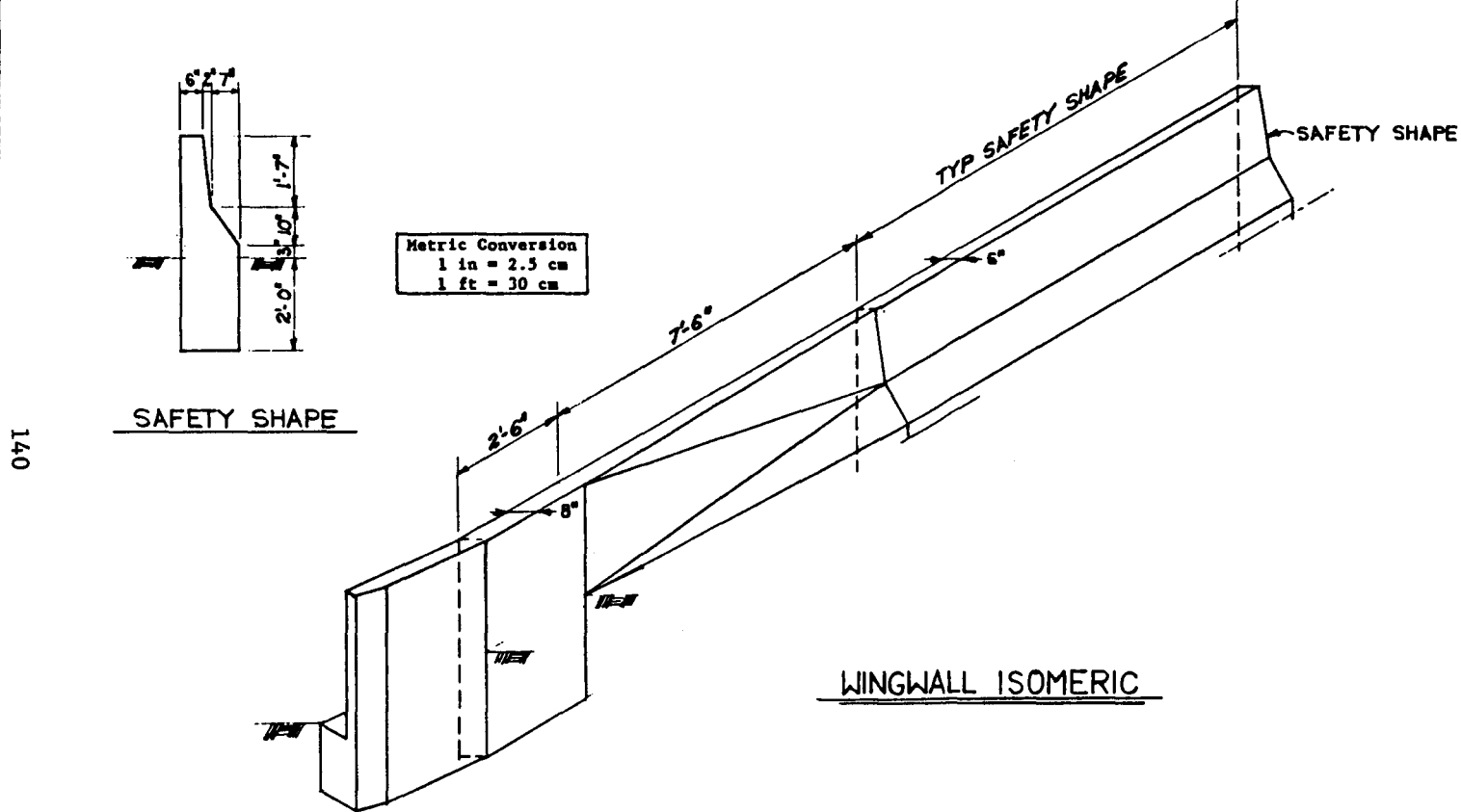


Figure 67. W-beam transition on tapered wingwall.

Barrier components with F, P, and RE prefixes are found in latest edition of "A Guide to Standardized Highway Barrier Rail Hardware," a report prepared and approved by the AASHTO-AGC-ARTBA Joint Cooperative Committee.



047

Figure 68. Tapered wingwall geometry - W-beam and thrie beam transitions.

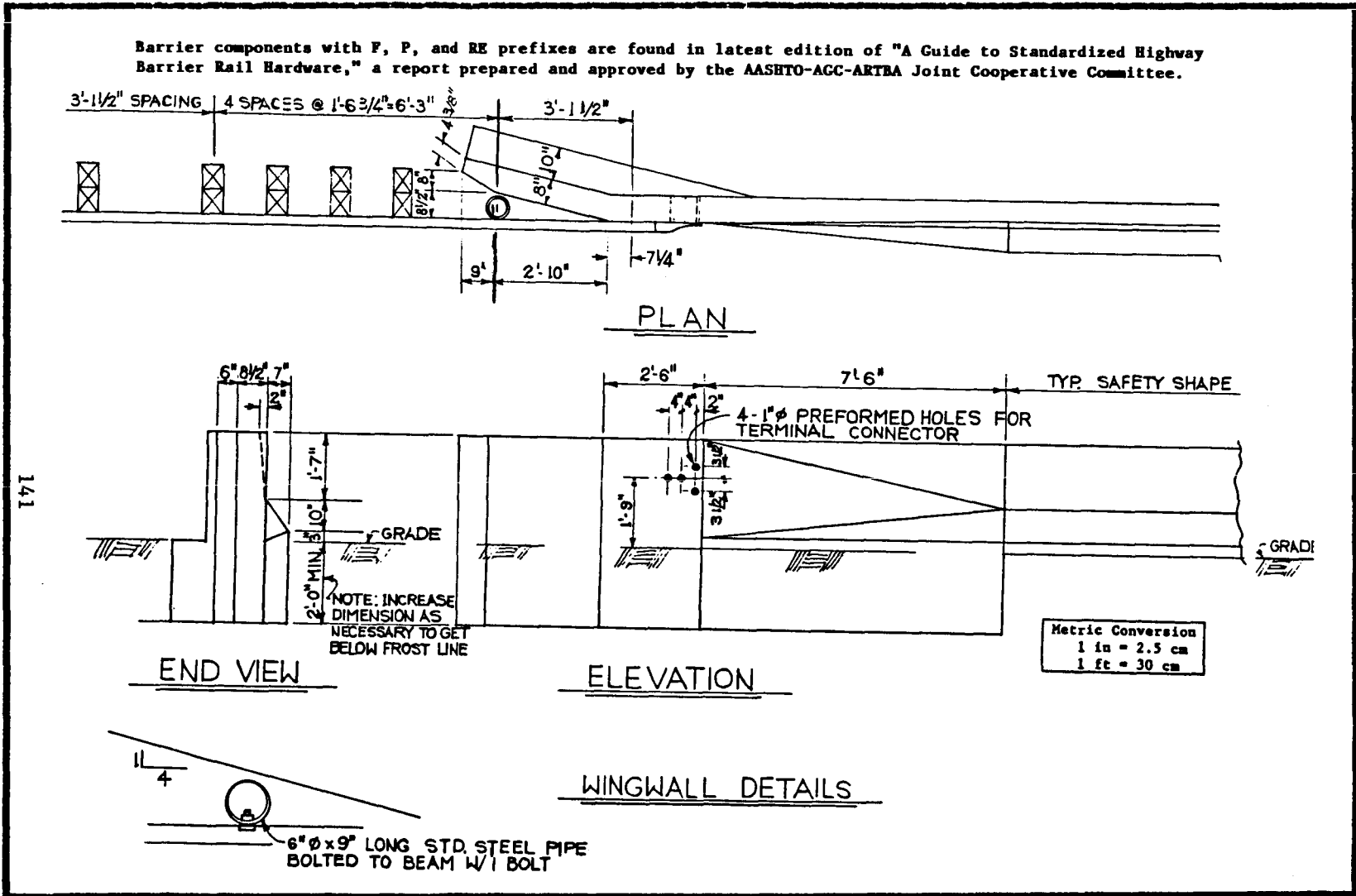


Figure 69. Tapered wingwall geometry for G4(1S) and G4(2W) systems.

Barrier components with F, P, and RE prefixes are found in latest edition of "A Guide to Standardized Highway Barrier Rail Hardware," a report prepared and approved by the AASHTO-AGC-ARTBA Joint Cooperative Committee.

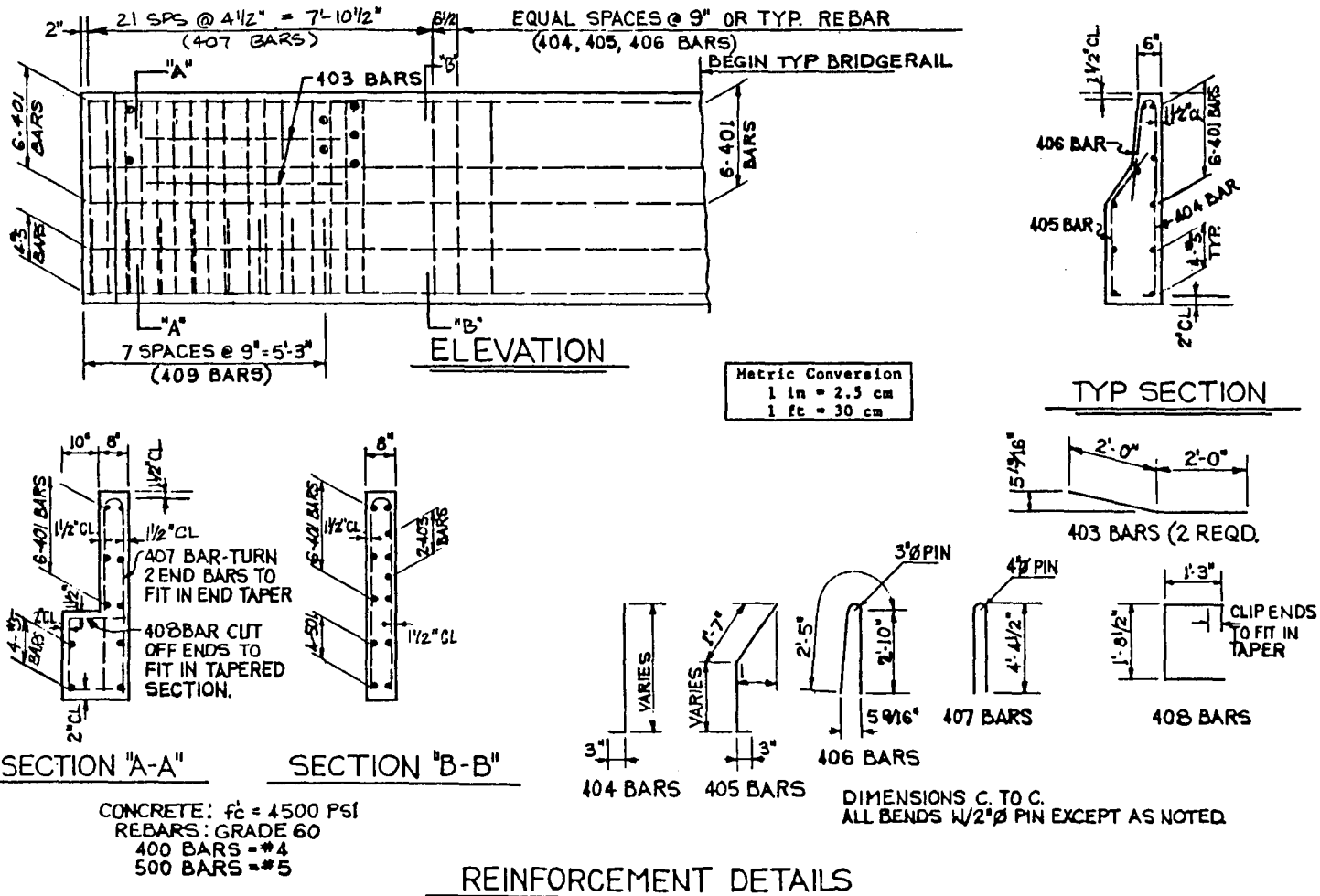
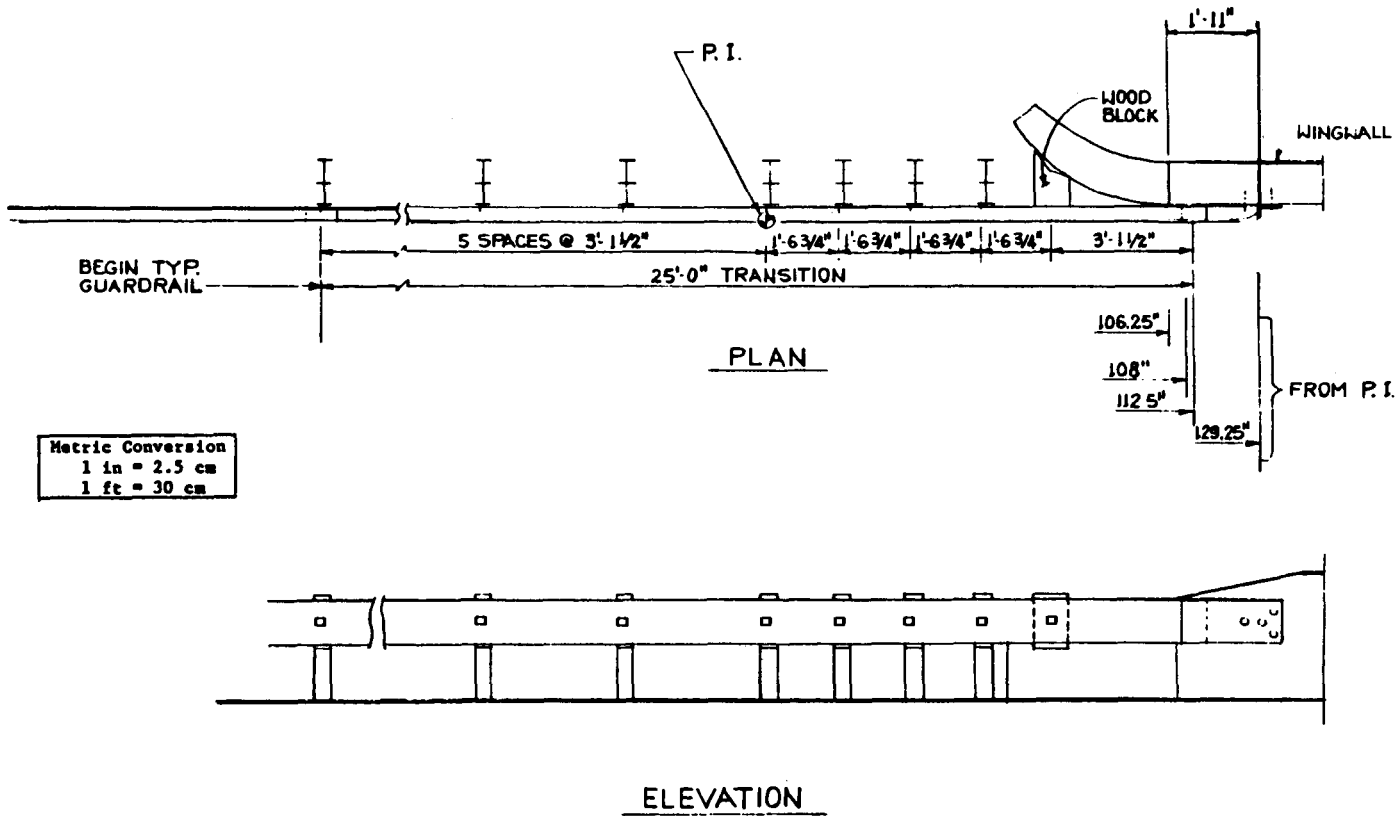


Figure 70. Wingwall reinforcement drawings for both tapered and straight wingwalls.

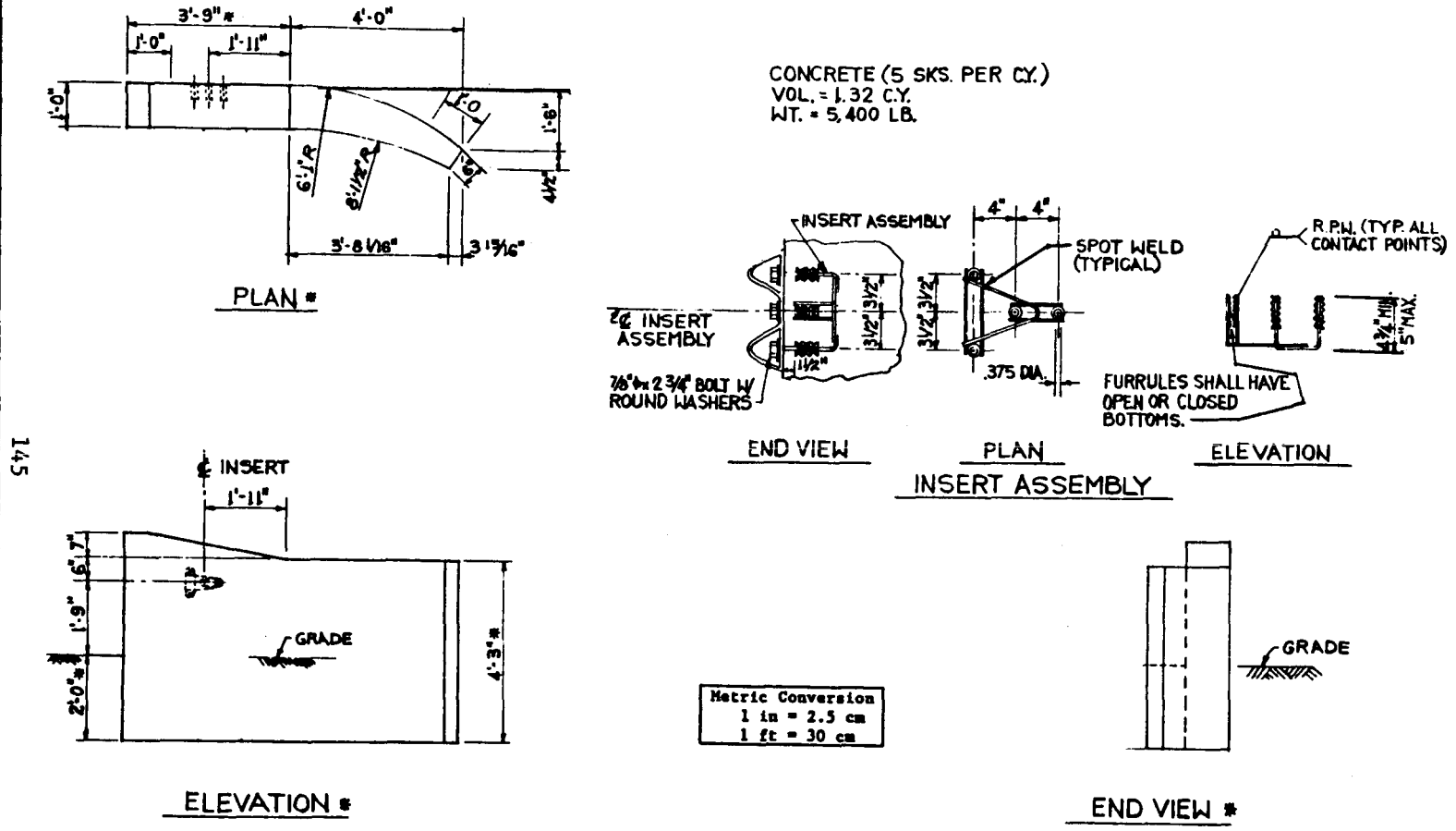
Barrier components with F, P, and RE prefixes are found in latest edition of "A Guide to Standardized Highway Barrier Rail Hardware," a report prepared and approved by the AASHTO-AGC-ARTBA Joint Cooperative Committee.



143

Figure 71. W-beam transition/curved wingwall North Carolina State standard.

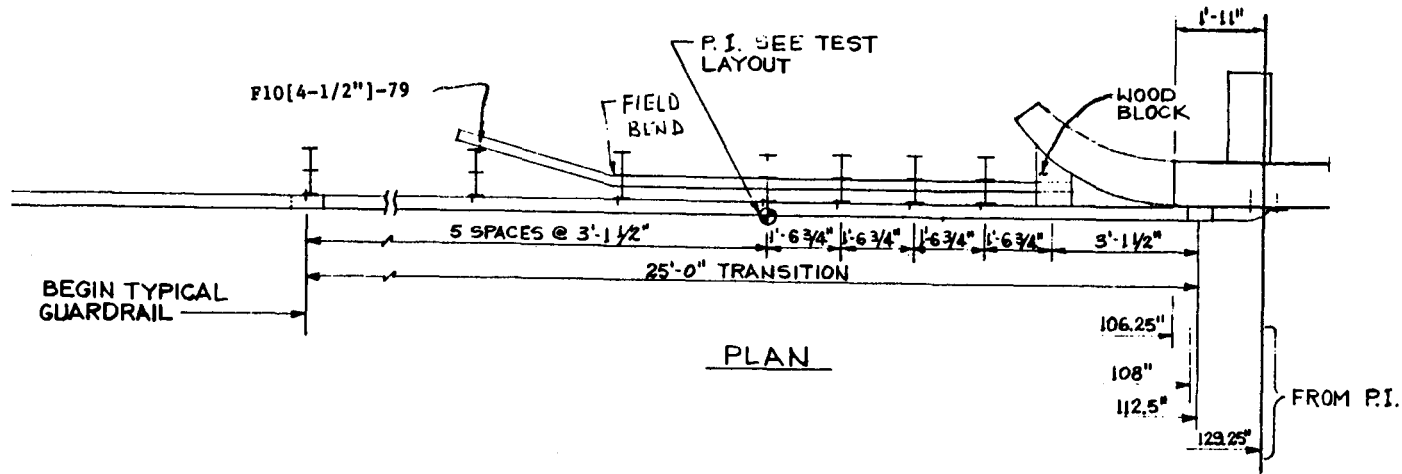
Barrier components with F, P, and RE prefixes are found in latest edition of "A Guide to Standardized Highway Barrier Rail Hardware," a report prepared and approved by the AASHTO-AGC-ARTBA Joint Cooperative Committee.



* AS TESTED, NOT A STANDARD

Figure 71. W-beam transition/curved wingwall North Carolina State standard (continued).

Barrier components with F, P, and RE prefixes are found in latest edition of "A Guide to Standardized Highway Barrier Rail Hardware," a report prepared and approved by the AASHTO-AGC-ARTBA Joint Cooperative Committee.



Metric Conversion
 1 in = 2.5 cm
 1 ft = 30 cm

946

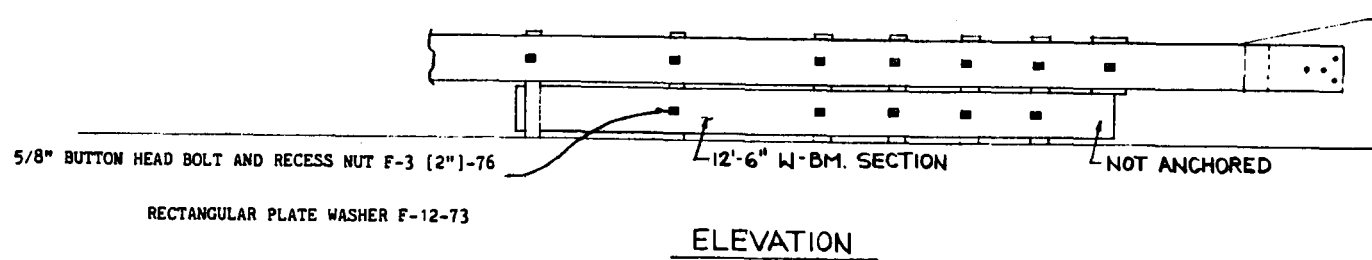


Figure 72. Modified North Carolina standard.

Barrier components with F, P, and RE prefixes are found in latest edition of "A Guide to Standardized Highway Barrier Rail Hardware," a report prepared and approved by the AASHTO-AGC-ARTRA Joint Cooperative Committee.

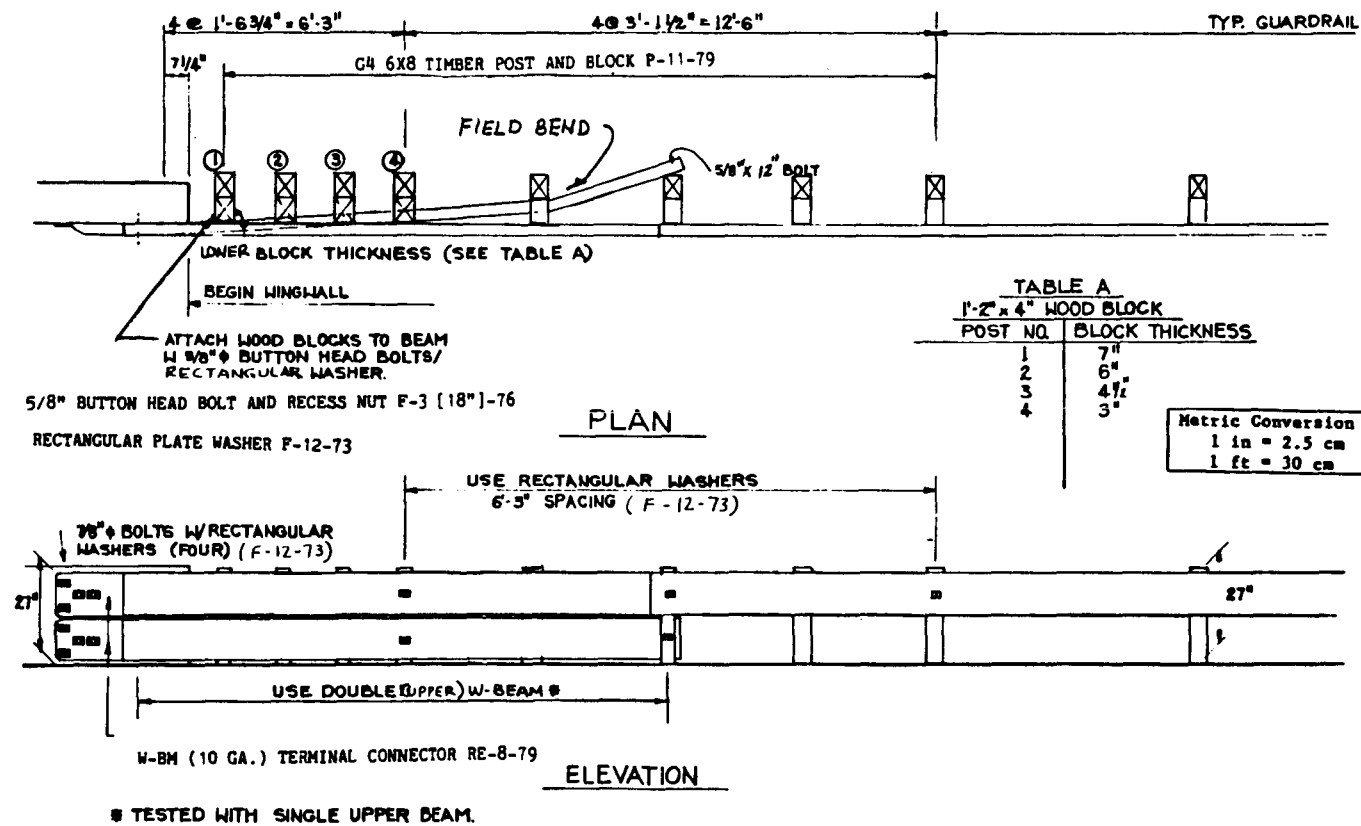


Figure 73. G4(2W) W-beam transition - straight wingwall.

Barrier components with F, P, and RE prefixes are found in latest edition of "A Guide to Standardized Highway Barrier Rail Hardware," a report prepared and approved by the AASHTO-AGC-ARTBA Joint Cooperative Committee.

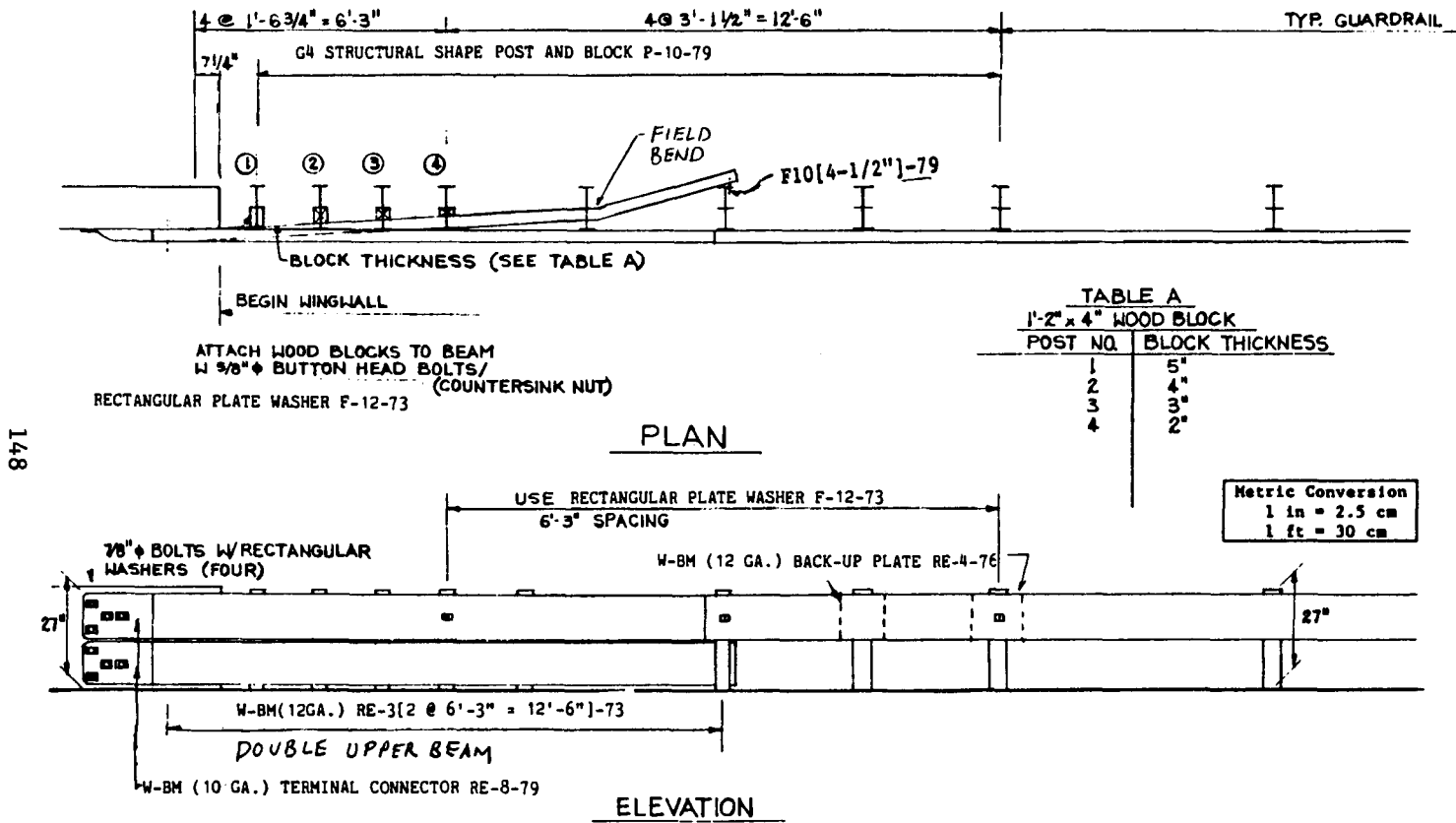


Figure 74. G4(1S) W-beam transition - straight wingwall.

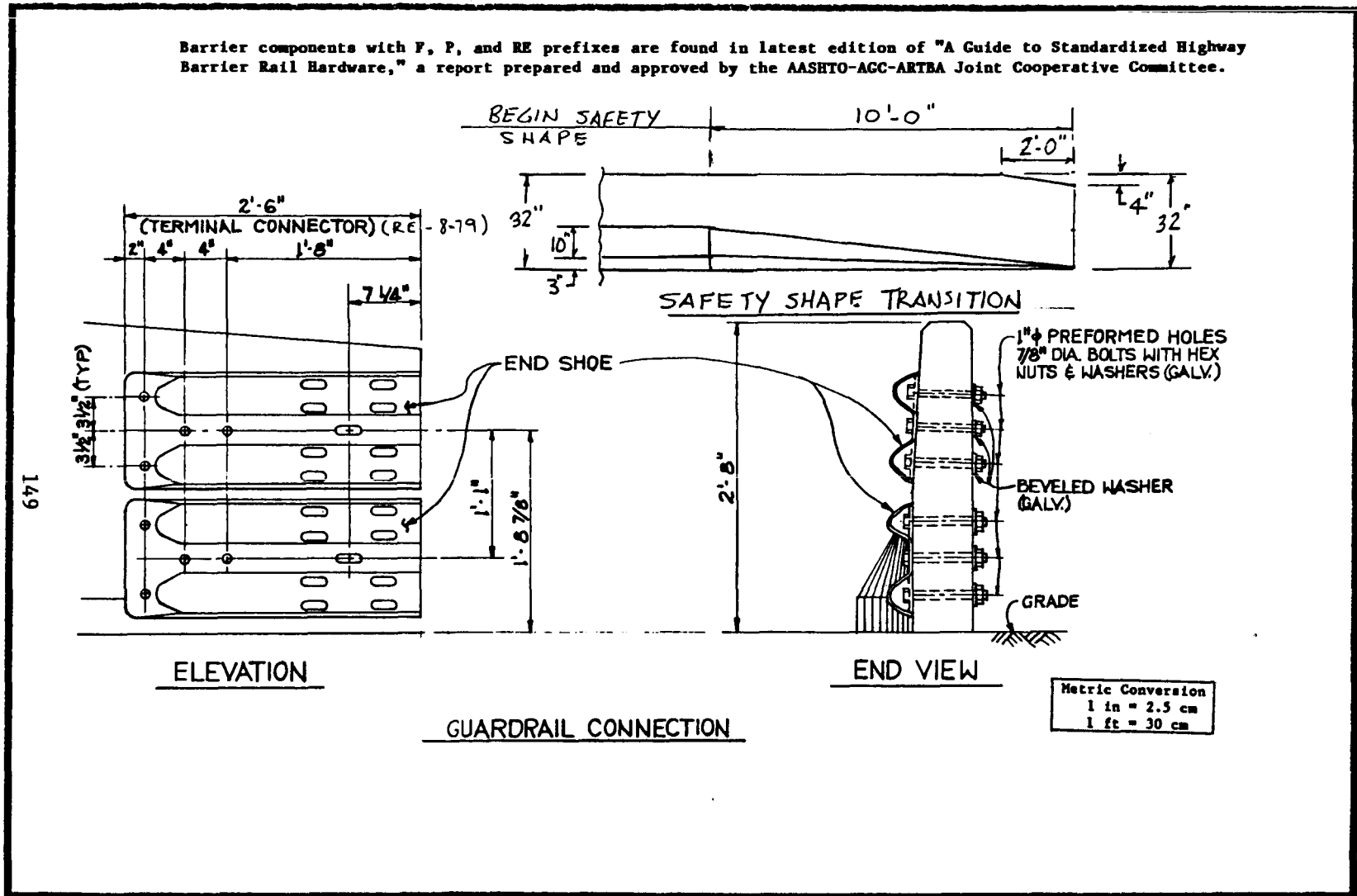
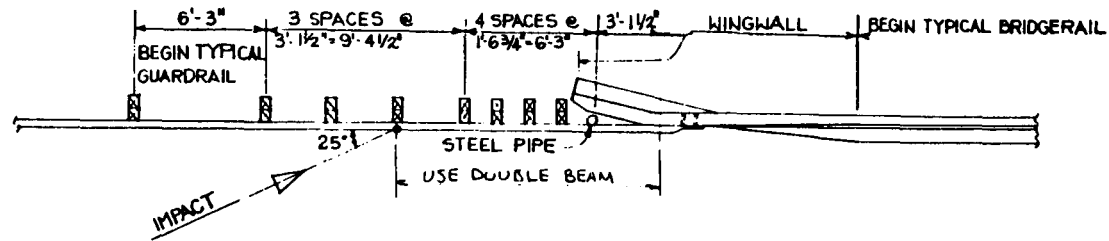


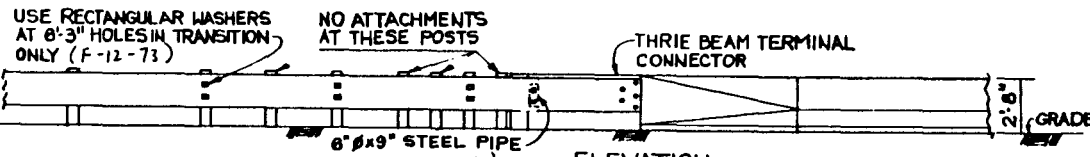
Figure 75. W-beam wingwall attachment details - straight wingwall.

Barrier components with F, P, and RE prefixes are found in latest edition of "A Guide to Standardized Highway Barrier Rail Hardware," a report prepared and approved by the AASHTO-AGC-ARTBA Joint Cooperative Committee.



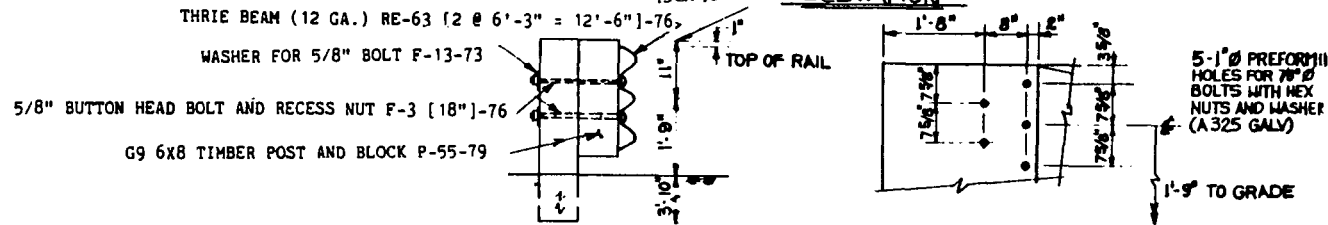
PLAN

Metric Conversion
 1 in = 2.5 cm
 1 ft = 30 cm



ELEVATION

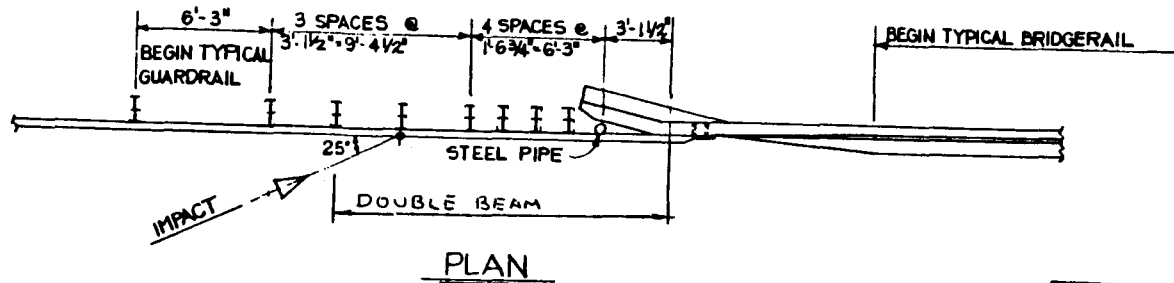
150



TYPICAL SECTION AT POST

Figure 76. G9 (wood post) thrie beam transition - tapered wingwall.

Barrier components with F, P, and RE prefixes are found in latest edition of "A Guide to Standardized Highway Barrier Rail Hardware," a report prepared and approved by the AASHTO-AGC-ARTRA Joint Cooperative Committee.



Metric Conversion
 1 in = 2.5 cm
 1 ft = 30 cm

151

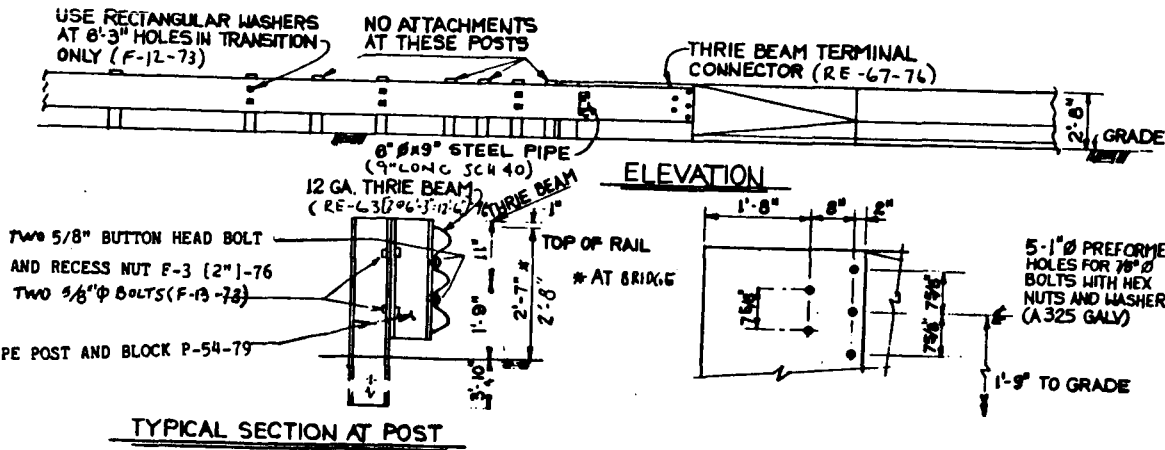
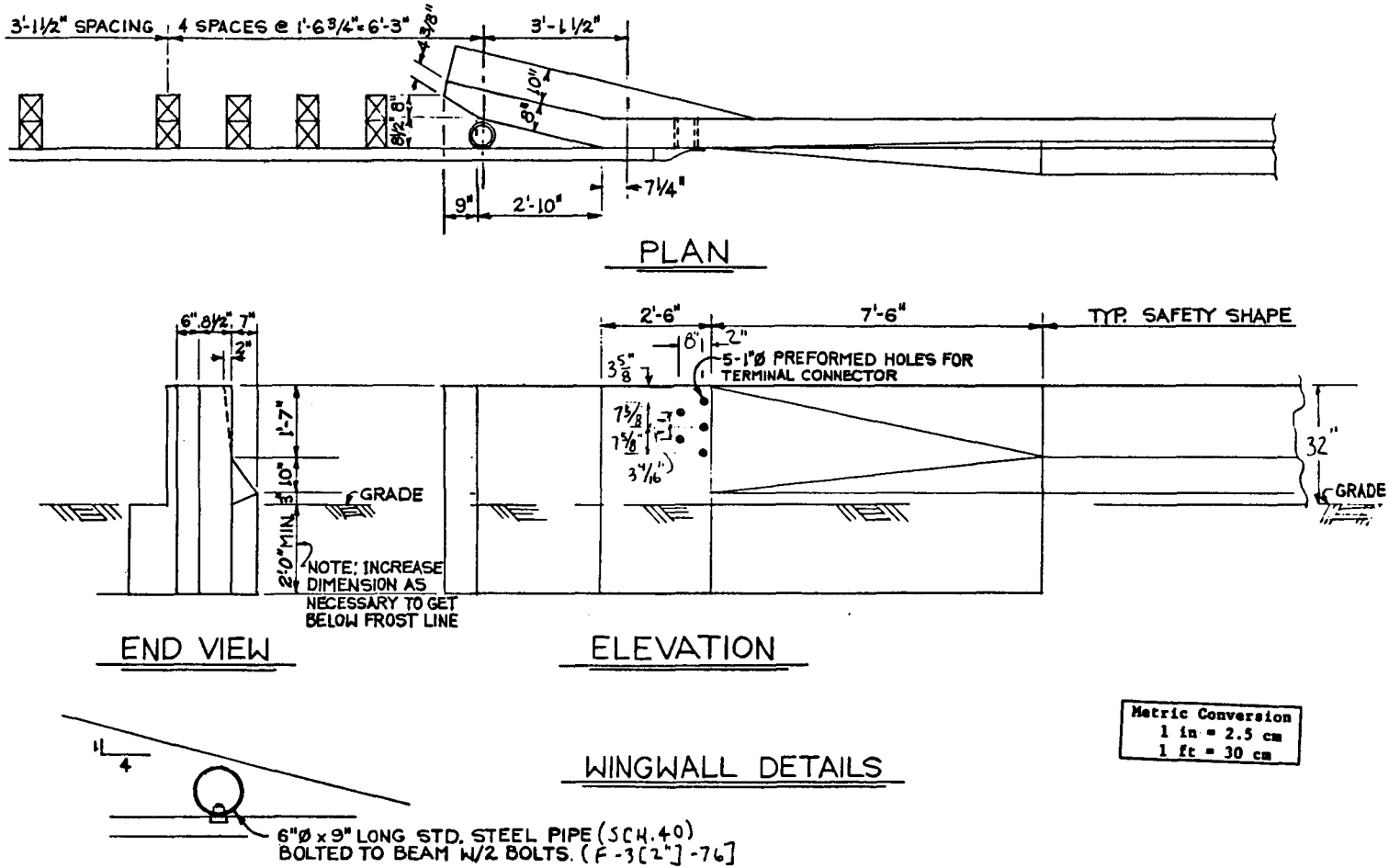


Figure 77. G9 (steel post) thrie beam transition - tapered wingwall.

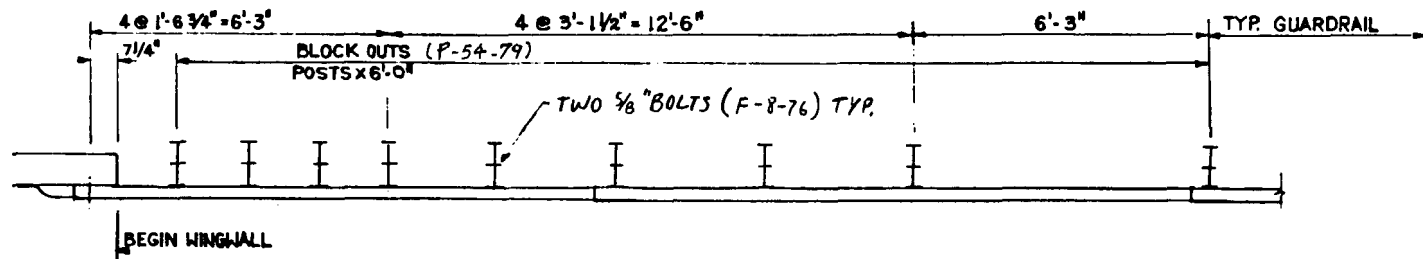
Barrier components with F, P, and RE prefixes are found in latest edition of "A Guide to Standardized Highway Barrier Rail Hardware," a report prepared and approved by the AASHTO-AGC-ARTBA Joint Cooperative Committee.



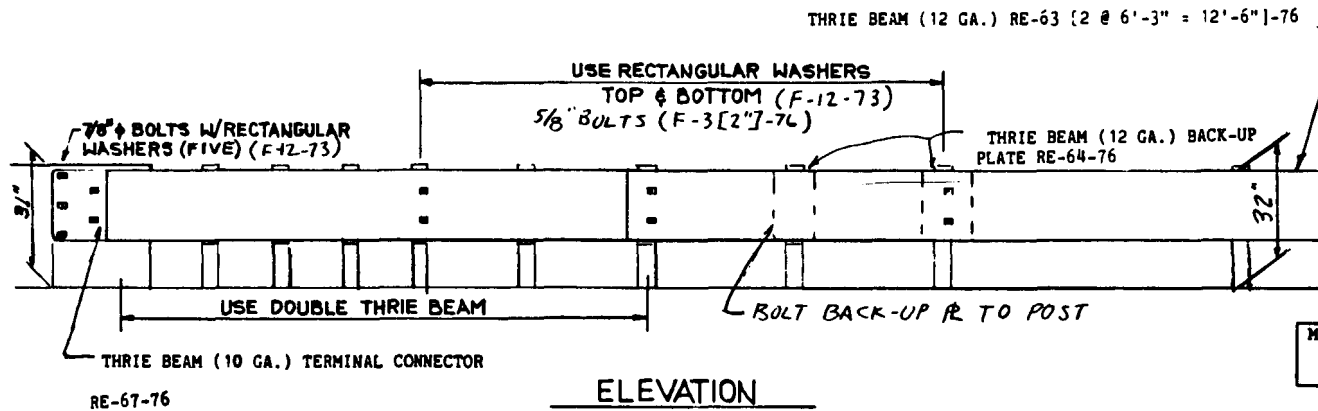
152

Figure 78. Tapered wingwall details for G9 thrie beam transition.

Barrier components with F, P, and RE prefixes are found in latest edition of "A Guide to Standardized Highway Barrier Rail Hardware," a report prepared and approved by the AASHTO-AGC-ARTBA Joint Cooperative Committee.



PLAN

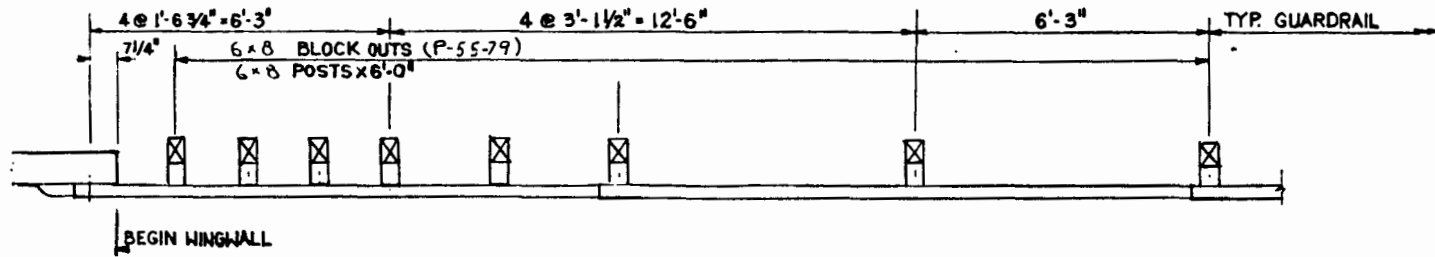


ELEVATION

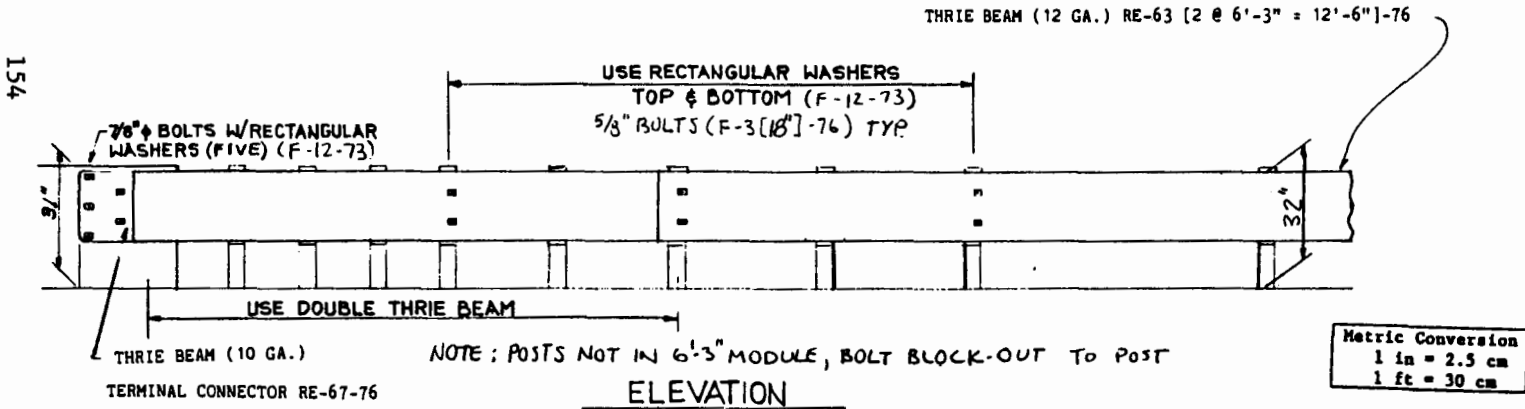
Metric Conversion
 1 in = 2.5 cm
 1 ft = 30 cm

Figure 79. G9 (steel post) transition - flat wingwall.

Barrier components with F, P, and RE prefixes are found in latest edition of "A Guide to Standardized Highway Barrier Rail Hardware," a report prepared and approved by the AASHTO-ACC-ARTBA Joint Cooperative Committee.



PLAN



ELEVATION

Metric Conversion
1 in = 2.5 cm
1 ft = 30 cm

Figure 80. G9 (wood post) transition - flat wingwall.

Barrier components with F, P, and RE prefixes are found in latest edition of "A Guide to Standardized Highway Barrier Rail Hardware," a report prepared and approved by the AASHTO-AGC-ARTBA Joint Cooperative Committee.

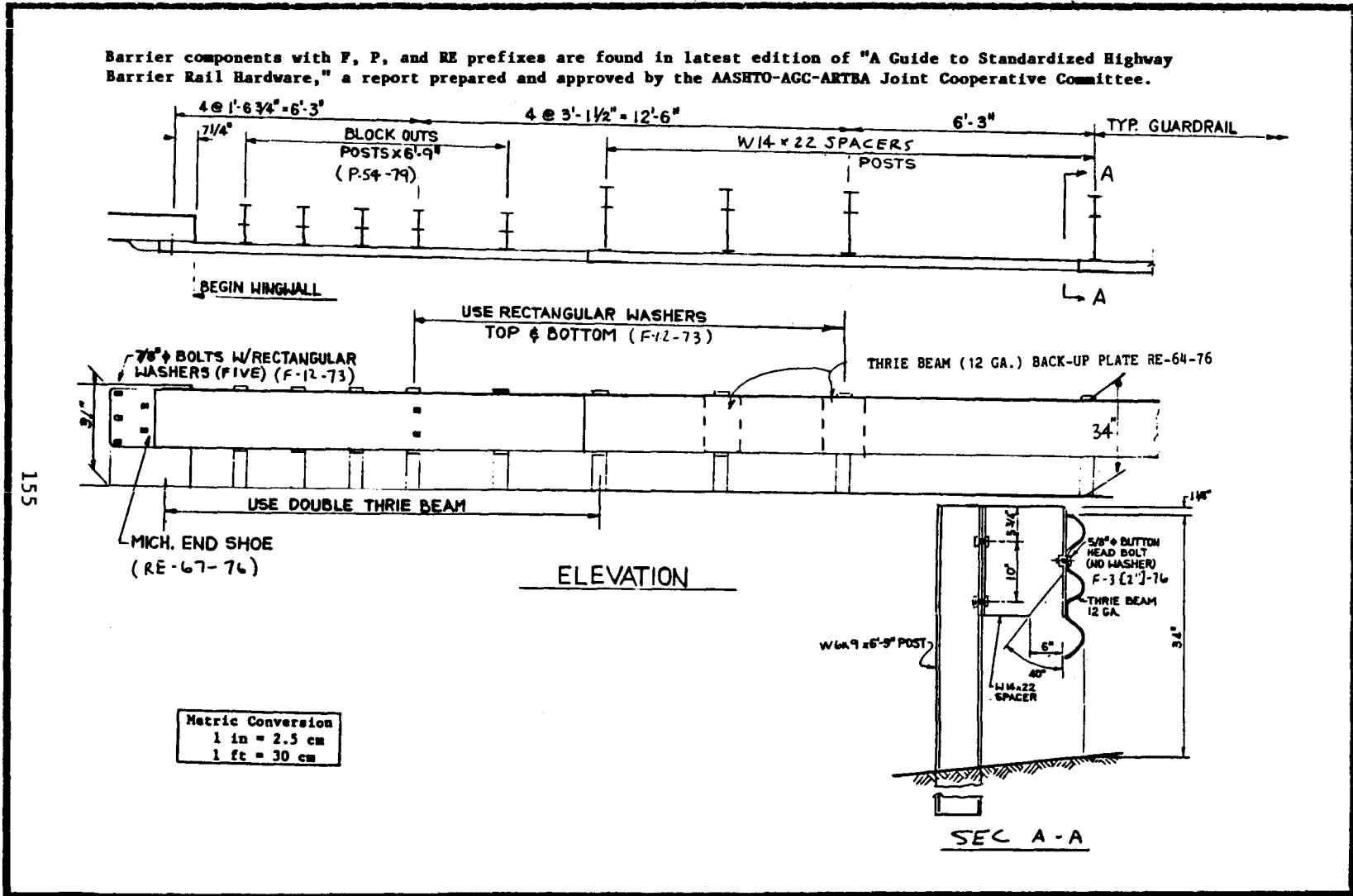


Figure 81. Modified thrie beam transition - flat wingwall.

Barrier components with F, P, and RE prefixes are found in latest edition of "A Guide to Standardized Highway Barrier Rail Hardware," a report prepared approved by the AASHTO-AGC-ARTBA Joint Cooperative Committee.

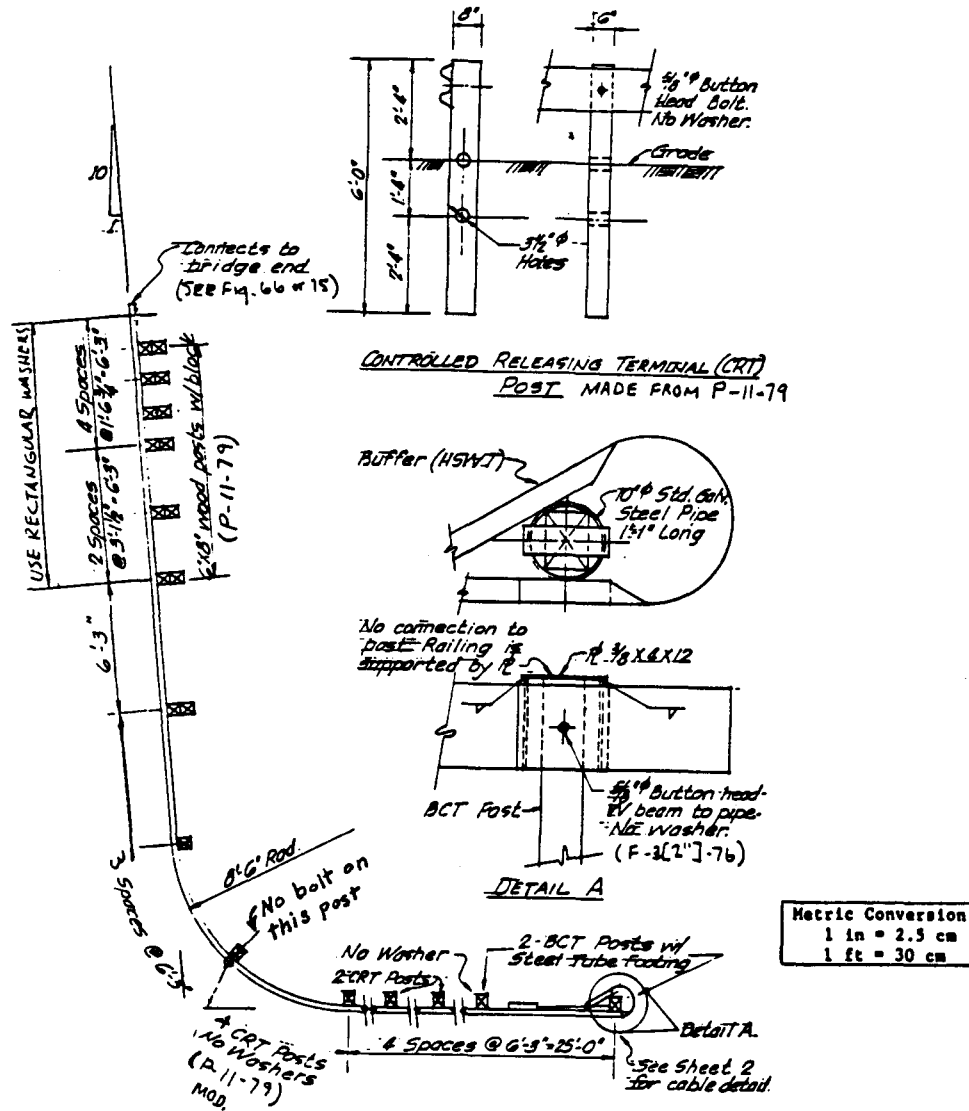


Figure 82. Intersecting roadway transition design. (sheet 1 of 2)

Barrier components with F, P, and RE prefixes are found in latest edition of "A Guide to Standardized Highway Barrier Rail Hardware," a report prepared and approved by the AASHTO-AGC-ARTBA Joint Cooperative Committee.

157

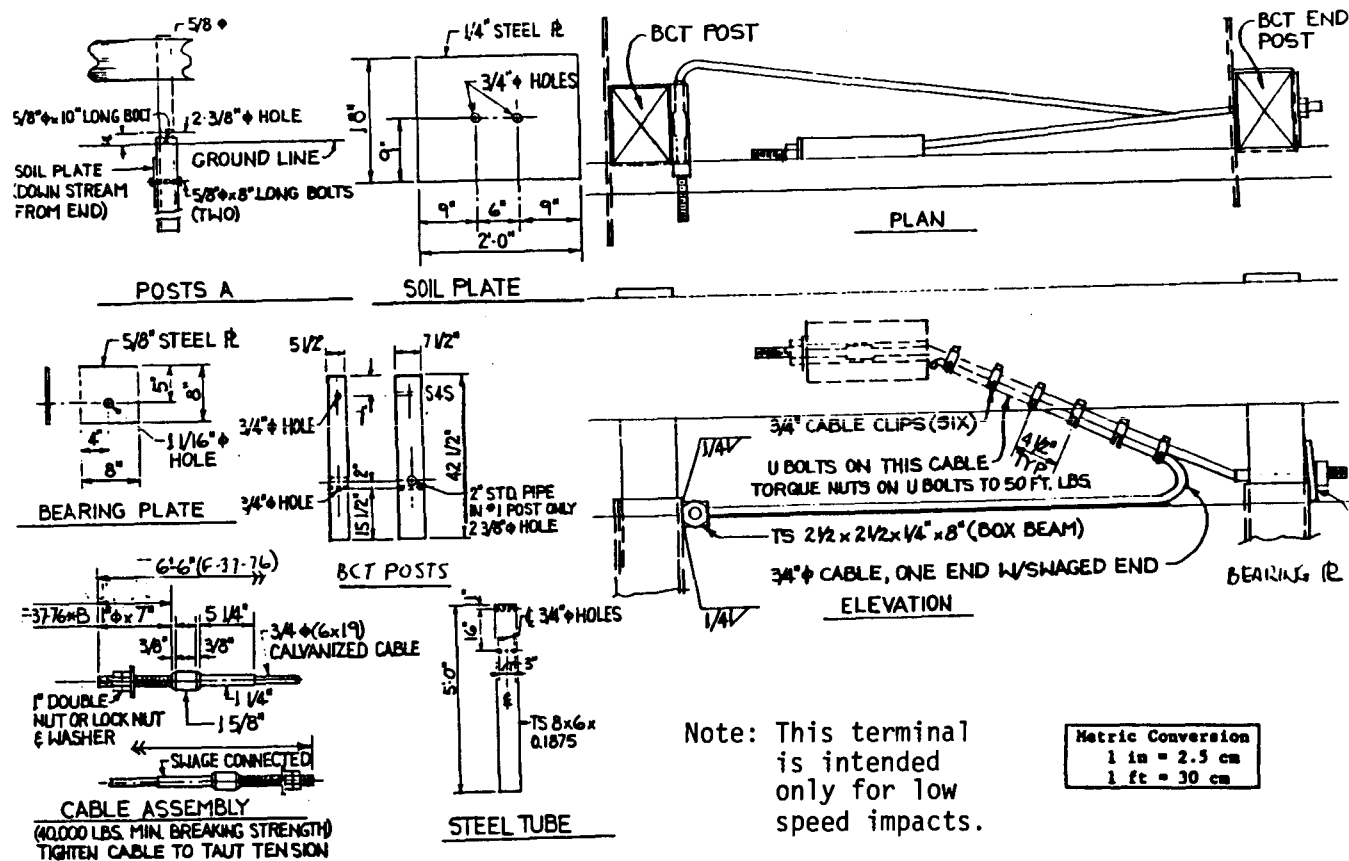
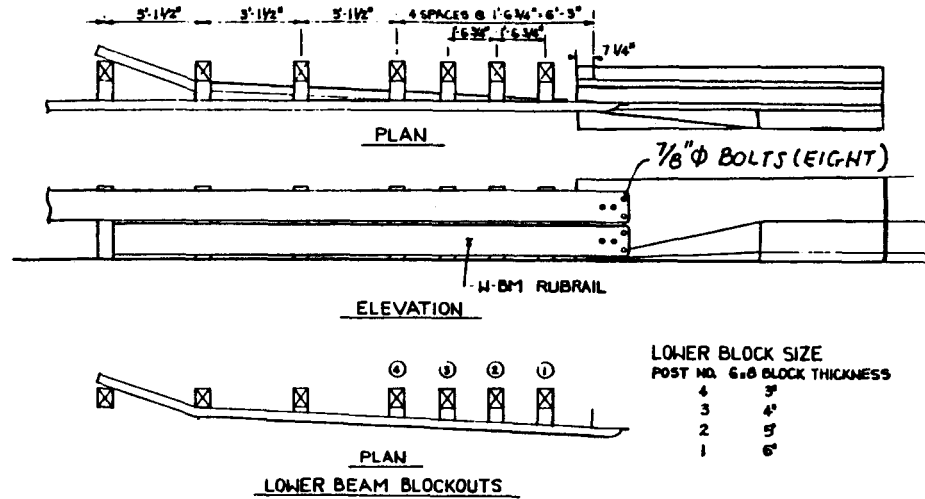


Figure 82. Intersecting roadway transition design (continued).
 (sheet 2 of 2)

Barrier components with F, P, and RE prefixes are found in latest edition of "A Guide to Standardized Highway Barrier Rail Hardware," a report prepared and approved by the AASHTO-AGC-ARTBA Joint Cooperative Committee.



LOWER BLOCK SIZE

POST NO.	6 x 8 BLOCK THICKNESS
4	3'
3	4'
2	5'
1	6'

158

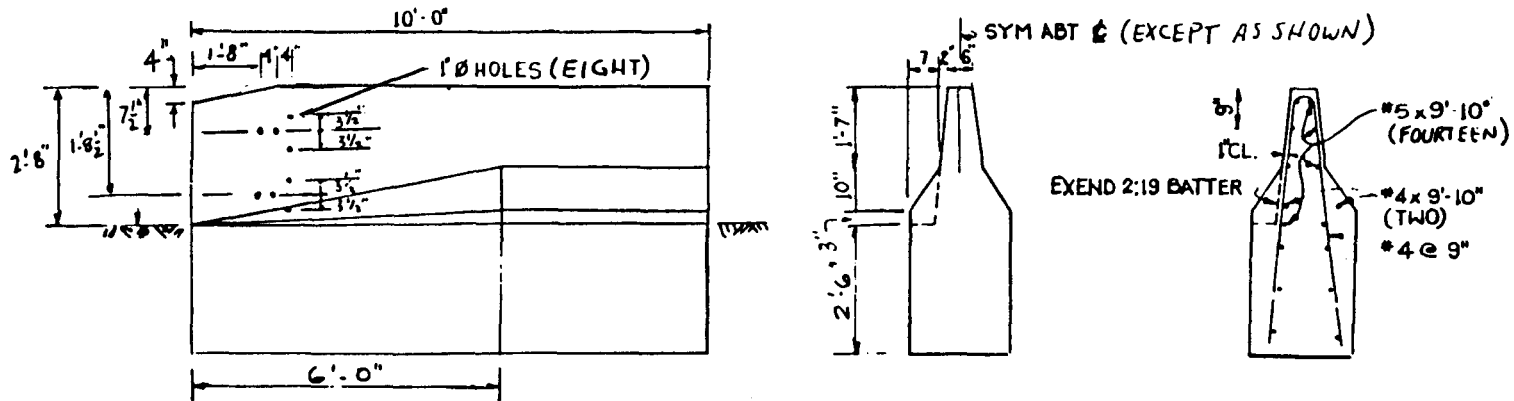


Figure 83. Independent end block drawing.

4. Transition With Curbs. The system tested was a modified State standard; the modifications were based on the findings of the project (e.g., reduced standard post spacing). Although redirection was achieved in the crash test, some snagging occurred and a recommendation for preventing the movement of the tapered curb is given in figure 84.

Appendix A contains drawings of transition systems that were tested in this project but are not recommended for installation.

Barrier components with F, P, and RE prefixes are found in latest edition of "A Guide to Standardized Highway Barrier Rail Hardware," a report prepared and approved by the AASHTO-AGC-ARTRA Joint Cooperative Committee.

160

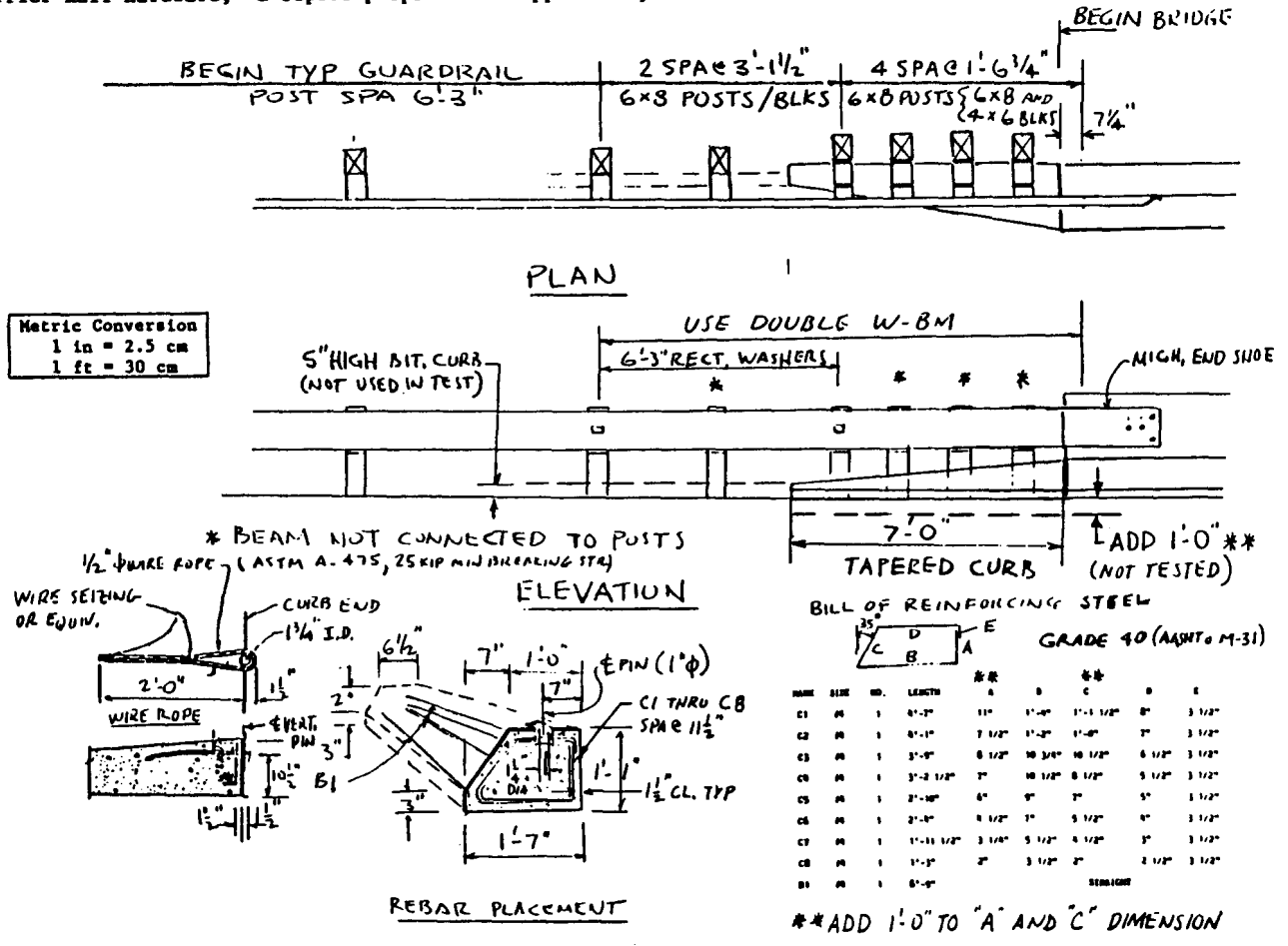
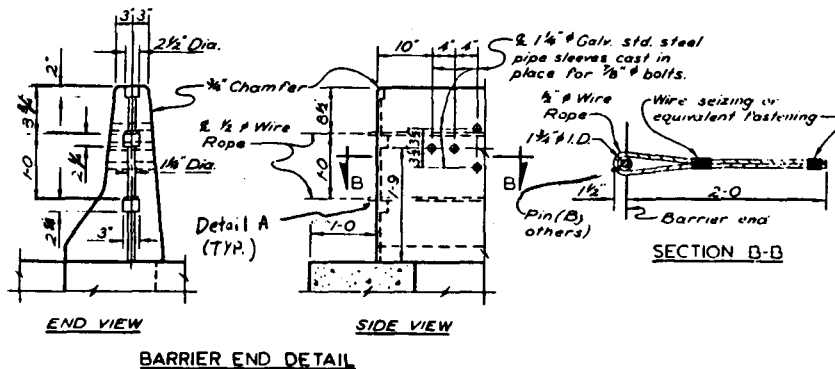


Figure 84. Barrier construction details, tapered curb.

Barrier components with F, P, and RK prefixes are found in latest edition of "A Guide to Standardized Highway Barrier Rail Hardware," a report prepared and approved by the AASHTO-AGC-ARTBA Joint Cooperative Committee.



Metric Conversion
 1 in = 2.5 cm
 1 ft = 30 cm

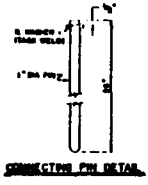
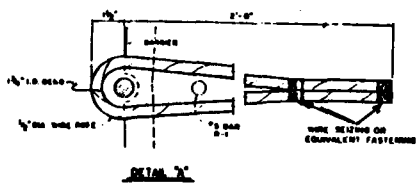
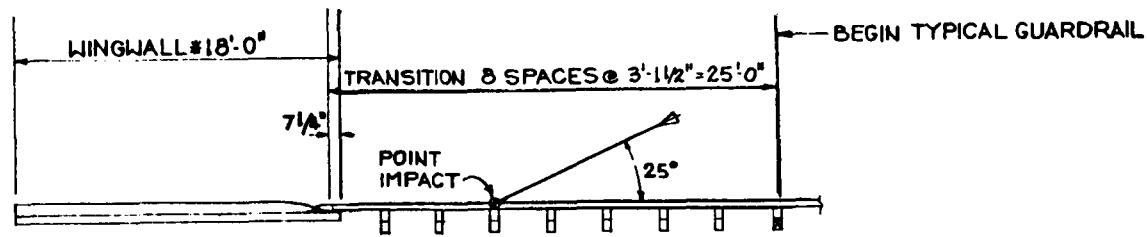


Figure 84. Barrier construction details, tapered curb (continued).

Appendix A
Transition Configurations

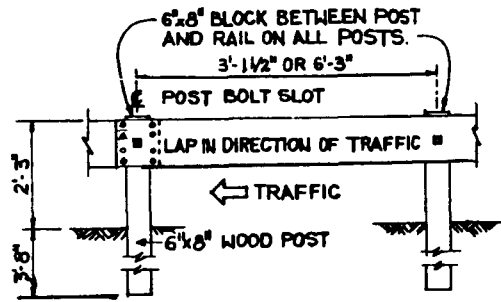
Appendix A contains drawings of transition systems that were tested in this project but are not recommended for installation.

163

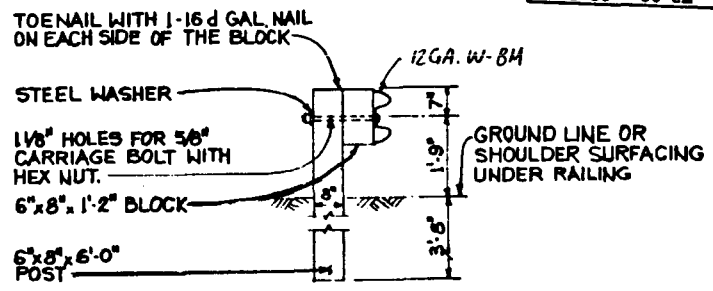


PLAN

Metric Conversion
 1 in = 2.5 cm
 1 ft = 30 cm



ELEVATION



TYPICAL SECTION AT POST

* AS TESTED, NOT STANDARD

Figure 85. LA-1 test installation drawing.

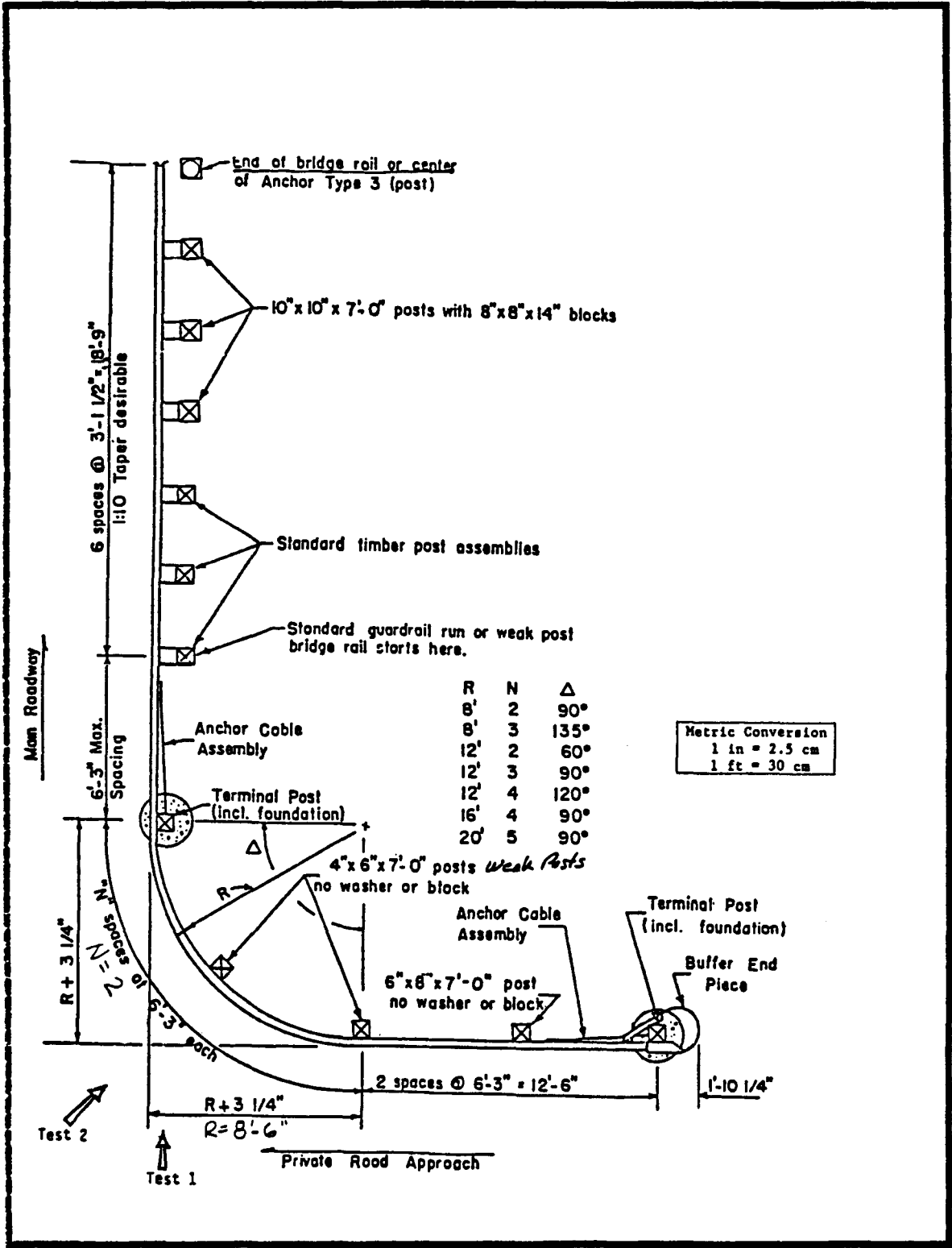


Figure 86. WA-1 test installation drawing.

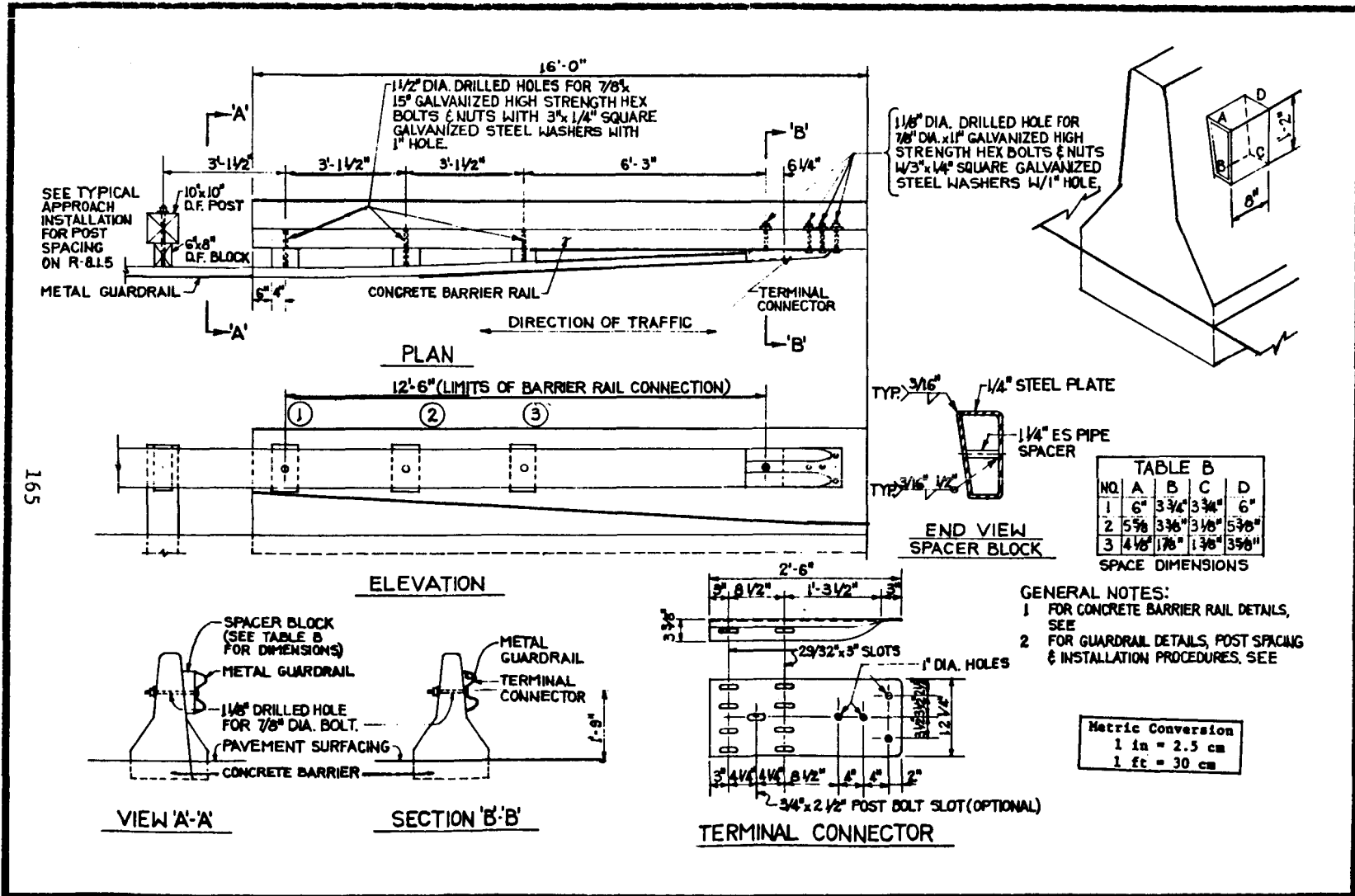
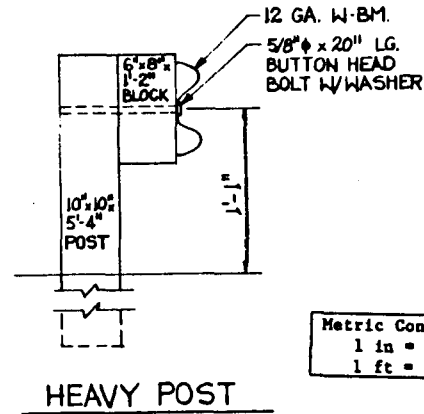
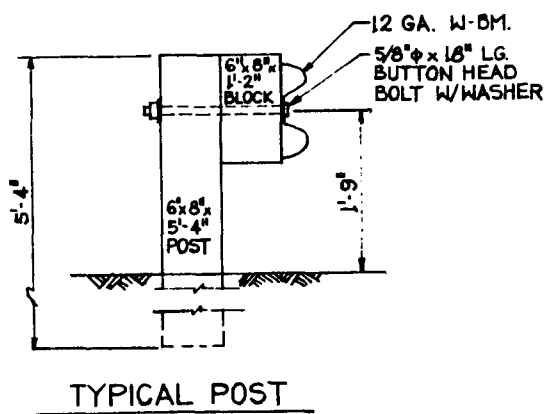
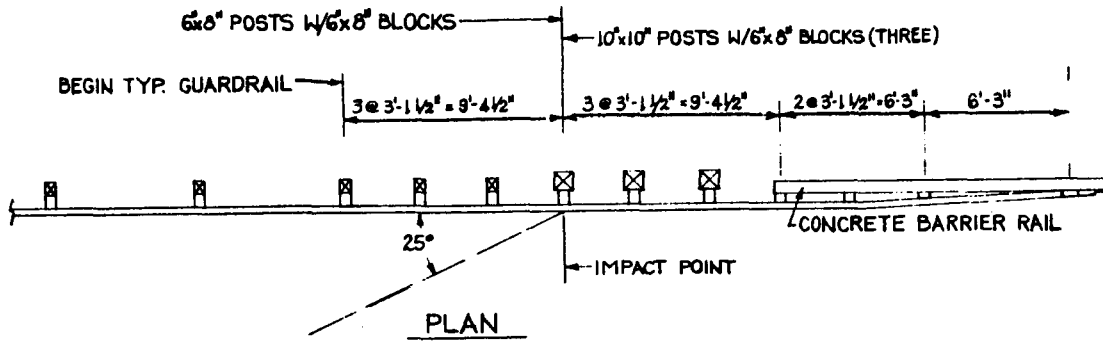
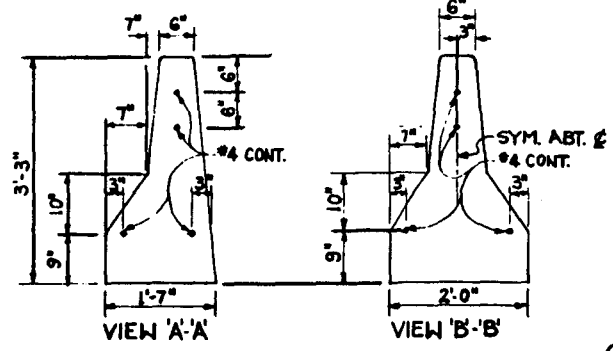
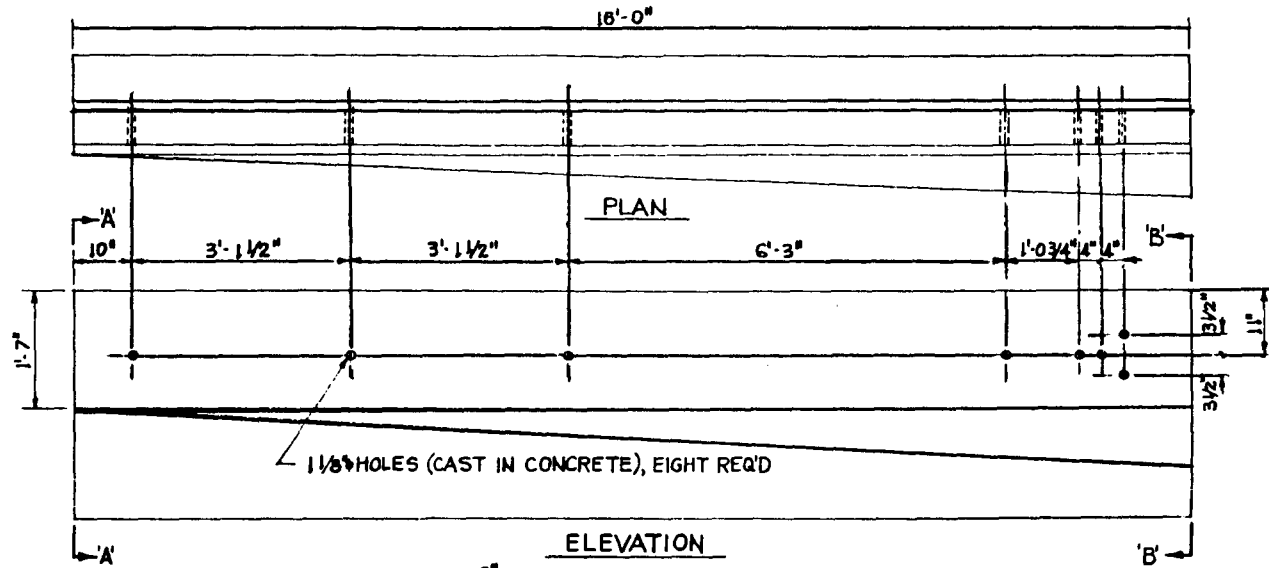


Figure 87. NV-1 test installation drawings.



Metric Conversion
 1 in = 2.5 cm
 1 ft = 30 cm

Figure 87. NV-1 test installation drawings (continued).



- NOTES:
 1. BARRIER MAY BE CAST INVERTED.
 2. REBAR GRADE 40.
 3. CONCRETE CLASS A OR AA (7 & 28 DAY CYLINDER REQ'D).

CLASS OF CONCRETE	CEM. RANGE SACKS PER CU. YD.	COARSE AGG. SIZE NO.	MAX. WATER GAL. PER SACK CEM.	MIN. COMPR. STR. (28 DAY) P.S.I.	STUMP RANGE INCHES NEV. T438	AIR RANGE PERCENT
A	6.0-7.5	467	6	3,000	1-4	-
AA	6.0-7.5	467	6	3,000	1-4	4-7

Metric Conversion
 1 in = 2.5 cm
 1 ft = 30 cm

CONCRETE END BLOCK

Figure 87. NV-1 test installation drawings (continued).

References

1. K. K. Mak and L. R. Calcote, "Accident Analysis of Highway Narrow Bridge Sites," FHWA Contract No. DOT-FH-11-9285, Final Report Nos. FHWA-RD-82-138, 139, 140, February 1983.
2. L. R. Calcote, "Development of a Cost-Effectiveness Model for Guardrail Selection," Report No. FHWA-RD-78-74, January 1980.
3. "Guide for Selecting, Locating, and Designing Traffic Barriers," American Association of State Highway and Transportation Officials, 1977.
4. J. D. Michie, "Recommended Procedures for the Safety Performance Evaluation of Highway Appurtenances," NCHRP Report 230, March 1981.
5. J. D. Michie, M. H. Ray, and W. N. Hunter, "Evaluation of Design Analysis Procedures and Acceptance Criteria for Roadside Hardware," Department of Transportation Contract No. DTFH61-82-C-00086, Draft Final Report, Southwest Research Institute, December 1985.
6. Joseph Bowles, Foundation Analysis and Design, 3rd Edition, McGraw Hill, Inc., New York, NY, 1982.
7. Karl Terzaghi, Theoretical Soil Mechanics, John Wiley and Sons, Inc., New York, NY, 1943.
8. J. F. Dewey, J. K. Jeyapalan, T. J. Hirsch, and H. E. Ross, "A Study of the Soil-Structure Interaction Behavior of Highway Guardrail Posts," Technical Report No. FHWA/TX-84/12+343-1, Texas State Department of Highways and Public Transportation, September 1982.
9. J. F. Sieler, "Effect of Depth of Embedment on Pole Stability," Wood Preserving News, Vol. 10, No. 11, November 1932, pp. 152-160.
10. D. L. Ivey, et al, "Test and Evaluation of W-Beam and Thrie-Beam Guardrails," Report No. FHWA/RD-82/071, June 1982.